T.C.
REPUBLIC OF TURKEY
HACETTEPE UNIVERSITY
GRADUATE SCHOOL OF HEALTH SCIENCES

EFFECTS OF NARINGENIN, BERBERINE, AND DELPHINIDIN PHYTOCHEMICAL COMPOUNDS ON BROWNING OF 3T3-L1 PREADIPOCYTE CELLS

MSc. Elif Didem ÖRS DEMET

Program of Nutrition and Dietetics
DOCTOR OF PHILOSOPHY THESIS

ANKARA
2024

T.C.
REPUBLIC OF TURKEY
HACETTEPE UNIVERSITY
GRADUATE SCHOOL OF HEALTH SCIENCES

EFFECTS OF NARINGENIN, BERBERINE, AND DELPHINIDIN PHYTOCHEMICAL COMPOUNDS ON BROWNING OF 3T3-L1 PREADIPOCYTE CELLS

Elif Didem ÖRS DEMET (MSc.)

Program of Nutrition and Dietetics
DOCTOR OF PHILOSOPHY THESIS

ADVISOR OF THE THESIS
Assoc. Prof. Zeynep GÖKTAŞ, PhD

ANKARA
2024

APPROVAL PAGE

EFFECTS OF NARINGENIN, BERBERINE, AND DELPHINIDIN PHYTOCHEMICAL COMPOUNDS ON BROWNING OF 3T3-L1 PREADIPOCYTE CELLS

Elif Didem ÖRS DEMET, MSc

Supervisor: Assoc. Prof. Zeynep GÖKTAŞ, PhD

This thesis study has been approved and accepted as a PhD dissertation in "Nutrition and Dietetics Program" by the assesment committee, whose members are listed below, on 08.03.2024.

Chairman of the Committee :	*Prof. Efsun KARABUDAK, PhD* *Sanko University*
Member :	*Prof. Neslişah RAKICIOĞLU, PhD* *Hacettepe University*
Member :	*Prof. Zehra BÜYÜKTUNCER DEMİREL, PhD* *Hacettepe University*
Member :	*Prof. Mustafa ÇELEBİER, PhD* *Hacettepe University*
Member :	*Prof. Abdullah ÖKSÜZ, PhD* *Necmettin Erbakan University*

This dissertation has been approved by the above committee in conformity to the related issues of Hacettepe University Graduate Education and Examination Regulation.

13 Mart 2024

Prof. Müge YEMİŞCİ ÖZKAN, MD, PhD

Director

DECLARATION OF PUBLICATION AND INTELLECTUAL

Enstitü tarafından onaylanan lisansüstü tezimin/raporumun tamamını veya herhangi bir kısmını, basılı (kağıt) ve elektronik formatta arşivleme ve aşağıda verilen koşullarla kullanıma açma iznini Hacettepe Üniversitesine verdiğimi bildiririm. Bu izinle Üniversiteye verilen kullanım hakları dışındaki tüm fikri mülkiyet haklarım bende kalacak, tezimin tamamının ya da bir bölümünün gelecekteki çalışmalarda (makale, kitap, lisans ve patent vb.) kullanım hakları bana ait olacaktır.

Tezin kendi orijinal çalışmam olduğunu, başkalarının haklarını ihlal etmediğimi ve tezimin tek yetkili sahibi olduğumu beyan ve taahhüt ederim. Tezimde yer alan telif hakkı bulunan ve sahiplerinden yazılı izin alınarak kullanılması zorunlu metinlerin yazılı izin alınarak kullandığımı ve istenildiğinde suretlerini Üniversiteye teslim etmeyi taahhüt ederim.

Yükseköğretim Kurulu tarafından yayınlanan **"Lisansüstü Tezlerin Elektronik Ortamda Toplanması, Düzenlenmesi ve Erişime Açılmasına İlişkin Yönerge"** kapsamında tezim aşağıda belirtilen koşullar haricince YÖK Ulusal Tez Merkezi / H.Ü. Kütüphaneleri Açık Erişim Sisteminde erişime açılır.

- o Enstitü / Fakülte yönetim kurulu kararı ile tezimin erişime açılması mezuniyet tarihimden itibaren 2 yıl ertelenmiştir. (1)
- ✓ Enstitü / Fakülte yönetim kurulunun gerekçeli kararı ile tezimin erişime açılması mezuniyet tarihimden itibaren 6 ay ertelenmiştir.(2)
- o Tezimle ilgili gizlilik kararı verilmiştir.

13/03/2024

Elif Didem ÖRS DEMET

1"Lisansüstü Tezlerin Elektronik Ortamda Toplanması, Düzenlenmesi ve Erişime Açılmasına İlişkin Yönerge"

(1) Madde 6. 1. Lisansüstü tezle ilgili patent başvurusu yapılması veya patent alma sürecinin devam etmesi durumunda, tez danışmanının önerisi ve enstitü anabilim dalının uygun görüşü üzerine enstitü veya fakülte yönetim kurulu iki yıl süre ile tezin erişime açılmasının ertelenmesine karar verebilir.

(2) Madde 6. 2. Yeni teknik, materyal ve metotların kullanıldığı, henüz makaleye dönüşmemiş veya patent gibi yöntemlerle korunmamış ve internetten paylaşılması durumunda 3. şahıslara veya kurumlara haksız kazanç imkanı oluşturabilecek bilgi ve bulguları içeren tezler hakkında tez danışmanının önerisi ve enstitü anabilim dalının uygun görüşü üzerine enstitü veya fakülte yönetim kurulunun gerekçeli kararı ile altı ayı aşmamak üzere tezin erişime açılması engellenebilir.

*(3) Madde 7. 1. Ulusal çıkarları veya güvenliği ilgilendiren, emniyet, istihbarat, savunma ve güvenlik, sağlık vb. konulara ilişkin lisansüstü tezlerle ilgili gizlilik kararı, tezin yapıldığı kurum tarafından verilir *. Kurum ve kuruluşlarla yapılan işbirliği protokolü çerçevesinde hazırlanan lisansüstü tezlere ilişkin gizlilik kararı ise, ilgili kurum ve kuruluşun önerisi ile enstitü veya fakültenin uygun görüşü üzerine üniversite yönetim kurulu tarafından verilir. Gizlilik kararı verilen tezler Yükseköğretim Kuruluna bildirilir. Madde 7.2. Gizlilik kararı verilen tezler gizlilik süresince enstitü veya fakülte tarafından gizlilik kuralları çerçevesinde muhafaza edilir, gizlilik kararının kaldırılması halinde Tez Otomasyon Sistemine yüklenir*

** Tez danışmanının önerisi ve enstitü anabilim dalının uygun görüşü üzerine enstitü veya fakülte yönetim kurulu tarafından karar verilir.*

ETHICAL DECLARATION

In this thesis study, I declare that all the information and documents have been obtained in the base of the academic rules and all audio-visual and written information and results have been presented according to the rules of scientific ethics. I did not do any distortion in data set. In case of using other works, related studies have been fully cited in accordance with the scientific standards. I also declare that my thesis study is original except cited references. It was produced by myself in consultation with supervisor Assoc. Prof. Dr. Zeynep GÖKTAŞ and written according to the rules of thesis writing of Hacettepe University Institute of Health Sciences.

Elif Didem ÖRS DEMET

ACKNOWLEDGEMENTS

There are not enough words to thank my thesis advisor, Assoc. Prof. Dr. Zeynep GÖKTAŞ, who has always supported me from the beginning of my academic career. She is the best advisor in the world, who has shown and made me feel loved and she always had faith, patience, and trust in me. She always supported and encouraged me to do better. One of the biggest opportunities in life was to be her student and I will always try my best to be worthy of her.

I would like to thank TÜBİTAK 1001-The Scientific and Technological Research Projects Funding Program and TÜBİTAK BİDEB 2211-A for supporting me financially during my studies.

I would like to thank my Prof. Dr. Mustafa ÇELEBIER, Assoc. Prof. Dr. Tuğba GÜLSÜN INAL, Dr. Tuba REÇBER, and Dr. Duygu SEVIM for helping me and supporting me whenever I needed it. I would like to express my gratitude towards my research colleagues, with whom I worked together in laboratory analyses and experiments: Res. Asst. Aslıhan AĞAÇDIKEN, Res. Asst. Kübra UÇAR BAŞ, Res. Asst. Dilem TUĞAL ASLAN, Assist. Res. Asst. Ayşegül SIVASLIOĞLU and Res. Asst. Gülcan UYSAL YELER. I am glad that I worked with you and I am thankful to have had you as my teammates. I am grateful to be part of such a team.

I would like to thank all the professors and assistants of Necmettin Erbakan University, Department of Nutrition and Dietetics, for their support during the thesis process and all my dear friends who never withheld their moral support and were with me throughout the whole process. In particular, I'd like to thank Şenay Burçin ALKAN, Semra KAPLAN, Nicoletta BATTAGLIA, Arife MACIT, Manel and Maryam NASR.

I am profoundly grateful to my beloved husband, Atıf Emre DEMET, and his family, especially Aliye DEMET and Hikmet DEMET. Their unwavering support and encouragement were crucial, particularly during the final stages of my PhD.

I owe the biggest thanks to my family: my dear mother Zeliha ÖRS and my father Ali ÖRS, my sisters Leyla ÖRS and Özlem Deniz ÖRS BODUR, my brother-in-law Samet BODUR and my dear nephew Alper Eren BODUR. Last but not least, I want to thank myself for the hard work throughout my PhD journey.

Last but not least, I want to thank myself for the hard work throughout my PhD journey

ABSTRACT

ÖRS DEMET, ED. Effects of Naringenin, Berberine, and Delphinidin Phytochemical Compounds on Browning of 3T3-L1 Preadipocyte Cells. Hacettepe University, Graduate School of Health Sciences, Nutrition and Dietetics Program, Doctor of Philosophy Thesis, Ankara, 2024. Obesity, a complex global health challenge, demands innovative treatment strategies. Plant-derived bioactive compounds, including flavanones, alkaloids, and anthocyanins, hold promise for combating obesity-related complications. This study explored the effects of delphinidin, naringenin, and berberine – compounds with known anti-obesity potential – on 3T3-L1 preadipocyte cells to unravel their impact on browning of adipose cells. This study investigated the impacts of delphinidin, naringenin, and berberine in both free and liposomal forms on the browning process in 3T3-L1 preadipocyte cells. The expression of key browning markers (PRDM16, PPARγ, PGC1-α, CIDEA, and UCP1) was assessed and triglyceride levels were measured to evaluate lipid metabolism. Quantitative Real Time PCR and Elisa analyses were employed to quantify gene and protein expression levels, respectively, with statistical significance determined by p-values ($p<0.05$). These findings indicate a complex interaction between the tested phytochemicals and adipocyte browning. Free form of delphinidin showed potential in promoting browning through increased PRDM16 expression ($p=0.037$) but did not significantly affect beige-specific gene expressions or reduce triglyceride levels except during maturation. High-dose liposomal form of naringenin during maturation increased UCP1 gene expression significantly ($p=0.035$), indicating potential for browning, but did not impact triglyceride levels. Liposomal form of berberine significantly enhanced UCP1 expression ($p=0.002$) and reduced triglyceride levels in differentiation ($p<0.05$), suggesting its efficacy in inducing adipocyte browning. Safety assessments, evaluated with cell viability assays (MTT), indicated that all compounds were safe in free form after 24 hours, with adverse effects noted after 48 hours. This study highlights the differential impacts of delphinidin, naringenin, and berberine on the browning of adipocytes, with berberine showing the most consistent and significant effects in promoting browning and affecting lipid metabolism. These findings lay groundwork for anti-obesity therapeutics, yet comprehensive *in vitro* and *in vivo* studies are essential to validate and expand the browning potential of delphinidin, naringenin, and berberine to treat obesity.

Key Words: Naringenin, Berberine, Delphinidin, 3T3-L1 Preadipocyte Cells, Brown Adipose Tissue, Obesity

Funding source: This dissertation was supported by TÜBİTAK 1001-The Scientific and Technological Research Projects Funding Program. The project number was 220S742.

ÖZET

ÖRS DEMET, ED. Naringenin, Berberin ve Delfinidin Fitokimyasal Bileşenlerinin 3T3-L1 Preadipozit Hücrelerinin Kahverengileşmesi Üzerine Etkisi. Hacettepe Üniversitesi Sağlık Bilimleri Enstitüsü Beslenme ve Diyetetik Programı Doktora Tezi, Ankara, 2024. Obezite dünyada ve ülkemizde hızla artan önemli bir halk sağlığı sorunudur. Obezite kompleks bir hastalık olup, bireyin yaşam süresini kısaltmakta ve sosyo-psikolojik ve fiziksel açıdan yaşamı olumsuz etkilemektedir. Son yıllarda obezitenin engellenmesi ve tedavisi için yapılan araştırmalar adipoz doku üzerine yoğunlaşmaktadır. İnsanlarda farklı fonksiyonlara sahip üç adipoz doku vardır: beyaz, kahverengi ve bej adipoz doku. Adipoz dokuların morfolojik yapıları, metabolik fonksiyonları, biyokimyasal özellikleri ve gen ekspresyon yolakları farklıdır. 1) Beyaz adipositler küresel şekilli hücrelerdir ve hacimlerinin %90'ını tek bir sitoplazmik lipit damlacığı oluşturur. Beyaz adipoz deponun temel fonksiyonu vücuda alınan fazla enerjiyi açlık durumunda organizmanın kullanması için trigliserit formunda depolamaktır. 2) Kahverengi adipositlerin hücre yapısı incelendiğinde beyaz adipositlere göre daha küçük çaplı olduğu ve birkaç küçük lipit damlacığı içerdiği gösterilmiştir. Kahverengi yağ dokusunda titremeye bağlı olmayan termojenez gerçekleşir. Titremeye bağlı olan termojenezde soğuğa maruz kalma sonucu kas aktivitesinin artması sonucu ısı oluşumu gerçekleşir. Kahverengi adipositlerin sitoplazmasında daha fazla sayıda mitokondri bulunur. Bunlar eşleşmemiş protein-1 (UCP -1) içerir ve titremeye bağlı olmayan termojeneze aracılık eder. Kahverengi adipoz dokunun en önemli belirteçlerinin arasında PRDM16, PPARγ, PGC1-α, CIDEA ve UCP1 genleri bilinmektedir. 3) Son yıllarda yapılan çalışmalarda "bej adipoz doku" (uyarılabilir kahverengi adipoz doku) olarak adlandırılan üçüncü bir adipoz doku tespit edilmiştir. Bej adipositler beyaz adiposit fenotipindedir, büyük lipid damlacıkları içerir. Bej adipositlerde bazal koşullarda UCP-1 ekspresyonu yoktur. Soğuğa maruziyet veya β3-adrenerjik aktivatörleri ile kahverengi adipoz dokuya benzerler. Bu değişim beyaz adipoz dokunun kahverengileşmesi olarak adlandırılmaktadır ve zayıflama da etkili olup obezite tedavisinde kullanımı araştırılmaktadır. Yapılan hayvan çalışmalarında besinlerin yapısında bulunan besin ögeleri ve biyoaktif bileşenlerin, vücut yağ kompozisyonunun azalmasında, kahverengi adipoz dokunun aktifleştirilmesinde ve beyaz adipoz dokunun kahverengileşmesinde rol oynadığı gösterilmiştir. Vücut yağ kompozisyonuna olan etkisi araştırılmış fakat kahverengileşme üzerine etkisi net olarak bilinmeyen ve son yıllarda öne çıkan fitokimyasallar naringenin, berberin ve delfinidindir. Naringenin (4',5,7-trihidroksiflavanon) renksiz ve acı bir bileşen olup en fazla greyfurtta olmak üzere portakal, limon ve mandalina gibi turunçgillerde ve düşük miktarda olmak üzere domates ve domates ürünlerinde bulunmaktadır. Naringeninin önemli bir özelliği ise obeziteye karşı etkisidir. Adipoz dokusunun kütlesindeki azalma ve preadiposit proliferasyonunun inhibisyonu sağladığı incelenmektedir. Berberin pek çok bitkisel ilaçta doğal olarak bulunan bitki alkoloididir ve genellikle diyarenin tedavisinde kullanılsa da geçtiğimiz yıllarda pek çok farklı metabolik faydası keşfedilmiştir. In vivo ve in vitro çalışmalar berberinin insülin direnci ve hiperlipidemi gibi bazı önemli metabolik hastalıklarda iyileşme sağlayabileceği gösterilmiştir. Delfinidin pek çok pigmentli meyve ve sebzede bolca bulunan antosiyaninlerin majör bir sınıfıdır. Antosiyaninlerin obesite üzerine pozitif

etkileri olduğu gösterilmiş olsa da, delfinidinin adipojenez ve kahverengileşme üzerine etkilerini inceleyen çalışmalar sınırlı sayıdadır. Bu üç fitokimyasalın biyoraralılığı ve stabilitesi düşüktür, bu nedenle nanoenkapsülasyon tekniği ile enkapsüle edilip fitokimyasalların stabilitesini arttırılıp ve yıkımını azaltabilmektedir. Bu taşıyıcıların küçük boyutta olmaları hücre için alımını kolaylaştırmakta ve böyle biyoyararlılığı arttırabilmektedir. Artmış çözünürlük ve stabilite, kontrollü salınım, hedefe yönelik dağıtım gibi özellikler sayesinde nanoenkapsülasyon tekniği ile uygulanan doz miktarı da azaltılabilmektedir. Bu çalışmanın amacı nanoenkapsüle ve serbest halde farklı dozlarda naringenin, berberin ve delfinidin biyoaktif bileşenlerinin 3T3-L1 pre-adiposit hücre kültüründe diferansiyasyon ve maturasyon sürecinde termojenez ve kahverengileşme üzerine etkilerini incelemektir. Çalışma in vivo 3T3-L1 pre-adipoz hücrelerinin üzerinde yapılmıştır. İki farklı aşamada tedavi uygulanmıştır: diferensiyasyon ve maturasyon. Bir sonraki aşamada saf naringenin ve berberin lipozomal formunda enkapsüle edilmiştir. Bu partiküller ayrıca boş olarak hazırlanıp nano taşıyıcılar da test edilmiştir. Naringenin, berberin ve delfinidin ve tüm nanopartiküller spesifik konsantrasyonlarda PBS'de (phosphate buffered saline) çözülecektir ve 4°C'de saklanmıştır. Lipozomal naringenin ve berberin kapsüller fiziksel ve kimyasal konşulları test edilmiştir. Kapsüle edilmemiş naringenin, berberin ve delfinidin, nanoenkapsüle naringenin, berberin ve bunların boş partikülleri farklı konsantrasyonlarda medyuma eklenmiştir. Bir sonraki aşamada hücre canlılığı testi, gen ekspresyon seviyeleri (C/EBPβ, PPARγ, FABP4, UCP-1, PGC1-α, PRDM16, CIDEA) ve hücre içi trigliserit ve protein konsantrasyonu ölçülmüştür. Gen ve protein ekspresyon seviyelerini ölçmek için sırasıyla Kantitatif Gerçek Zamanlı PCR ve Elisa analizleri kullanılmıştır. Araştırma sonucu elde edilecek veriler SPSS 22.0 programıyla değerlendirilmiştir ve istatistiksel anlamlılık p değerleri ($p<0.05$) ile belirlenmiştir. Bu çalışmadan elde edilen bulgular özetle verilmiştir: 1) Naringenin ve berberinin kapsüllenmiş lipozomal formu başarıyla üretilmiştir. 2) Fiziksel olarak en stabil enkapsüle edilmiş naringenin ve berberin siyah renkli tüplerde +4°C'de muhafaza edilen olarak bulunmuştur. 3) Enkapsüle edilmiş naringenin ve berberin formülasyonunun daha HPLC ölçümü ile fitokimyasalların serbest formundan daha stabildir. 4) Delfinidin adipogenez anahtar düzenleyicilerin ifade seviyelerini değiştirmemiştir (PPARγ, C/EBPβ, FABP4). 5) Delfinidin yağ hücrelerinin kahverengileşmenin üzerinde katkıda bulunabilir (PRDM16'nın artan ifadesi). Bununla birlikte, delfinidin diğer kilit düzenleyicilerin (PGC1-α, CIDEA, UCP1) ifadeleri değişmemiştir. 6) Delfinidin sadece maturasyon sürecinde trigliserit seviyelerini düşürmüştür. 7) Delfinidin kahverengi adipoz dokunun temel proteinlerin, özellikle de UCP-1 seviyeleri üzerinde olumlu bir etkiye sahip olmayabilir. Ancak, PGC1-α protein konsantrasyonu doza bağlı olarak artmıştır. 8) C/EBPβ, serbest ve lipozomal naringenin uygulamasından sonra, gen ekspresyon seviyelerini değişmemiştir. Bununla birlikte, PPARγ gen ekspresyon seviyeleri lipozomal 20 μM, 10 μM ve 5 μM naringenin sonrasında önemli ölçüde düşmüştür. Ayrıca, naringenin maturasyon sürecinde FABP4 seviyelerini azaltmıştır. Bu sonuçlara dayanarak, naringenin'in adipogenez üzerindeki etkisi belirsizdir. 9) Serbest naringenin ile tedaviden sonra PGC1-α gen ekspresyon seviyeleri maturasyonda önemli ölçüde yükselmiştir, ancak diferansiyasyon da değildi. 10) CIDEA gen ekspresyon seviyeleri diferansiasyon serbest 20 μM naringenin uygulandıktan sonra diğer gruplara kıyasla daha yüksek bulunmuştur. 11) UCP1 gen ifade seviyeleri, diferansiyasyon sürecinde kapsüllü 20 μM, 10 μ ve serbest 10 μM naringenin formlarında önemli ölçüde daha yüksek

incelenmiştir. Naringenin yağ hücrelerinin kahverengileşmesinin erken evresi üzerinde etkili olabilir. 12) PRDM16, diferansiyasyon da tüm naringenin grupları için benzer gen ekspresyon seviyeleri sergilemiştir, ancak maturasyonda bu gen ekspresyon seviyeleri naringenin uygulamasından sonra yukarı doğru düzenlenmiştir. 13) Hem serbest hem de lipozomal naringenin UCP1 ve PPARγ protein konsantrasyonunu değiştirmemiştir. Ancak, naringenin PGC1-α protein konsantrasyonunu önemli ölçüde arttırdığı gözlenmiştir. 14) Naringenin diferansiyasyon ve maturasyon aşamalarında trigliserit seviyelerini azaltmamıştır. 15) Berberin tedavisinden sonra PPARγ, C/EBPβ ve FABP4 gen ekspresyon seviyeleri diferansiyasyon da tüm gruplarda benzerdi, ancak maturasyonda PPARγ gen ekspresyon seviyeleri berberinin lipozomal 20 μM'ında önemli ölçüde daha düşük bulunmuştur; FABP4 gen ekspresyon seviyeleri maturasyonda serbest 10 μM'da diğer gruplardan önemli ölçüde daha düşük incelenmiştir. Berberin tedavisinin adipositlerin adipogenezini etkileyebileceği düşünülmektedir. 16) CIDEA seviyeleri diferansiyasyon da tüm berberin formlarında benzerdi, ancak berberinde CIDEA ifadesi tüm berberin gruplarına kıyasla serbest 10 μM' da önemli ölçüde daha yüksek incelenmiştir. 17) PGC1-α ekspresyon seviyeleri diferansiyasyon sürecinde serbest 5 μM' da lipozomal 20 μM ve lipozomal 10 μM berberine kıyasla daha yüksek saptanmıştır. Şaşırtıcı bir şekilde, boş berberin maturasyon sürecinde bu geni arttırmıştır. 18) Berberin her iki süreçte de PRDM16 seviyelerini önemli ölçüde değiştirmemiştir. Şaşırtıcı bir şekilde, void B maturasyon sürecinde bu geni arttırmıştır. 19) UCP1 seviyelerin en yüksek seviyesi diferansiyasyon sürecinde serbest 20 μM ve 10 μM ve maturasyon sürecinde serbest 20 μM ve 10 μM berberinde görülmüştür. Bu sonuçlar berberinin 3T3-L1 adipositlerinde kahverengileşmeyi indükleyebileceğini düşündürmektedir. 20) UCP1 protein konsantrasyonu açısından serbest naringenin, serbest berberin, lipozomal naringenin ve lipozomal berberin grupları için anlamlı bir fark bulunmamıştır. 21) PPARγ ve PGC1-α protein konsantrasyonu berberin tedavisinden sonra pozitif olarak etkilenmiştir. 22) Berberinin lipozomal formu sadece diferansiyasyon sürecinde trigliserit seviyesindeki azaltmıştır. 23) Tüm fitokimyasalların 24 saat sonra serbest formda kullanımının güvenli olabileceğini gösterilmiştir. Ancak, berberin ve naringenin'in serbest ve lipozomal formları yan etkiler hücre canlılık testinde 48 saat sonra incelenmiştir.

Bu çalışmanın sınırlılığı, karmaşık transkripsiyonel ve post-transkripsiyonel düzenlemeyi içeren bej adipogenez yollarının analiz edilmemesidir. Bu nedenle, adiposit kahverengileşmesini ve metabolik etkilerini açıklayan moleküler mekanizmaları tam olarak anlamak için daha fazla çalışma yapılması gerekmektedir. Sonuç olarak, bu bulgular obezite ile mücadele için terapötiklerin geliştirilmesi için önemli bir farklı yol sağlayabilir. Bununla birlikte, delfinidin, naringenin ve berberinin kahverengileşme etkisini doğrulamak ve bu fitokimyasalları pratik obezite karşıtı tedavi olarak potansiyel olarak uygulamak için daha fazla in vitro ve in vivo çalışma gereklidir.

Anahtar Kelimeler: Naringenin, Berberin, Delfinidin, 3T3-L1 Preadiposit Hücreleri, Kahverengi Yağ Dokusu

Destekleyen Kurumlar: Bu proje TÜBİTAK 1001- Bilimsel ve Teknolojik Araştırma Projelerini Destekleme Programı 220S742 numaralı proje kapsamında desteklenmiştir.

TABLE OF CONTENTS

SYMBOLS AND ABBREVIATIONS

ACC	Acetyl-CoA Carboxylase
AMPK	Adenosine Monophosphate-Activated Protein Kinase
ATGL	Adipose Triglycerides Lipase
B	Berberine
BAT	Brown Adipose Tissue
BCA	Protein Quantification
C/EBP	CCAAT/Enhancer Binding Protein
cDNA	Complementary DNA
ChREBP	Carbohydrate Responsive Element-Binding Protein
CIDEA	Cell Death Inducing DFFA Like Effector A
CPT1A	Carnitine Palmitoyltransferase 1A
CREG1	Cellular Repressor of E1A-stimulated Genes 1
D	Delphinidin
DMEM	Dulbecco's modified Eagle's medium
DMSO	Dimethyl sulfoxide
EF	Encapsulation Efficiency
ELISA	Enzyme-Linked Immuno Sorbent Assay
FABP4	Fatty Acid Binding Protein 4
FAS	Fatty Acid Synthase
FBS	Fetal Bovine Serum
FGF21	Fibroblast Growth Factor 21
FoxO1	Forkhead transcription factor O1
G6Pase	Glucose-6-phosphatase
GLP-1	Glucagon-Like Peptide-1
HMG-CoA	3- Hydroxy 3-Methylglutaryl-Coa
HNF4	Hepatic Nuclear Factor 4 Alpha
HPLC	High-Performance Liquid Chromatography
IBMX	Isomethyl-butylxanthine
IL-1	Interleukin-1
IL-6	Interleukin-6

IRS-1	Insulin Receptor Substrate-1
LIPO	Liposomal Form
LC	Loading Capacity
LDLR	Low-Density Lipoprotein Receptor
MCP-1	Monocyte Chemoattractant Protein
N	Naringenin
OLZ	Olanzapine
PA	Palmitic Acid
PBS	Phosphate-Buffered Saline
PCSK9	Proprotein Convertase Subtilisin/Kexin Type 9
PEPCK	Phosphoenolpyruvate Carboxykinase
PGC1-α	Peroxisome Proliferator-Activated Receptor-Gamma Coactivator-1alpha
PI	Polydispersity Index
PPARγ	Peroxisome Proliferators-Activated Receptor Γ
PRDM16	PR Domain Containing 16
RT-PCR	Reverse transcription-polymerase chain reaction
SEM	Scanning Electron Microscope
SMARCD1	SWI/SNF Related, Matrix Associated, Actin Dependent Regulator of Chromatin, Subfamily D, Member 1
Soy-PC	Soy L-α-phosphatidylcholine
SREBP1	Sterol Regulatory Element-Binding Protein 1c
STZ	Streptozotocin
TC	Total Cholesterol
TG	Triglyceride
TNF-α	Tumor Necrosis Factor Alpha
UCP1	Uncoupled Protein-1
V	Void
WAT	White Adipose Tissue
ZP	Zeta Potential

FIGURES

TABLES

1. INTRODUCTION

1.1. Theoretical Framework

Obesity is an important public health problem that is quickly expanding in the world. It is a multifactorial complex disease, and it represents a serious public health issue with a rapidly increasing incidence in all age groups worldwide (1). Obesity is associated with a decreased quality of life by incrementing the risk of many diseases such as diabetes, cardiovascular diseases, various types of cancer, and osteoarthritis (2).

In humans, there are three adipose tissues with different functions: beige, brown, and white adipose tissue. The beige adipose tissue resembles brown adipose tissue to cold exposure or ß3-adrenergic activators (presence of uncoupled protein-1expression (UCP-1) small lipid droplets). Browning of adipose tissue and increasing brown adipose tissue activity is a new and promising approach to the management of the aforementioned diseases (3).

Bioactive components such as phytochemicals play an important role in the browning of white adipose tissue. Naringenin, berberine, and delphinidin are some of these phytochemical components. Naringenin regulates gluconeogenesis (4), lipolysis, and lipogenesis-related gene expression (5, 6), reducing inflammation in adipose tissue (7), and lowering plasma lipid levels through activation of adenosine monophosphate-activated protein kinase (AMPK). Thus, naringenin reduces body weight, fat accumulation, hyperlipidemia, and hyperglycemia by suppressing the proliferation of preadipocytes, increasing fatty acid oxidation in hepatocytes (8), and regulating white adipose tissue in mice (9). Berberine has been reported to protect rodents from weight gain and fat accumulation (10, 11). Berberine has been shown to affect brown adipose tissue by improving cold tolerance, reducing fat accumulation, and increasing mitochondrial content and thermogenic markers (such as peroxisome proliferator-activated receptor-gamma coactivator-1alpha (PGC1α), cell death inducing dffa like effector A (CIDEA), and UCP1 (12). It has also been reported that berberine not only increases the activity of brown adipose tissue but also stimulates the browning of the white ones (13). Delphinidin has many biological effects such as anti-inflammatory, anti-angiogenic, anti-cancer, anti-adipogenesis, antimicrobial, and neuroprotective

(14-24). Delphinidin has been demonstrated to lower the viability, growth, and maturation of 3T3-L1 cells by diminishing the levels of peroxisome proliferators-activated receptor Γ (PPARγ) (25). it was observed that delphinidin enhances the phosphorylation of AMPK and acetyl-CoA carboxylase (ACC), while it reduces the levels of PPARγ, CCAAT/enhancer-binding protein alpha (C/EBPα), SREBP1, and FAS. This leads to a decrease in lipid concentrations and small fat droplets, mitigating fat formation and advancing lipid metabolism (26).

However, the stability and bioavailability of these phytochemicals in the free form are very low. The nanoencapsulation technique has been developed to increase these properties. They can increase the stability of encapsulated components and reduce their degradation (27-29). The small size of these carriers facilitates their uptake into the cell and thus increases bioavailability. In addition, targeted delivery can be achieved with ligands that can be added to the surfaces of these carriers (30). Nanocarriers can provide controlled release of encapsulated components. Thanks to features such as increased solubility and stability, controlled release, and targeted delivery, the amount of dose administered with the nanoencapsulation technique can also be reduced (31). Nano-encapsulated phytochemicals can be used in combating obesity and activating brown adipose tissue (31, 32).

1.2. Aim and Hypotheses

The purpose of this study is to investigate the effects of administration of free naringenin, berberine, and delphinidin and encapsulated naringenin and berberine in different dosages to 3T3-L1 preadipocyte cell culture in differentiation and maturation stages on thermogenesis and browning processes. Hypotheses;

Hypothesis1: Administration of encapsulated naringenin and berberine decreases fat accumulation in 3T3-L1 cells.

Hypothesis 2: Administration of free naringenin, berberine, and delphinidin decreases fat accumulation in 3T3-L1 cells.

Hypothesis 3: Administration of free forms of naringenin, berberine, delphinidin and encapsulated forms of naringenin and berberine decreases the differentiation of 3T3-L1 cells.

Hypothesis 4: Administration of free forms of naringenin, berberine, delphinidin and encapsulated forms of naringenin and berberine increases browning markers in 3T3-L1 cells.

2. LITERATURE REVIEW

2.1. Berberine

Berberine is a natural product of quaternary ammonium salt from the group of isoquinoline alkaloids (2,3-methylenedioxy-9,10-dimethoxyprotoberberine chloride $C_{20}H_{18}NO_4^+$) (33) (Figure 2.1).

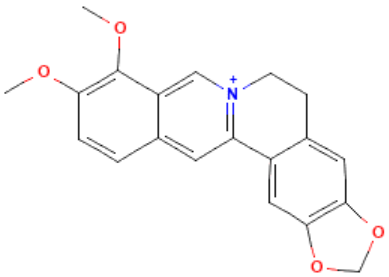

Figure 2.1. The chemical structure of berberine (34)

It is a plant alkaloid and a polyphenol extract isolated from several plants and roots, such as Berberis aristata (Tree Turmeric), Berberis vulgaris (Barberry), Berberis aquifolium (Oregon grape), Coptis chinensis (Coptis or Goldthread), Arcangelisia flava, and Hydrastis canadensis (goldenseal) (12, 35-37). Berberine is commonly used to treat gastrointestinal symptoms like diarrhea in Eastern Asia, on the other hand, its potential metabolic effects drew attention in past decades (38, 39). Berberine seems to have hypolipidemic, hypoglycemic, anti-inflammatory effects, and hypotensive (35, 39-41).

2.1.1. Pharmacokinetic Properties

Berberine has a low oral bioavailability and intestinal absorption. The oral bioavailability of berberine in rats was estimated to be less than 1% (42, 43). According to research, berberine's bioavailability in humans is just as low as it is in animal studies (44, 45). The main barriers to berberine in oral administration are as follows: self-aggregation in the stomach and small intestine's acidic environments (44), intestinal first-pass elimination, interaction with P-glycoprotein (P-gp) pumps, and distribution in the liver (46). This low bioavailability limits the beneficial effects

of berberine. In recent years, different strategies have been utilized in pharmaceutics to enhance bioavailability like: liposomes, microemulsions, solid lipid nanoparticles, and micelles.

These formulations increase the stability, circulation time, and endocytosis of an encapsulated medication while also enhancing the drug's solubility and permeability in the gastrointestinal system (29, 47, 48). Moreover, they facilitate the transfer of drugs from the lymphatic system to the gastrointestinal tract. These strategies increase the bioavailability of berberine in animal studies; nevertheless, human trials are required to assess these techniques.

Animal studies demonstrate that following oral treatment, berberine has a high tissue distribution. Berberine is rapidly distributed into the liver, kidneys, pancreas, muscle, brain, heart, fat, and lungs (49). The distribution of berberine has not been studied in humans. Berberine metabolism is mostly located in the liver in both rats and humans (50). According to clinical studies, CYP2D6 is the human cytochrome P450 (CYP) that is most responsible for creating berberine's metabolites, followed by CYP1A2, 3A4, 2E1, and CYP2C19 (51). There is no research on the excretion of berberine in humans. Berberine has a low oral bioavailability in humans due to limited intestinal absorption and quick *in vivo* metabolism. The majority of the total recoverable rate of berberine was eliminated through bile and urine (52).

2.1.2. Therapeutic Effect of Berberine

Anti-Obesity Activities

In recent studies, berberine’s anti-obesity effects via brown adipose tissue thermogenesis regulation and adipogenesis suppression have been shown (53, 54). In a cell study, berberine treatment (0.5, 1, 5, and 10 mcg) of 3T3-L1 cells during differentiation reduced the expressions of CCAAT/enhancer binding protein α (C/EBP α) and peroxisome proliferators-activated receptor γ2 (PPARγ2). Berberine prevented the phosphorylation of the cAMP-response element-binding protein (CREB) and the expression of C/EBPβ in the early stages of differentiation. These findings suggest that berberine may be effective in suppressing adipogenesis (53).

In another *in vitro* study, olanzapine (OLZ)-induced 3T3-L1 cells were treated with berberine (0.675, 1.25, 2.5, and 5 μM) for 6 days and it decreased triglyceride

and total cholesterol accumulation and suppressed the expressions of the sterol regulatory element binding proteins 1 (SREBP1), fatty acid synthase (FAS), peroxisome proliferator-activated receptor-γ (PPARγ), sterol regulatory element-binding protein 2 (SREBP2), low-density lipoprotein receptor (LDLR), and hydroxymethylglutaryl-coenzyme A reductase (HMG-CoA). Furthermore, berberine treatment reversed the phosphorylation level of AMPK, which was suppressed by OLZ treatment (55). Few animal studies confirm berberine's effects on weight loss (10, 12). Daily berberine injections (5mg/kg-1 per day) in diabetic (db/db) mice for 4 weeks prevented weight gain and lipid accumulation in adipose tissue (12). Moreover, in the same study, berberine treatment increased energy expenditure and improved cold tolerance and brown adipose tissue activity.

Berberine increased the development of inguinal brown-like adipocytes, mitochondrial biogenesis, and expression of UCP1, PGC1α, and CIDEA in both brown and white adipose cells through AMPK-related mechanisms. Berberine treatment also inhibited hypothalamic AMPK activity and when AMPK is genetically activated in the hypothalamus, it still did not prevent berberine-induced weight loss and activation of thermogenesis (12).

These results imply that berberine induces thermogenesis most likely through activating the AMPK and PGC1 pathways (56). In another animal study, OLZ-induced rats were treated with berberine (380mg/kg/day) for 2 weeks, and OLZ-induced weight gain and white adipose tissue fat accumulation were significantly alleviated without decreasing the food intake (10). Gene expression analysis showed that OLZ-induced suppression of UCP1 expression was restored with berberine treatment (10). There are few clinical trials investigating berberine’s capacity to lose body weight.

Anti-Diabetic Activities

Numerous studies demonstrated that berberine is effective in treating type 2 diabetes mellitus and insulin resistance (57-60). In a cell study, berberine treatment (5 μg/mL) of 3T3-L1 cells and L6 myotubes stimulated AMPK activity in both increased GLUT4 translocation in L6 cells and decreased lipid accumulation in 3T3-L1 cells (61). Similarly, in another research, berberine treatment caused an increase in glucose consumption and phosphorylation of AMPK in 3T3-L1 cells (62).

Furthermore, when primary rat islets were isolated from male Sprague-Dawley rats treated with berberine (1, 3, 10, and 30 μmol/L), glucose-stimulated insulin secretion was increased dose-dependently. Hepatic nuclear factor 4 alpha (HNF4) expression on both mRNA and protein concentration as well as glucokinase activity were all elevated (63). These studies suggest that berberine may show an insulinotropic effect. In an animal study, streptozotocin (STZ)-induced diabetic mice were treated with 100mg/g/day berberine orally for 4 weeks and blood glucose levels were significantly lowered while plasma insulin levels were raised compared to the control group (57).

In a different study, berberine was given to diabetic rats, induced by STZ, at a dosage of 120 mg/kg/day for five weeks. This led to a significant increase in both plasma and intestinal levels of glucagon-like peptide-1 (GLP-1), plasma insulin levels, and the count of pancreatic beta cells (64). Additionally, when berberine was administered orally at a dose of 380 mg/kg/day to STZ-induced diabetic Sprague-Dawley rats, there was a notable reduction in fasting glucose levels. The levels of Phosphoenolpyruvate carboxykinase (PEPCK) and Glucose-6-phosphatase (G6Pase) saw a decrease in the liver, leading to diminished hepatic steatosis. Furthermore, the liver's expression of fatty acid synthase (FAS) was suppressed. Activity levels of several transcription factors, including Forkhead transcription factor O1 (FoxO1), sterol regulatory element-binding protein 1c (SREBP1), and carbohydrate responsive element-binding protein (ChREBP), were also lowered. These findings indicate that berberine positively impacts fasting blood glucose by directly suppressing gluconeogenesis in the liver (65).

Clinical studies show similar results. In a clinical trial, when berberine was administered (0.5g/3 times per day for 3 months) to individuals recently diagnosed with type 2 diabetes, plasma HbA1c, fasting blood glucose, and postprandial glucose levels were significantly reduced. When berberine was administered to type 2 diabetes patients with the poorly controlled disease, fasting blood glucose and HOMA-IR levels were dropped by 28.1 and 44.7%, respectively (66). In a different clinical trial, berberine (1g/day) was administered to 106 individuals with type 2 diabetes for three months, and similarly, fasting and postprandial plasma glucose levels and HbA1C

levels significantly reduced (54). According to these results, berberine may act as a hypoglycemic agent via the AMPK pathway or gluconeogenic pathway.

Anti-Hyperlipidemic Activities

Berberine seems to be promising for its anti-hyperlipidemic effects (67-69). In a study, HepG2 human hepatoma cells were treated with berberine in various concentrations (5, 10, and 15 μg/mL) and AMPK phosphorylation and AMPK activity were significantly increased. In comparison to the control group, there was a significant reduction in the production of lipids and triglycerides. (67).

Similarly, in another study HepG2 cells were treated with berberine (2.5, 5, 10, 15, and 25 μg/mL) and mRNA and protein cpncentration of proprotein convertase subtilisin/kexin type 9 (PCSK9) were significantly decreased in a dose-dependent manner. PCSK9 downregulates LDL receptor post-transcriptionally by detaching it from the cell surface and shuttling it to the lysosomes for degradation (68). Moreover, another study showed that berberine upregulates LDL receptor expression independent of sterol regulatory element binding protein (SREBP), but dependent on ERK activation (70).

In animal studies, berberine shows similar effects (67). In a study, high-fat diet fed male Syrian golden hamsters were treated with berberine (100mg/kg/day, orally) twice a day for 10 days and plasma LDL cholesterol and liver fat storage were significantly reduced (67). Furthermore, in another study, treatment of hyperlipidemic hamsters with berberine (50 mg/kg or 100 mg/kg twice a day) for 10 days decreased serum cholesterol by 40% and LDL cholesterol by 42% (70).

Another study suggested that berberine may be involved in upregulating the reverse cholesterol transport. When dyslipidemic hamsters were treated with CETP inhibitor torcetrapib, introducing berberine significantly stimulated reverse cholesterol transport (71). In a clinical trial, patients with type 2 diabetes and hyperlipidemia were treated with berberine (1.0g/day) for 3 months and plasma TG, total cholesterol, and LDL cholesterol levels were significantly decreased compared to the placebo group (54).

Similarly, in another study, when patients with type 2 diabetes treated with berberine (0.5g/day) for 3 months, plasma TG and total cholesterol levels were

significantly decreased however, there was no change in LDL cholesterol levels (66). A meta-analysis reviewing randomized controlled trials, demonstrated an average decrease in total cholesterol of 0.61 mmol/L, in TGs of 0.50 mmol/L, and in LDL cholesterol of 0.65 mmol/L, and an average increase in HDL cholesterol of 0.05 mmol/L (69). In a study with hypercholesterolemic patients, berberine administration (0.5g/twice a day) for 3 months reduced serum cholesterol by 29%, TGs by 35%, and LDL cholesterol by 25% (70).

These data suggest that berberine stimulates AMPK phosphorylation and activity and subsequently leads to an increase in fatty acid oxidation and a decrease in fatty acid and TG synthesis. Berberine seems to be effective as an anti-glycemic and anti-hyperlipidemic agent via various metabolic pathways. Although its effects on weight loss and hypertension seem to be more inconclusive, berberine may be an effective supplementation for metabolic syndrome patients. To better understand its effects, long-term clinical trials are needed.

2.1.3. Safety and Toxicity

According to a meta-analysis, type 2 diabetes, hyperlipidemia, and hypertension were all treated with berberine without any major side effects (58). Generally, animal research with berberine has revealed relatively little toxicity and adverse effects (72). In humans, more clinical studies assessed the safety of berberine reported only modest gastrointestinal reactions, including constipation and diarrhea (54, 60, 73). In a cohort study, berberine demonstrated safe, without any clinical deterioration or impact on creatinine level and liver function (74).

2.2. Delphinidin

Delphinidin (2-(3, 4, 5-trihydroxyphenyl) chromenylium-3, 5, 7-triol) is a polyphenolic ring structure based on diphenylpropane (Figure 2.2) (75). It is one of the most valuable polyphenol anthocyanidin classes, a subfamily of flavonoids, that includes different varieties as follows: cyanidin, delphinidin, pelargonidin, malvidin, peonidin, and petunidin (76). Many delphinidin-derived glycosides are known, and their stability and bioavailability vary according to their structure (77).

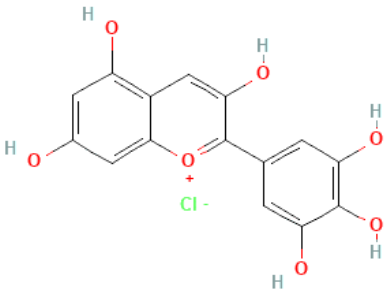

Figure 2.2. The chemical structure of delphinidin (78)

Delphinidin is found in a wide variety of brightly colored fruits and vegetables such as grapes, berries, black grapes, pomegranates, carrots, sweet potatoes, tomatoes, and pigmented cabbages (79, 80). According to studies conducted in recent years, delphinidin had anti-inflammatory, anti-angiogenic, anti-mutagenic, anti-cancer, anti-adipogenesis, anti-microbial, neuroprotective, hepatoprotective, and antioxidant properties (14-24).

2.2.1. Pharmacokinetic Properties

Administering 500 mg of 13C-isotope labeled cyanidin-3-glucoside to eight healthy participants enabled the tracking of its absorption, metabolism, and elimination through the analysis of 13C in blood, breath, urine, and feces. It was possible to detect metabolites up to 48 hours after consumption, with the estimated relative bioavailability being 12.4±1.4% (81).

The absorption of anthocyanins can take place both in the stomach and the intestines (82). The swift bioavailability noted in anthocyanins ingested orally suggests the involvement of a gastric transport mechanism like bilitranslocase, a carrier for organic anions, in the uptake of glycosylated anthocyanidins in their complete form (83). Anthocyanins are detectable in plasma in their unaltered state (84). Aglycones are found in plasma but are characterized by a short half-life due to their instability and likelihood of breaking down. It has been suggested that besides bilitranslocase, additional active transport systems might be involved in the uptake of whole anthocyanins in both the stomach and small intestine. Research utilizing rat jejunum in chamber assays has indicated that delphinidin aglycon can affect the sodium-glucose co-transporter 1 (SGLT-1), resulting in the inhibition of glucose

transportation. Although the levels of anthocyanins in the bloodstream may seem low, further investigation is needed to explore how delphinidin anthocyanins are distributed within various tissues. The specific glycosylation pattern of delphinidin could identify the main cellular targets. Numerous studies have established the presence of anthocyanins in different brain areas of pigs and rats, including the cortex, cerebellum, hippocampus, and striatum (85-87).

Peak levels of delphinidin were detected 2 hours post-consumption, whereas the glucuronide conjugates of delphinidin (phase II metabolites) were identified 6.3 hours afterward (88). The presence of intact delphinidin glycosides in the body is evidenced by the detection of delphinidin-3-sambubioside in the urine of healthy individuals (89).

The challenges of low bioavailability, instability at physiological pH levels, and delphinidin's high reactivity present significant hurdles for researchers. Efforts to enhance delphinidin's bioavailability have been pursued, aiming to utilize this natural plant pigment in dietary supplements and nutraceuticals within the food and pharmaceutical sectors. Strategies to increase its solubility, stability, and bioavailability have included microencapsulation using natural polymers, the creation of multiple emulsions, and the development of nano-formulations (27, 90, 91).

2.2.2. Therapeutic Effect of Delphinidin

Anti-Obesity Activities

Recent studies reported that delphinidin may be protective against obesity-related conditions such as oxidative stress, inflammation, insulin resistance, and steatosis by altering redox signaling in mice fed a high-fat diet (92, 93). In an animal study, Maqui berry supplementation with high amounts of delphinidin as an anthocyanin was shown to improve insulin response and reduce weight gain (94).

In another study, maqui berry improved insulin response and reduced weight gain in animals (95). Furthermore, delphinidin differentiation in subcutaneous white adipose tissue thermogenesis, multicellular lipid droplet formation, and gene expression are involved in de novo lipogenesis. In addition, delphinidin altered gene expression involved in subcutaneous white adipose cells thermogenesis, multicellular lipid droplet formation, and de novo lipogenesis. These changes are associated with

increased expression of carbohydrate response element binding protein b (Chrebpb) and sterol regulatory element binding protein 1c (Srebplc) and improved cellular repressor of adenovirus early region 1A-induced gene (Creg1) and fibroblast growth factor 21 (FGF21) signaling. In conclusion, supplementation of Maqui berry in the diet-induced thermogenesis of the brown-like phenotype in subcutaneous beige or white adipose cells (94).

A recent study elucidated the inhibitory effects of delphinidin on 3T3-L1 preadipocyte differentiation (96). Delphinidin has proven to be effective in reducing the buildup of lipids inside cells and enhancing the breakdown of fats, by influencing the regulation of genes and transcription factors involved in fat production. Its ability to decrease lipid levels is primarily due to its impact on the initial phase of fat cell development, which involves slowing down cell division by causing a delay in the G1 phase of the cell cycle.

It has also been observed that delphinidin inhibits the activity of early-stage fat development transcription factors such as C/EBPβ and C/EBPδ, along with intermediate markers like C/EBPα, PPARγ, and specific markers of fat cells including adiponectin and aP2 (FABP4). Moreover, treatment with delphinidin leads to the activation of Wnt1, Wnt10b, and the Wnt receptor Fzd2, as well as the Lrp5/6 co-receptors, while it deactivates Gsk3, a key component of the complex responsible for β-catenin breakdown.

In conclusion, delphinidin may inhibit adipogenesis by stabilization of β-catenin and activation of Wnt signaling during early differentiation of 3T3-L1 through inhibition of its degradative complexes. This is promising for the prevention of metabolic diseases, also of obesity (96). In similar studies, it has been reported that black soybean anthocyanins, which mainly contain delphinidin (25), and a delphinidin-3-O-β glycoside (derived from delphinidin) (26) may have beneficial effects on obesity by inhibiting adipocyte differentiation, stimulating basal lipolysis, and reducing adipogenesis.

Delphinidin exhibited a reduction of viability, proliferation, and differentiation of 3T3-L1 cells by reducing the expression of PPARγ (25). Wu et al. reported that supplementation of C57BL/6 mice with blueberry and mulberry juice containing delphinidin as the major anthocyanin for 12 weeks, inhibited weight gain, reduced

serum cholesterol levels, insulin resistance, leptin levels, and lipid accumulation, and thus may prevent obesity (97).

Anti-Diabetic Activities

Anthocyanins may control blood glucose levels and carbohydrate metabolism, as well as lower cardiovascular risk factors (98). Glucagon-like peptide-1 (GLP-1) secretion is increased by delphinidin in GLUTag cells via the Ca2+/calmodulin-dependent Ca2+-CaMKII pathway. Three hydroxyl groups or two methoxyl moieties in the aromatic ring of delphinidin are said to be essential for increasing GLP-1 secretion (99).

The findings indicate that delphinidin, in its liposomal form, could be developed into an effective approach for managing diabetes. In male BALB/c mice with diabetes induced by Streptozotocin (STZ), treatment with delphinidin at a concentration of 100 mg/mL, both in its free and liposomal forms, was conducted over 8 weeks (100). Additionally, in rats with STZ-induced diabetes, the oral administration of black currant extract (containing 1 mg of delphinidin per kg) at a dose of 5 mg/kg led to reduced blood glucose levels at both 30- and 60-minute marks, an increase in serum insulin levels, and a boost in GLP-1 levels at 15- and 30-minute marks after an intraperitoneal glucose injection (2 g/kg).

Furthermore, type-2 diabetic male kk-Ay mice, when given delphinidin-rich black currant extract alongside a high-sucrose diet for 2 to 7 weeks, experienced a notable reduction in serum glucose levels and an enhancement in basal GLP-1 levels. This improvement is attributed to the upregulated mRNA and protein expression of PC1/3 in the ileum (101).

According to clinical interventional studies, a high dosage of anthocyanins may be used to prevent and treat type 2 diabetes (102). Delphinidin increased AMPK alpha phosphorylation to protect pancreatic beta cells from damage caused by high glucose levels, and it also promoted cell glucose absorption. (103).

Delphinol R, a product that contains 35% total anthocyanins and 25% delphinidin, was able to reduce postprandial glucose and insulin in a clinical trial.

Delphinidin led to reductions in insulin levels and fasting blood sugar in a manner that depended on the dose. Furthermore, it brought about betterment in blood

sugar levels when given to individuals with pre-diabetes (102). In a clinical study, delphinidin-rich maqui berry extract Delphinol® (≥25% delphinidin anthocyanin) supplementation significantly inhibited postprandial blood glucose increase, after carbohydrate challenge (95).

Anti-Hyperlipidemic Activities

Delphinidin supplementation has been reported to stimulate lipolysis and inhibit adipogenesis by regulating the expression of adipogenic transcription factors and target genes and effectively reducing intracellular lipid accumulation.

Delphinidin was observed to reduce the levels of PPAR, C/EBP, SREBP1, and FAS while increasing the phosphorylation of AMPK and acetyl-CoA carboxylase (ACC). This action leads to a decrease in lipid concentrations and small fat droplets, diminishes fat cell development, and boosts fat metabolism (26).

The promotion of lipid accumulation brought on by palmitic acid (PA) has been connected to SWI/SNF related matrix-associated actin-dependent regulator of chromatin subfamily B member (SMARCD1) inhibition. By restoring SMARCD1 expression in hepatocytes, delphinidin exhibits inhibitory effects on lipid accumulation and cell senescence brought on by PA (104).

Delphinidin significantly reduces the accumulation of TGs in HepG2 cells and lowers the expression of CPT1A, SREBF1, and fatty acid synthase (FASN) without changing the activity of AMPK, (21). Human umbilical vein endothelial cells (HUVECs) were exposed to delphinidin's protective effects against oxidized low-density lipoprotein (oxLDL)-induced cellular damage. In a concentration-dependent manner, delphinidin was shown to significantly repair the oxLDL-induced viability loss in HUVECs (105).

2.2.3. Safety and Toxicity

However, the volume of *in vitro*, *in vivo*, and human research completed to date is minimal; therefore, it's premature to assert that consuming foods high in delphinidin or supplementing with delphinidin invariably leads to health benefits. With only a handful of studies conducted so far, further in-depth research on both animals and humans is essential to ascertain the health safety of delphinidin intake. Moreover,

investigating how delphinidin might interact with drugs when administered concurrently, particularly at elevated doses, is imperative. Additional research is needed to thoroughly comprehend the metabolic processes involving delphinidin and to resolve any potential safety issues.

2.3. Naringenin

Naringenin, 5,7-dihydroxy-2- (4-hydroxyphenyl) -2,3-dihydrochromen- 4-one is a flavonoid, specifically a flavanone (9). Naringenin is colorless and flavorless and its molecular weight is 272.26 g/mol (Figure 2.3).

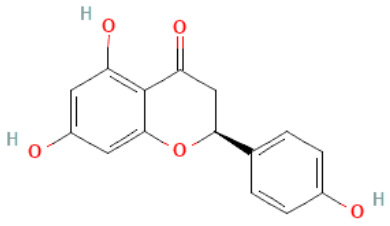

Figure 2.3. The chemical structure of naringenin (106)

The main sources of naringenin are citrus fruits and juices such as oranges, grapefruits, and bergamots (107). Naringenin has several notable pharmacological properties, e.g., antioxidant, anti-cancer, anti-inflammatory, anti-obesity, antimicrobial, and anti-diabetic in animal models and humans (6, 8, 108-111).

2.3.1. Pharmacokinetic Properties

Recently, the bioavailability and pharmacokinetic properties of naringenin have been thoroughly studied (108, 112). To summarize, naringin exhibits low absorption in the human body via the gastrointestinal tract. It is typically transformed into its aglycone form, naringenin, by oral cavity enzymes, epithelial cells of the small intestine, and intestinal microbes.

Naringenin has a 15% oral bioavailability, and due to its poor solubility, a small amount is absorbed in the human gastrointestinal tract (113). Naringenin is distributed in the gastrointestinal tract, trachea, lungs, kidney, and liver (114). Naringenin undergoes phase I (demethylation or oxidation by cytochrome P450 monooxygenases)

and phase II (sulfation, glucuronidation, or methylation) metabolism in the intestine and hepatic cells (108).

The primary method of excretion is through urine, while some metabolites are also present in the feces. The therapeutic potential of naringenin is severely limited by its limited oral bioavailability. One of the recommended strategies to solve this problem is the use of nano-formulations (28, 115).

2.3.2. Therapeutic Effect of Naringenin

Anti-Obesity Activities

One of the more important therapeutic effects of naringenin is its anti-obesity activity. The proliferation of 3T3-L1 pre-adipocytes was significantly reduced in a dose-dependent manner after 48 hours of naringenin (5-100 μM) treatment (116). This did not affect adipogenesis gene expression (STAT3 and PPAR-γ) or TG accumulation during adipocyte differentiation (116).

Insulin resistance is linked to increased levels of the pro-inflammatory cytokine tumor necrosis factor-alpha (TNF-α). Naringenin (100 μM) treatment of 3T3-L1 adipocytes for 30 min significantly decreased the TNF-induced FFA secretion. Naringenin treatment increased the levels of the cytosolic nuclear factor of kappa light polypeptide gene enhancer in B-cell inhibitor, alpha (IκB-α), and reduced the levels of protein extracellular signal-regulated kinases (p-ERK) (117). Administration of naringenin (20 μM) markedly reduced both insulin-induced glucose uptake and the insulin-triggered translocation of GLUT4 in 3T3-L1 adipocytes as well as in mature human fat cells (118).

Inflammation of adipose tissue caused by obesity is mediated by toll-like receptors (TLRs), also plays a role in insulin resistance and type 2 diabetes mellitus (T2DM). Naringenin (10-100 μM) treatment in 3T3-L1 differentiating adipocytes significantly reduced TLR2 expression in a dose-dependent manner. In addition, inflammatory mediators, such as monocyte chemoattractant protein (MCP)-1 levels and TNF-α, significantly decreased (119). Moreover, naringenin reduced the expression of TLR2 in adipocytes that was stimulated by TNF-α and by macrophage co-culture. Naringenin's suppression of NF-κB and JNK signaling was connected to these effects (119).

Treatment of 3T3-L1 differentiating and differentiated adipocytes with naringenin (25 μM) led to reduced mature adipocyte function and suppression of adipogenesis (120). After naringenin was administered to immature 3T3-L1 cells (0-120 h), lipid accumulation was inhibited. Furthermore, the protein expression of aP2, PPAR, adiponectin, and signal transducer and activator of transcription 5A (STAT5A), all adipogenesis-related, was reduced. Naringenin administration prevented insulin-induced glucose uptake in mature differentiated 3T3-L1 adipocytes, decreased tyrosine phosphorylation of insulin receptor substrate-1 (IRS-1), and decreased levels of adiponectin, indicating induction of insulin resistance (120).

The ability of naringenin to inhibit insulin activity in adipocytes *in vitro* raises the risk of a negative effect on glucose homeostasis in humans (118, 120). In a recent study, treatment with naringenin (8 μM) for 7 to 14 days increased thermogenesis in human white adipocytes (121). The rate of oxygen consumption was higher at rest, at maximum, and in reserve, all of which were adenosine triphosphate (ATP)-linked.

Adipose TG lipase (ATGL), adiponectin, CREBpβ, PGC-1α, and PGC-1β, which are all involved in fat oxidation, were all increased by naringenin therapy. According to this study, naringenin increased human adipocytes' thermogenesis, energy expenditure, and insulin sensitivity (121). Naringenin treatment decreases adipocyte growth, suggesting that adipocytes may have anti-inflammatory effects and may induce the browning of adipose cells (119). However, more research is needed to fully understand how naringenin affects adipose tissue.

Anti-Diabetic Activities

Naringenin has been thoroughly researched for its potential to combat diabetes. This involves several mechanisms, such as enhancing glucose uptake in the body's periphery, reducing glucose production in the liver, influencing insulin sensitivity and secretion, decreasing glucose absorption in the intestines, affecting glucose transporters, and interacting with PPARγ (120, 122-124).

Naringenin has been demonstrated to prevent the development of metabolic syndrome by upregulating PPARα through the action of AMPK. Furthermore, naringenin has been shown to inhibit SGLT1 and hence impairs glucose uptake (125, 126), and also inhibits intestinal α-glucosidase activity *in vivo* thereby delaying the

absorption of carbohydrates (127). Therefore, these results suggested that naringenin reduces postprandial glucose incursion comparable with metformin. In many *in vitro* studies, naringenin lowered the absorption of D-glucose by inhibiting a renal and intestinal Na+-glucose co-transporter (128).

N (10–150 μM) stimulated the absorption of glucose in skeletal muscle by activating the AMK pathway (129).

In a different study, naringenin (6-100 μM) was discovered to be important for regulating hyperglycemia because it decreased the generation of hepatic glucose and suppressed the level of cellular adenosine triphosphate. (130). Moreover, naringenin inhibited the hepatic gluconeogenic pathway and caused diabetes mellitus, like metformin (131). Through the activation of the PI3K pathway, naringenin (50 μM) was able to counteract the pancreatic β-cell damage brought on by cytokine-mediated apoptosis and promoted cell survival (132).

Rats with diabetes induced by streptozotocin and fed a high-fat diet received naringenin treatment. It (25 mg/kg) demonstrated a potent α-glucosidase inhibitory activity by competitive inhibition with oligosaccharide residues and α-limited dextrin for the binding site. Furthermore, naringenin regulated the expression of TNF-α and GLUT4, these had hypoglycemic action and insulin-sensitizing (127).

Naringenin treatment (50 mg/ kg) in Streptozotocin (STZ)-Nicotinamide rat model decreased the hyperglycemia and also TG levels (133). This effect was not achieved through the inhibition of alpha-glucosidase activity but rather through the reduction of carbohydrate uptake from the gastrointestinal tract. In a different study, naringenin at a dosage of 50 mg/kg showed antihyperglycemic properties by lowering fasting glycosylated hemoglobin and blood glucose levels, while elevating insulin levels (134). At this dosage, naringenin was effective in managing insulin resistance and metabolic syndrome.

n a scenario where a high fructose diet was the cause, the beneficial outcomes could be attributed to its ability to improve tyrosine phosphorylation, enhance insulin sensitivity, and reduce nitro oxidative stress. (135). Furthermore, the administration of naringenin at 25 and 50 mg/kg/day led to a reduction in changes to serum glucose, insulin, and pro-inflammatory cytokines like IL-6, IL-1beta, and TNF-alpha that are associated with diabetes (136).

Anti-Hyperlipidemic Activities

The ability of naringenin to decrease lipid levels have been studied (137, 138) and there are some mechanisms of action. One of the mechanisms involved the suppression of cholesterol production by targeting two key enzymes: 3-hydroxy 3-methylglutaryl-CoA (HMG-CoA) reductase and acyl-CoA: cholesterol acyltransferase (ACAT). Additionally, there was an enhancement in the breakdown of fatty acids through the activation of several pathways including adipose triglyceride lipase (ATGL), uncoupling protein 1 (UCP1), and peroxisome proliferator-activated receptors alpha and gamma (PPARα and PPARγ).

In experiments with human liver cells (HepG2) treated with cholesterol, naringenin was observed to increase both the mRNA and protein levels of the LDL receptor (LDLR) in a concentration-dependent manner (ranging from 12.5 to 50 μM). This increase in LDLR was also accompanied by a rise in the mRNA and protein levels of sterol regulatory element-binding protein 2 (SREBP-2) (139). Furthermore, naringenin significantly increased the mRNA and protein expression of hepatic CYP7A1, an enzyme that produces bile acids from cholesterol through PPARγ activation, indicating a higher liver clearance of cholesterol (139).

Naringenin has been demonstrated to be helpful in preventing obesity-related dyslipidemia by lowering blood levels of triglyceride (TG), total cholesterol (TC), and LDL-C (140, 141). This is as a result of increased fatty acid oxidation and decreased TG accumulation in hepatocytes and adipocytes. (122).

In male C57BL/6J mice made obese through a high-fat diet, administering naringenin orally via gavage at doses of 25, 50, and 100 mg/kg/day for 8 weeks led to a reduction in body and liver weights, as well as decreases in plasma LDL cholesterol, liver triglycerides, and total liver cholesterol levels, all in a manner that correlated with the dose (142). In addition, proprotein convertase subtilisin/kexin type 9 (Pcsk9) mRNA expression was discovered to be downregulated in the liver, although Ldlr protein concentration and phospho-AMPK alpha (p-AMPK α) protein concentration were found to be upregulated.

PCSK9, which is mostly produced by hepatocytes, reduces the amount of LDL receptors on the membrane by binding to it and activating lysosomal degradation.

(143). Due to naringenin's ability to suppress Pcsk9 mRNA expression, plasma LDL-C levels may be decreased by boosting hepatic LDLR concentration (142).

In a recent study involving humans, individuals with class 1 obesity and high cholesterol were given a daily oral dose of N (450 mg) for 90 days. This treatment led to a decrease in body weight and lowered levels of plasma triglycerides, total cholesterol, and LDL cholesterol (144).

In a human study, obese patients with hypercholesterolemia received daily oral naringenin (450 mg) for 90 days, that decreased body weight and plasma TG, TC, and LDL-C levels.

2.3.3. Safety and Toxicity

Few studies examined the adverse effects of naringenin in its pure form or in foods on humans. According to a study, naringenin’s inhibitory actions on cytochrome P450 enzymes cause grapefruit juice to either inhibit or raise the concentration of medications that are processed in the liver, which can change pharmacokinetics and cause toxicity (51).

A randomized, placebo-controlled, single-ascending-dosage clinical research was conducted to examine the side effects of naringenin based on a dose of 135 mg (145). This study involved 18 participants and found no negative impacts or alterations in certain markers indicating liver and kidney health, including levels of blood creatinine, urea nitrogen, potassium, and albumin, even when the naringenin dosage was increased from 150 mg to 900 mg. This naringenin was extracted from whole oranges (Citrus sinensis), which were comprised of 28% naringenin (146).

Despite these findings, it's suggested that further research with larger groups of participants is necessary to fully assure the safety of naringenin extracted from Citrus sinensis. This call for further study comes in the light of another research, which showed that pure naringenin at a concentration of 8 μM could enhance the expression of genes related to heat production and increase energy use in human fat cells (121).

Following this, another study aimed to identify the precise naringenin dosage needed to achieve a concentration of 8 μM in the bloodstream. The results indicated that consuming 300 mg of naringenin extracted from Citrus sinensis twice a day was effective in reaching the desired blood concentration, showing positive effects in

human subjects (146). In conclusion, according to a recent study, naringenin is a relatively safe and nontoxic bioactive compound (147).

Table 2.1. Chemical and physical properties of berberine, naringenin and delphinidin (34) (106) (78)

	Berberine	**Naringenin**	**Delphinidin**
Molecular Formula	$C_{20}H_{18}NO_4^+$	$C_{15}H_{12}O_5$	$C_{15}H_{11}ClO_7$
Molecular Weight	336.4 g/mol	272.25 g/mol	338.69 g/mol
XLogP3-AA	3.6	2.4	3.0
Physical Description	Yellow solid	White to light yellow solid	Purple, oily liquid
Melting Point	145°C	251°C	350 °C
Solvent	Methanol	Ethanol	Methanol
pH	7.0	7.0	7.4

2.4. Adipose Tissue

Adipose tissue is a heterogeneous endocrine organ consisting of white adipose tissue (WAT), brown adipose tissue (BAT), and beige adipose tissue (148) (Table 2.2). Different types of adipose tissue have characteristics determined by their origin, anatomical distribution, and metabolic functions (149). Brown adipocytes develop from myf5 positive (myf5+) precursors, similar in origin to muscle cells, whereas white and beige adipocytes develop from myf5 negative (myf5-) precursors (150).

WAT is composed of white adipocytes containing a large lipid droplet covering 85-90% of its cytoplasm (151). It functions as an active endocrine organ that regulates various activities such as insulin sensitivity (152). Its main function is to store excess energy intake in the form of TGs (lipogenesis), but it also provides energy substrate to tissues by hydrolyzing TGs to fatty acids and glycerol (lipolysis) in cases of prolonged fasting or high energy demand (153).

Brown adipose tissue consists of brown adipocytes, which are smaller and contain numerous lipid droplets (154). The most important feature of brown adipocytes that distinguishes them from white adipocytes is the presence of a large number of mitochondria containing uncoupled protein-1 (UCP1). This contributes to energy expenditure as a result of increased basal metabolic rate by mediating non-shivering

thermogenesis. (154). In thermogenesis due to shivering, heat generation occurs as a result of increased muscle activity due to exposure to cold (155). BAT development begins in the intrauterine period. It is an important organ for thermoregulation at birth and in early childhood. BAT rate decreases with age due to the increase in body surface area. Positron emission tomography/computed tomography (PET/CT) showed that BAT activation is also present in adult humans. Therefore, it is thought that increasing BAT activity may be an effective method in the treatment of obesity (156).

Beige adipose tissue is the third type of adipose tissue that has recently been identified to have different characteristics from WAT and BAT (157). Beige adipocytes in WAT contain large lipid droplets and phenotypically look similar to white adipocytes (11). Beige adipocytes, which do not express UCP1 under basal conditions, show BAT-like activity with UCP1 expression when stimulated by cold exposure, (11, 158), β3-adrenergic receptor activators (158, 159), or some dietary factors (11, 160). Stimulation of beige adipose tissue, which is phenotypically similar to WAT, to show BAT-like activity is defined as "browning of white adipose tissue" and is more likely to happen in the adipose tissue beneath the skin (161, 162).

Changes in circulating adipokines with the increase in white adipose tissue and reduces in BAT activity, which is important for thermogenesis and increased energy expenditure, play a role in the pathogenesis of obesity.

It has been recently studied that the browning of white adipose tissue may be effective in weight loss by demonstrating the presence of functional BAT in adult humans (163, 164). Therefore, the browning of adipose tissue may be used in the treatment of obesity (162, 165).

Table 2.2. Comparison between white, brown, and beige adipose tissue (166)

Data	WAT	BAT	Beige
Origin	Myf5- cells	Myf5+ cells	Myf5- cells (differentiation or trans differentiation)
Function	Energy storage and endocrine tissue	Thermogenesis and endocrine tissue	Adaptive thermogenesis (under stimuli)
Phenotype	White-fat phenotype	Brown-fat phenotype	White-fat phenotype that acquires a brown-fat phenotype under stimuli
Mitochondria	Low	Abundant	Present (upon stimulation)
UCP1 expression	Absent	Present	Present (under stimuli)
Protein markers	Lipoprotein lipase, leptin, adiponectin	PGC1α, PRDM16	CD137, PRDM16, Tmem26

The maturation of preadipose cells into adipose cells is called adipogenesis. The process of adipogenesis is regulated by some transcription factors. Adipocytes begin their life cycle as mesenchymal stem cells. Differentiation from mesenchymal stem cells to adipocytes occurs with the expression of some transcription regulator proteins. During the initial phases of adipogenesis, hormonal signals trigger the activation of CCAAT/enhancer-binding protein (C/EBP)- β and C/EBP-γ genes. Following this activation, peroxisome proliferator-activated receptor γ (PPARγ), a regulatory factor C/EBP-α, adiponectin, and fatty acid binding protein 4 (FABP4) genes become active, contributing to the concluding stages of adipocyte formation (167, 168). Unlike white fat cells, brown fat cells originate from Myf5-negative cells, which means they have a common precursor with muscle cellsPRDM16 is a determinant transcription factor in brown adipose tissue formation. Increased PRDM16 expression leads to both the formation of new brown adipocytes and the browning of white adipocytes (169). PRDM16 stimulates PPARγ co-activator-1α (PGC-1α) and browning genes. With this activation, new brown adipocytes form in brown adipose tissue and the volume of brown adipose tissue increases.

In white adipose tissue, mesenchymal stem cells are stimulated via PRDM16 and PGC-1α and the cells transform into beige preadipocytes instead of white (170). PGC-1α increases mitochondrial biogenesis by stimulating UCP1 protein expression

in both brown and beige adipocytes. Beige adipocytes can be formed directly from mesenchymal stem cells by PRDM16 induction or by differentiation of white adipocytes (171). This phenomenon is also referred to as browning (172).

Recent studies propose that inducing the browning of WAT and enhancing the activity of BAT represent a fresh and promising strategy for managing obesity. This approach aims to boost energy expenditure by promoting thermogenesis (173, 174). *In vitro* and *in vivo* studies have demonstrated that certain elements and bioactive constituents found in food may contribute to these effects (156, 175, 176).

Beige fat cells originate from mesenchymal stem cells ($Myf5^{-}$) and share similarities with white fat cells, whereas brown fat cells originate from $Myf5^{+}$ precursor cells and are closely linked to muscle lineage (150).

2.5. Nanoencapsulated Phytochemicals in Combating Obesity

Phytochemicals are naturally occurring compounds found in plants, offering numerous health benefits, including antioxidant, anti-inflammatory, and anticarcinogenic properties (177). Due to their chemical instability, break down quickly when exposed to environmental factors like oxygen, temperature, light, or pH.

These factors limit the development of phytochemicals as dietary components and their integration into foods. This instability poses a significant challenge to harness these compounds' health benefits. Due to their diverse biological functions for disease prevention and health promotion, phytochemicals received a lot of attention in the pharmaceutical sector. Their potential in preventing chronic diseases such as cancer, cardiovascular diseases, and diabetes has been recognized (178).

However, because of the low water solubility and high vulnerability to degradation of phytochemicals, their use in food has been limited. Studies demonstrated that the methods of micro- and nanoencapsulation may significantly improve the stability, characteristics, and bioavailability of phytochemicals (179). This technology involves wrapping the phytochemicals in a protective coating to shield them from environmental stressors, thereby enhancing their stability and absorption in the human body (180).

The key factors to determine nanoparticles' stability, bioavailability, biodistribution, and metabolism are the following: nanoparticle size, polydispersity

index (size homogeneity), zeta potential (surface charge), chemical and physical stability, loading capacity, and encapsulation efficiency (181).

Encapsulation technologies hold the promise of overcoming the inherent challenges associated with phytochemicals, making it possible to incorporate these beneficial compounds into a wider range of food products and pharmaceutical applications. To develop nanoparticles for diagnosing and treating diseases like cancer, scientists have explored a wide range of organic and inorganic materials to create various structures and functions.

However, when addressing chronic conditions such as obesity, nanoparticles should be made from materials that are compatible with the body, break down naturally, and have minimal side effects. This requirement ensures that the developed nanoparticles can be safely used in long-term applications without adverse effects on human health. Therefore, nanoparticles must be synthesized from biocompatible and biodegradable materials.

These nanoparticles demonstrate significantly differential absorption efficiency in the increased adipose tissue over other tissues. Additionally, nanoparticles can improve the absorption of phytochemicals into cells in adipose tissue and prevent them from interacting with the body's biological environment too early (31). This delivery system can potentially lead to more effective treatments for obesity and various metabolic disorders, making phytochemicals a powerful tool in the fight against chronic diseases.

Nanoencapsulation

Nanotechnology is the manipulation, production, and use of materials with at least one dimension less than 100 nm (179, 182). The potential of nanotechnology has been investigated in various nutrition areas, this includes the creation of novel functional foods and beverages, enhancing nutrient delivery systems, designing nano tracers to ensure food safety and security, and progressing food preservation techniques (183, 184).

Encapsulation, which permits the creation of fresh delivery systems for bioactive substances, is another major effect of nanotechnology. New functional foods

and beverages were eventually developed as a result of the encapsulation's increased water solubility, stability, functionality, and bioavailability (185).

Nanoparticles, nanoemulsions, nanoliposomes, nanofibers, and materials exhibiting nanostructures represent just a handful of the diverse range of nanoencapsulation methods that have been innovated.

Liposome

A lipid vesicle with a spherical shape, composed of one or multiple lipid bilayers, is referred to as a liposome. These structures are formed utilizing phospholipids (for example, phosphatidylcholine), which consist of hydrophilic head and hydrophobic tail groups. In an aqueous solution, the head and tails self-organize into the typical lipid bilayer structure. As a result of the inclusion of both lipid and aqueous phases in their structure, liposomes have a special structural property that allows them to entrap hydrophilic, lipophilic, and amphiphilic molecules. (186, 187).

Some of the typical liposome production techniques include sonication, extrusion, micro-emulsification, freeze-thawing, and micro-fluidization (188-190). The liposome may be produced in various forms, such as small unilamellar liposome vesicles, large unilamellar vesicles, and multilamellar vesicles, with sizes ranging from the nanoscale to microscale, thanks to its composition flexibility and a variety of production methods. Given that a liposome consists of a lipid bilayer encapsulating an aqueous solution, hydrophilic substances can be dissolved in the inner core but struggle to cross the bilayer unless it merges with other bilayers, such as those of a cell membrane. In such instances, the hydrophilic solute is then transported into the cell.

Moreover, hydrophobic substances can be securely carried by incorporating them into the liposome's lipid bilayer. Liposomes have been utilized as carriers for both nutrients and pharmaceuticals, thanks to their carrying capacity and biological safety. Additionally, the liposome's size and structure are influenced by the method used in its preparation. (191).

Liposomes have been used to encapsulate a variety of food ingredients, including flavor enhancers, essential oils, amino acids, vitamins, minerals, coloring agents, enzymes, antioxidants, antimicrobial compounds, phytochemicals, and omega-3 fatty acids (192).

Numerous liposomal formulations have received FDA approval, such as Doxil for ovarian cancer treatment, DaunoXome for advanced HIV-related Kaposi's sarcoma, and Amphotec for combating fungal infections. Liposomes serve as effective carriers for delivering phytochemicals in the battle against chronic diseases like obesity, owing to their ability to encapsulate both water-soluble and fat-soluble substances, along with their compatibility with biological systems. While trans-resveratrol, curcumin, and quercetin could potentially be embedded within the non-polar region of their phospholipid tails, hydrophilic phytochemicals such as EGCG have the capability to be enclosed within the aqueous core of liposomes (193).

The stability, ability to dissolve in water, absorption into the body, and effectiveness against obesity of these plant-derived compounds will all be improved by liposomal encapsulation (194-196).

Another significant feature of liposomes is the ability to combine many phytochemicals with complementary effects into a single vesicle. To optimize the targeted distribution of phytochemicals to particular cells with increased therapeutic efficiency, target ligands can be further conjugated to the surface of liposomes (197).

In order to combat obesity and associated comorbidities, liposome administration of phytochemicals is a very promising method.

3. METHODOLOGY

3.1. Time and Location of Research

This research was carried out between September 2019 and November 2022 at Hacettepe University, Department of Nutrition and Dietetics and Faculty of Pharmacy, Research Laboratories. In this study, 3T3-L1 preadipocyte cells supplied by ATCC company were used (ATCC®CL-173TM, USA). With the decision numbered 52338575-121 on 23.10.2019, an ethics committee was not required from the Hacettepe University Animal Experiments Local Ethics Committee Commission (Appendix 1). The reason was that the cell line was purchased from a supplier and no live vertebrate animals were used for this purpose.

3.2. Research Design

The research design is summarized in Figure 3.1. The application of liposomal and free forms were divided into the following groups: free naringenin (20 μM, 10 μM, and 5 μM), liposomal naringenin (20 μM, 10 μM, and 5 μM), free berberine (20 μM, 10 μM, and 5 μM), liposomal berberine (20 μM, 10 μM, and 5 μM), free delphinidin (20 μM, 10 μM, and 5 μM), along with a void and a control group. There were two samples for each group.

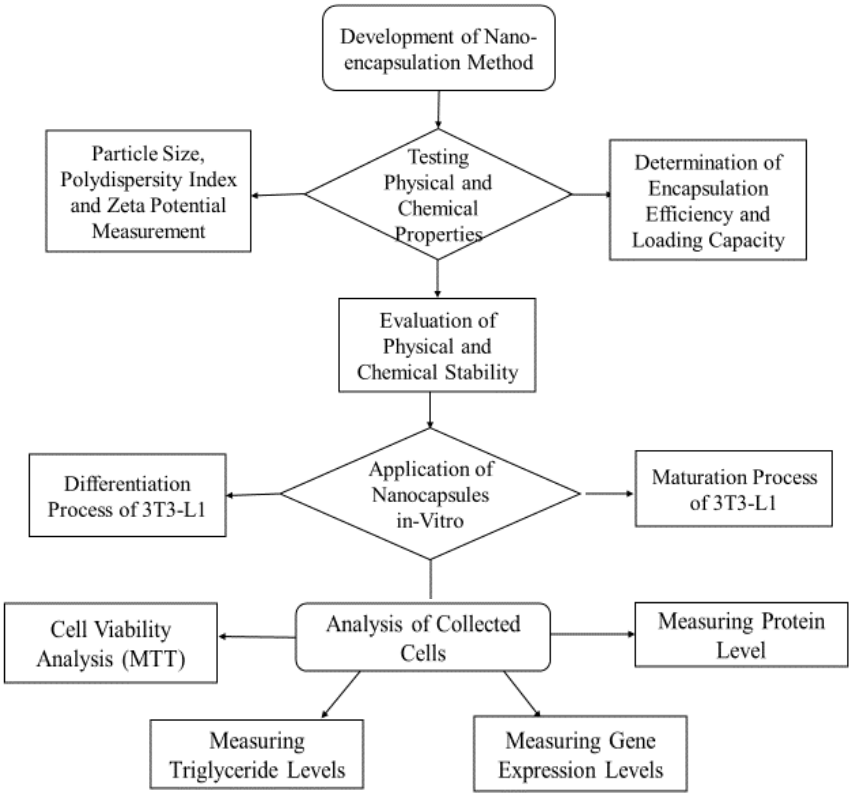

Figure 3.1. Flowchart of research design

3.2.1. Development of Encapsulation Method

Naringenin (≥93% TCI CHEM, N0072, Cas No. 67604-48-2), berberine (≥95% Cayman, 10006427, Cas No. 633-65-8), and delphinidin chloride (≥97% Cayman, 11012, Cas No. 528-53-0) phytochemicals were purchased. The liposomal encapsulation method for berberine (B) and naringenin (N) was developed based on the method published by Zu et al. (194).

In addition, these liposomal particles were prepared as void (V). Since the amount of delphinidin chloride (D) is insufficient for the nanoencapsulation protocol, it was only prepared in free form. The high cost of delphinidin, coupled with insufficient funding from the project, prevented us from proceeding with its encapsulation

Liposomal particle were prepared using a mixture containing Soy L-α-phosphatidylcholine (Soy-PC, P5638-500G, Sigma-Aldrich, CAS No. 8002-43-5), cholesterol (C8667-5G, Sigma-Aldrich, Cas. No. 57-88-5), chloroform (Merk 1024312500, Cas. No. 67-66-3), phosphate-buffered saline (PBS, Cegrogen H0500-

540-500 mL, Cas. No. 7778-77-0) (194). First of all, stock solutions were prepared. Berberine and naringenin were dissolved in chloroform (15mg/mL and 25mg/mL, respectively), Soy-PC was dissolved in chloroform (400mg/2mL), and cholesterol was dissolved in chloroform (100mg/2mL). Liposomal particles were prepared as reported in the following table (Table 3.1):

Table 3.1. Content of liposomal formulation

	Berberine	**Naringenin**	**Soy-PC**	**Cholesterol**
B-lipo	3mg (from stock 200µl)	--	50mg (from stock 250µl)	10mg (from stock 200µl)
N-lipo	--	5mg (from stock 200µl)	50mg (from stock 250µl)	10mg (from stock 200µl)
V-lipo	--	--	50mg (from stock 250µl)	10mg (from stock 200µl)

The mixture was completely dried under nitrogen gas (TAB-24 Nitrogen evaporator, Teknosem). After suspending the mixture with PBS, the suspension was sonicated (Bandelin Sonopuls HD 2070 homogeniser) for 30 minutes on ice. The samples were centrifuged (Labnet PRISM Microcentrifuge, USA) at 5,000 rpm for 7 minutes and the supernatant formed was transferred to new tubes. The prepared liposome were passed through 0.22 µm Millex® filters (EMD Millipore Corporation, Billerica) to eliminate substances that cannot dissolve. The void particle was prepared using the above methods without adding the phytochemicals. The liposomal particles were prepared at Hacettepe University, Faculty of Health Sciences, Department of Nutrition and Dietetics, Research Laboratories. The free form of phytochemicals was prepared using a mixture of dimethyl sulfoxide (DMSO, Sangon Biotech A503039) and B, N, and D (1 mg).

Particle Size, Zeta Potential, and Morphology

The average liposomal particle size, polydispersity index (PI), and zeta potential (ZP) values of the prepared V, N, and B particles were measured using a Zetasizer Nanoseries-ZS (Malvern Model: Zetasizer Nano ZSP).

Three consecutive measurements were made for each formulation at Hacettepe University Faculty of Pharmacy, Research Laboratories (194). The morphology and size of the particles were determined using a GAIA3+Oxford XMax 150 EDS electron microscope (Tescan). The electron microscope images were measured at Hacettepe University Faculty of Pharmacy, Hacettepe University Advanced Technologies Application and Research Center (HUNITEK).

Encapsulation Efficiency and Loading Capacity

The total amount of liposomal encapsulate phytochemical was measured by high-performance liquid chromatography (HPLC).

HPLC analyses were conducted using a Shimadzu UFLC system. The chromatographic setup included a solvent delivery unit (Shimadzu LC-20AB) and a diode array detector (Shimadzu SPD-M20A). Sample injection was facilitated by an autosampler (Shimadzu SIL-20AC), while the column (Shimadzu CTO-20AC) was maintained in an oven. Chromatographic separations were performed on a Discovery® HS C18 Column (75 ×4.6 mm, 3 μm) using an isocratic elution of ACN:0.1% Formic acid in water (40:60, v/v) as the mobile phase. The column temperature was regulated at 30 °C with a flow rate of 1.0 mL/min. Injection volume was set at 10 μL, and detection wavelengths were 280 nm for N and 266 nm for B, respectively. Peak identification was confirmed by comparing retention times.

Data acquisition and analysis were performed using the LabSolutions software (version 1.25, Shimadzu). Quantification of N and B in the samples was accomplished through calibration curves generated using least squares regression, correlating concentration to peak areas for N and B.

Non-encapsulated (free) N and B were separated from encapsulated N and B using an ultrafiltration method with centrifugation at 4500 × g for 60 minutes. After that, the free forms were measured by the HPLC system (194, 196). In order to calculate the loading capacity, N and B were dried using a freeze dryer system and they were measured at Hacettepe University, Faculty of Pharmacy, Pharmaceuticals, and Cosmetics AR-GE and Quality Control Laboratory (HUNIKAL).

The encapsulation efficiency (EF) and loading capacity (LC) of N and B in the particles were calculated according to the following equations:

$$EF\ \% = \frac{Amount\ of\ active\ substance\ -\ Amount\ of\ free\ active\ substance}{Amount\ of\ active\ substance} \times\ 100\%$$

$$LC\% = \frac{Amount\ of\ active\ substance * Volume\ -\ Amount\ of\ free\ active\ substance * Volume}{Nano\ capsule\ weight} \times\ 100\%$$

In-Vitro Release Study

The *in vitro* release behaviors of free N-B and lipo N-B were performed in the dissolution medium composed of 40 mL PBS (0.1 M) and 10 mL methanol (20:80, v/v) using a dialysis method. Quantities corresponding to 1.0 mg of N and B were dispersed in 2 mL of 1×PBS and subsequently inserted into 44 mm dialysis membranes (Bio Basic CA).

These dialysis bags were then immersed, using a thread, into a beaker filled with 50 mL of dissolution medium (maintained at 37°C) and stirred at 250 rpm. Every two hours for 24 h, 2 mL of the dissolution medium was taken and it was replaced by fresh medium. The N-B released from both free and liposomal formulations into the surrounding medium at each specified time interval was quantified utilizing the HPLC system. (196).

Physical and Chemical Stability

The stability of newly prepared liposomal particles was assessed in transparent or opaque tubes across three temperature settings (4°C, 22°C, and 37°C) over a span of 10 days, evaluating both physical and chemical properties.

The average particle diameter, zeta potential, and polydispersity index (PI) were assessed at two-hour intervals during the initial 10 hours, then daily for a span of 5 days, concluding with a final measurement on the tenth day. The chemical stability of liposomal N, B encapsulated were measured using the HPLC system every day for 5 days and the tenth day.

3.2.2. 3T3-L1 Cell Application

3T3-L1 purchased from ATCC is a fibroblast isolated from the embryo of a mouse. 3T3-L1 pre-adipocyte cells (fibroblast) were grown in Dulbecco’s modified

Eagle's medium (DMEM) containing fetal bovine serum (FBS), penicillin (100 units/mL), and streptomycin (100mg/mL).

The cells were incubated at 37°C in 95% humidity and 5% CO2. The differentiation of 3T3-L1 pre-adipocyte cells was induced by adding 0.5M isomethyl-butylxanthine (IBMX), 1μM dexamethasone, and 10μg/mL insulin to medium (Growth Media) containing 10% FBS, 1% antibiotic, and DMEM. Each media was prepared fresh and stored at 4°C. Two days later, the media was replaced with new media produced by adding 10μg/mL insulin to the first medium. About one month after differentiation was induced, most of the cells (approximately 90%) had differentiated into mature adipocyte cells (194, 198). The 3T3-L1 pre-adipocyte cells at Hacettepe University Faculty of Pharmacy were checked every two days.

The old growth medium of the cells was aspirated and replaced with a fresh growth medium containing 20% FBS or 10% FBS. Basic fibroblast growth factor (b-FGF) was added to fresh media to stimulate the growth of cells. Most of the cells (90%) grew and they were seeded in 12-well plates.

After the literature review, free forms of N, B, and D and encapsulate formulations of N and B to be tested in cells were determined as 20, 10, and 5 μM concentrations (96, 121, 199). In addition, the void capsule was added as a control group for encapsulated formulations. For the free form, PBS was added to the growth medium as a control group.

Treatment concentrations of 20, 10, and 5 μM were given to each well. 3T3-L1 cells were cultured with this medium. The treatment was applied at each medium change during the differentiation process and One Step-RNA Reagent (Bio Basic CA) was added after the cells had matured. Cells were aspirated from the dish into pre-labelled tubes. Cells were harvested 24 to 48 hours after this administration (Days 7-8) (Fig.3.2).

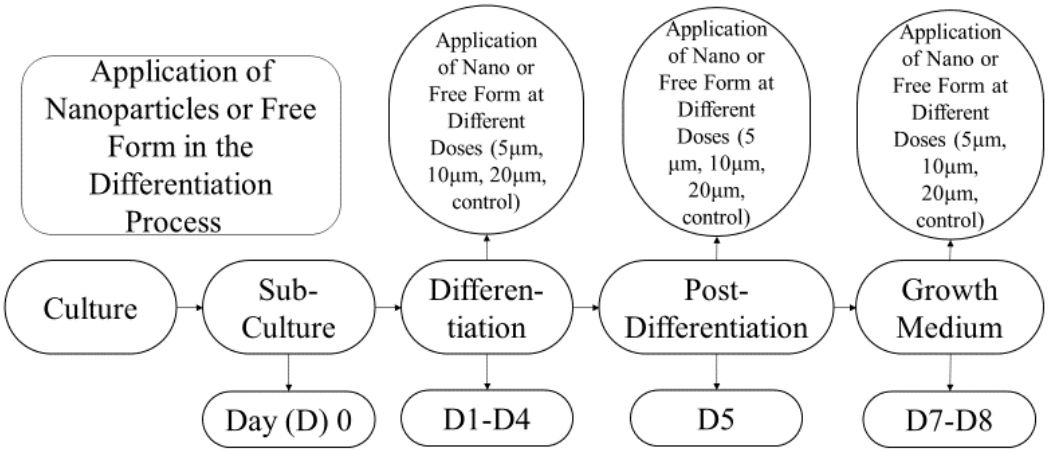

Figure 3.2. Application of liposomal or free form of delphinidin, naringenin and berberine in the differentiation process

The same treatment was applied to 3T3-L1 cells in the maturation process, but on different days (Fig.3.3). Free N, B, and D or encapsulated N and B were added to the growth medium at different concentrations. The treatments were applied 20 µl per well. Treatment concentrations were divided into the following groups: free naringenin (20 µM, 10 µM, and 5 µM), liposomal naringenin (20 µM, 10 µM, and 5 µM), free berberine (20 µM, 10 µM, and 5 µM), liposomal berberine (20 µM, 10 µM, and 5 µM), free delphinidin (20 µM, 10 µM, and 5 µM), along with a void and a control group. The cells were harvested 48 hours after maturation (194, 200).

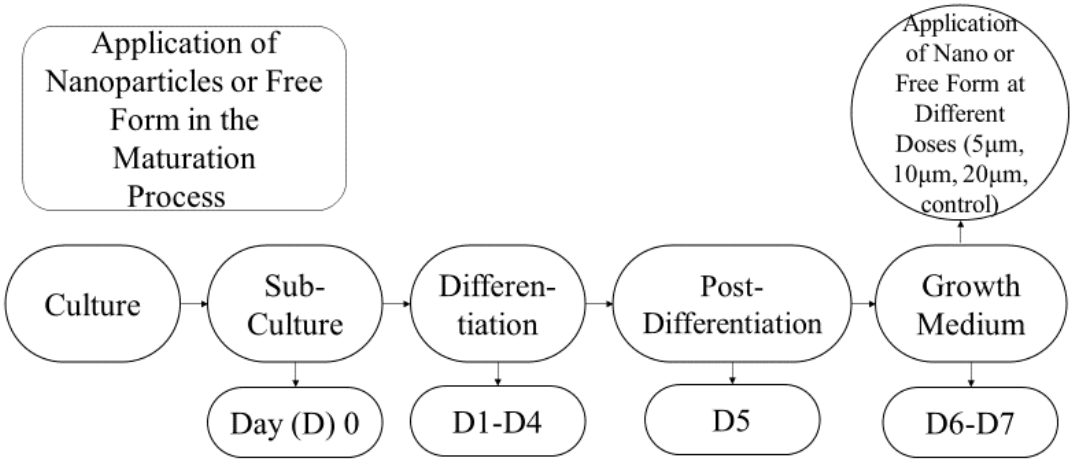

Figure 3.3. Application of liposomal or free forms of delphinidin, naringenin and berberine in the maturation process

3.3. Data Collection

3.3.1. Measuring Gene Expression Levels

Gene expression was measured in three key steps: RNA extraction, Reverse transcriptase, and Real-time PCR.

RNA Extraction

RNA extraction kit (One Step-RNA Reagent, Bio Basic CA) was used for the isolation of total RNA from samples. The reagent, a mono-phasic solution of phenol and guanidine isothiocyanate, was an improvement of the single-step RNA isolation method developed by Chomczynski and Sacchi (201).

While homogenizing or lysing the samples, One Step-RNA Reagent preserved RNA integrity while breaking down cells and dissolving their components. The introduction of chloroform, succeeded by centrifugation, partitioned the solution into an aqueous phase and an organic phase. RNA was specifically retained within the aqueous phase. After transferring the latter to a new tube, the RNA was recovered by precipitation with isopropyl alcohol. After removing the aqueous phase, it was possible to recover the DNA and proteins in the sample by sequential precipitation. Ethanol precipitation facilitated the extraction of DNA from the interphase, while a subsequent precipitation using isopropyl alcohol isolated proteins from the organic phase.

The main steps for RNA extraction were: homogenization, phase separation, RNA precipitation, RNA wash, and redissolving the DNA. Finally, the samples were dropped (1 to 2 μL) onto the measurement window of BioSpec-nano (Shimadzu Biospec Nano, JP). The concentration of RNA was measured at Hacettepe University Faculty of Pharmacy, Pharmaceuticals and Cosmetics AR-GE and Quality Control Laboratory (HUNIKAL). The concentration of RNA in the samples was directly calculated by BioSpec-nano.

Reverse Transcriptase Protocol

Complementary DNA (cDNA) was obtained from RNA with OneScript® Plus cDNA Synthesis Kit (Applied Biological Materials Inc-ABM, CA, catalog no: G236).

The kit included a Moloney-Murine Leukemia Virus Reverse Transcriptase engineered with genetic alterations to eliminate RNase H activity, thereby enhancing its thermal stability. This unique variant enzyme provides increased cDNA yields, capable of generating cDNA sequences up to 12 kb longer, and operates effectively at elevated temperatures (50°C - 55°C), aiding in the disruption of secondary structures typically found in GC-rich RNA templates. OneScript® Plus was developed incorporating abm's RNaseOFF Ribonuclease Inhibitor, which offers enhanced resilience to oxidation compared to traditional human RNase inhibitors that are highly susceptible to oxidation.

Reverse Transcriptase reactions should be assembled in an RNase-free environment. First of all, the sample was thawed. The components in the kit were mixed on ice and the sample was added. After that, the tube was incubated for 15 minutes at 50-55°C to perform cDNA synthesis. The incubation was measured at Hacettepe University Faculty of Health Sciences, Department of Nutrition and Dietetics, Research Laboratories (Piko® Thermal Cyclers by Thermo Fisher Scientific, USA). The synthesized first-strand cDNA was ready for amplification by PCR.

Real-Time PCR for Primer Testing

Before starting the Real-Time PCR sample testing, all designed primers (PPARγ, C/EBPβ, PGC1-α, CIDEA, FABP4, UCP1, PRDM16) were tested for the specific gene and efficiency. The primer sequences for the target genes are provided in Table 3.2. BlasTaq™ 2X qPCR MasterMix from Applied Biological Materials Inc-ABM (CA, catalog no: G891) was utilized to evaluate all the designed primers. This kit contains Taq Polymerase which provides a rapid extension rate. BlasTaq™ possesses polymerase and exonuclease activities in the 5'-3' direction but lacks exonuclease activity in the 3'-5' direction.

Additionally, it generates amplicons with 3'-dA tails. cDNA was diluted into 20 ng, 4 ng, 0.8 ng, 0.16 ng, 0.032 ng, and 0.0064 ng/µL (5-series dilution) with nuclease-free water. Subsequently, the individual components of the kit were mixed and the cDNA sample was added to the designated wells. The detection of gene expression was measured by Lightcycler 480 (Roche company) at Hacettepe

University, Faculty of Health Sciences, Department of Nutrition and Dietetics, Research Laboratories. The efficiency of the designed primers contained in each sample was calculated by using the standard curve (x-axis is Lg cDNA amount, y-axis is Ct) and delta Ct curve (x-axis is Lg cDNA amount, y-axis is delta Ct (target-endogenous gene). The slope of the standard curve should be between 3.2-3.4, while the slope of the delta Ct curve should be <±0.1. Experiments or primer designs were repeated when the slope was not in the range.

Table 3.2. Primer sequences of target genes

Gene name		Primer sequences
PPARγ	Forward	GTACTGTCGGTTTCAGAAGTGCC
	Reverse	ATCTCCGCCAACAGCTTCTCCT
C/EBPβ	Forward	GGTTTCGGGACTTGATGCA
	Reverse	CAACAACCCCGCAGGAAC
PGC1-α	Forward	GAATCAAGCCACTACAGACACCG
	Reverse	CATCCCTCTTGAGCCTTTCGTG
CIDEA	Forward	AGAAGGTCCTACTGACCCCC
	Reverse	ACCCGGTGTCCATTTCTGTC
FABP4	Forward	TGAAATCACCGCAGACGACAGG
	Reverse	GCTTGTCACCATCTCGTTTTCTC
UCP1	Forward	CCTGCCTCTCTCGGAAACAA
	Reverse	GTAGCGGGGTTTGATCCCAT
PRDM16	Forward	GATGGGAGATGCTGACGGAT
	Reverse	TGATCTGACACATGGCGAGG

Real-Time PCR for Sample Testing

Sample cDNAs were tested with Real-Time PCR protocol to measure gene expression levels. BlasTaq™ 2X qPCR MasterMix (Applied Biological Materials Inc-ABM, CA, catalog no: G891) was set up to perform quantitative real-time analysis of DNA samples. This kit contained Taq Polymerase providing a rapid extension rate and robust performance. BlasTaq™ has 5'-3' polymerase and 5'-3' exonuclease activities, lacks 3'-5' exonuclease activity, and produces 3'-dA-tailed amplicons.

After that, individual components were mixed with the kit on ice and the cDNA sample was added to the designated wells. The detection of gene expression was measured by Lightcycler 480 (Roche company) at Hacettepe University, Faculty of Health Sciences, Department of Nutrition and Dietetics, Research Laboratories. The gene expression was calculated with the following formula:

$$deltaCt\ (\Delta Ct) of\ target\ gene\ in\ experimental\ group\ \ = Ct\ (target\ gene) - Ct\ (endogenous\ gene)$$

$$\Delta C_t\ of\ target\ gene\ in\ control\ group = C_t\ (target\ gene) - C_t\ (endogenous\ gene)$$

$$\Delta\Delta C_t = \Delta C_t\ of\ target\ gene\ in\ experimental\ group - \Delta C_t\ of\ target\ gene\ in\ control\ group$$

$$Fold\ change = 2 \times \Delta\Delta C_t$$

3.3.2. Measuring Protein Concentration

Protein concentration were measured in three key steps: Protein Extraction, Protein Quantification (BCA), and ELISA protocol.

Protein Extraction Protocol

Protein extraction was used to isolate proteins from the sample. After RNA was separated in the tube, DNA and protein remained. An interphase, a lower organic layer with proteins and DNA, and a transparent upper aqueous layer with RNA. Isopropanol is used to precipitate RNA from the aqueous layer and ethanol is used to precipitate DNA from the interphase layer. Isopropanol precipitation separates the protein from the phenol-ethanol supernatant.

There were three basic steps of protein purification: precipitation of the protein, washing of the proteins, and solubilization of the proteins. Firstly, the samples were centrifuged for 5 minutes at 5,000 rpm at 4°C to precipitate DNA and washed with isopropanol. Secondly, the protein was resuspended with a washing solution (0.9009 g of urea in 95% ethanol and 5% water with DEPC) and centrifuged it at 9,000 rpm for 5 minutes at 4°C, and then discarded the supernatant twice.

Finally, the pellet was resuspended in 200 µL of 1% SDS, centrifuged for 10 minutes at 11,000 rpm at 4°C, and the supernatant was transferred to a new tube.

BCA Protein Assay

BCA protein assay kit (Thermoscientific, Pierce™ BCA Protein Assay Kit, USA) is a detergent-compatible formulation based on bicinchoninic acid (BCA) for the colorimetric detection and quantitation of total protein of the samples. In this assay, the well-known reduction of Cu^{+2} to Cu^{+1} by protein in an alkaline medium was combined with the very sensitive and specific colorimetric detection of the cuprous cation (Cu^{+1}).

This process involved employing a unique reagent comprising bicinchoninic acid. The combination of two BCA molecules with one cuprous ion resulted in the formation of the purple-hued reaction product utilized in this analysis. This water-soluble complex exhibited a significant absorbance at 562 nm that was almost linear with increasing protein concentrations over a broad working range (20–2000 μg/mL). The molecular arrangement of proteins, the quantity of peptide bonds, and the existence of four specific amino acids (cysteine, tyrosine, cystine, and tryptophan) have been documented as factors contributing to color development with BCA.

The plate reader was at Hacettepe University Faculty of Health Sciences, Department of Nutrition and Dietetics, Research Laboratories (BioTek Synergy Htx multi-mode reader). The protein concentration present in each sample was determined utilizing the "protein standard curve," which was established by plotting the average Blank-corrected 562 nm measurement for each BSA standard against its concentration in μg/mL.

ELISA Protocol

UCP1, PPAR-γ, PGC1-α protein concentrations of protein extracts were measured using a sandwich enzyme immunoassay (ELISA) kit (ELK Biotechnology, Wuhan). The analysis was performed in duplicate in 3T3-L1 cells after treatment with liposomal encapsulated phytochemicals or free form in different doses. The microtiter plate was pre-coated with an antibody specific to the protein (UCP1, or PPAR-γ, or PGC1-α). A biotin-conjugated antibody specific to the protein was added to the microtiter plate wells along with standards or samples.

Afterward, a mixture of avidin linked with Horseradish Peroxidase (HRP) was introduced into each well of the microplate and left to incubate. Subsequently, a TMB substrate solution was applied, resulting in a color change only in wells containing the designated protein, biotin-conjugated antibody, and avidin linked with the enzyme. The sulfuric acid solution was added to stop the enzyme-substrate reaction. The alteration in color was assessed spectrophotometrically at a wavelength range of 450nm ± 10nm. The plate reader was at Hacettepe University Faculty of Health Sciences, Department of Nutrition and Dietetics, Research Laboratories (BioTek Synergy Htx multi-mode reader). The protein concentration in the samples was

determined by correlating the optical density (OD) readings of the samples with the values obtained from the standard curve.

3.3.3. Measuring Triglyceride Levels

The Triglyceride Colorimetric Assay kit (Cayman Chemical Company, USA) was used for triglyceride quantification of the samples. The analysis was performed in duplicate in 3T3-L1 cells after treatment with encapsulated phytochemicals or free form in different doses by colorimetry method. Before the analysis, the cell pellet was resuspended in 1-2 mL of cold diluted Standard Diluent and sonicated.

The Triglyceride Colorimetric Assay relies on the enzymatic breakdown of triglycerides by lipase, resulting in the formation of glycerol and free fatty acids. The amount of glycerol released is then quantified using a coupled enzymatic reaction system. Glycerol kinase catalyzed a process in which the glycerol produced in the first reaction was phosphorylated to produce glycerol-3-phosphate. Glycerol-3-phosphate underwent oxidation catalyzed by glycerol phosphate oxidase, resulting in the generation of hydrogen peroxide and dihydroxyacetone phosphate. A vivid purple color was produced from the redox-coupled reaction of 4-aminoantipyrine, N-Ethyl-N-(3-sulfopropyl)-m-anisidine, and H2O2 was catalyzed by peroxidase. The absorbance was measured at 530-550 nm.

The plate reader was at Hacettepe University Faculty of Health Sciences, Department of Nutrition and Dietetics, Research Laboratories (BioTek Synergy Htx multi-mode reader). The concentration of triglycerides contained in each sample was calculated with the help of the “triglyceride standard curve” created by using the absorbance values of standard solutions with known triglyceride concentrations.

3.3.4. Cell Viability Assays (MTT)

The MTT Assay Kit (from Elabscience Biotechnology, USA) was used for assessing cell proliferation and cytotoxicity. MTT, also known as 3-(4,5-dimethylthiazol-2-yl)-2,5-diphenyl tetrazolium bromide, undergoes reduction by certain mitochondrial dehydrogenases, resulting in the formation of a dark purple crystalline product called formazan. DMSO completely dissolves formazan and has an absorbance of about 570 nm. The color changes in intensity depending on how many

and how quickly cells proliferate; the more cytotoxic the cells, the lighter was the color. A direct correlation was observed in the cells between the intensity of color and the cell count. 3T3-L1 preadipocytes were cultured in a 96-well plate and exposed to various concentrations (5, 10, and 20 μM) of both free and encapsulated phytochemicals for 24 and 48 hours.

The resulting absorbance was measured at Hacettepe University Faculty of Health Sciences, Department of Nutrition and Dietetics, Research Laboratories (BioTek Synergy Htx multi-mode reader). The concentration of cell survival rate was calculated as a percentage of cell viability and two replicates were performed for each treatment. The formula was as follows: the OD value of each test well was subtracted from the OD value of the blank group.

3.4. Statistical Analyses

Statistical analyses were performed with the use of the computer program SPSS 22.0. Parametric tests will be used for normally distributed variables, and non-parametric tests will be used for not normally distributed variables. Student's t test was used for normally distributed variables to compare differences between two groups.

Mann-Whitney U test was used for not normally distributed variables to compare differences between two groups. One-way ANOVA was used for normally distributed quantitative variables to compare more than two groups. Kruskal–Wallis analysis of variance was used for comparing not normally distributed variables.

One-way analysis of variance was used for normally distributed variables to compare the difference between the mean of three or more dependent groups. Instead, the Friedman test was used for those not normally distributed. Correlations among normally distributed quantitative variables were tested with the Pearson correlation coefficient. Spearman correlation was used for not normally distributed variables. A value of $p < 0.05$ was considered significant.

4. RESULTS

4.1. Characteristics of Encapsulated Phytochemical

4.1.1. Morphology of Particles

Encapsulated B and N were successfully synthesized. SEM images showed that both liposomal B and N displayed a spherical shape (Fig. 4.1). The mean encapsulated particle diameter of B and N measured approximately 215 nm and 207 nm, respectively.

Despite our initial aim to produce liposomal nanoparticles, after several attempts, we were unable to achieve this. Consequently, we proceeded to produce encapsulated liposomal forms (lipo). The PI values of lipo B and N were 0.30 and 0.35, respectively. The Zeta potentials of newly prepared encapsulated B and N were approximately -27 and -29 mV, respectively.

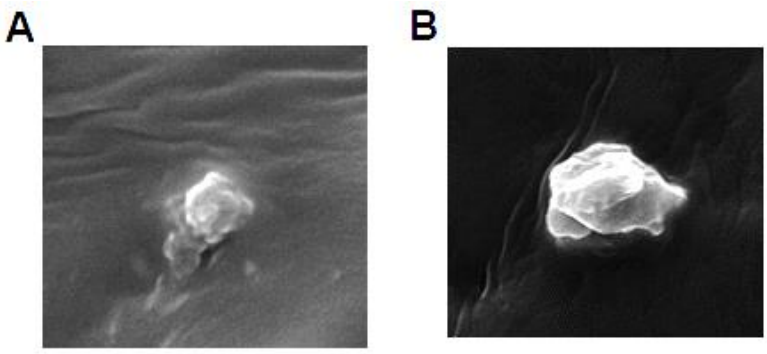

Figure 4.1. A scanning electron microscope (SEM) images of visual observation of liposomal forms of berberine (A) and naringenin (B)

4.1.2. Encapsulation Efficiency and Loading Capacity

The encapsulation efficiency of liposomal forms of B and N was 96.0% and 94.6%, respectively. Furthermore, berberine and naringenin loading capacity in B-lipo and N-lipo was 21.1% and 19.2%, respectively. The total amount of phytochemicals encapsulated in liposomes was measured using HPLC. For this purpose, a 20 ppm standard stock solution of berberine and naringenin (Figure 4.2) was prepared and analyzed by HPLC under optimal conditions

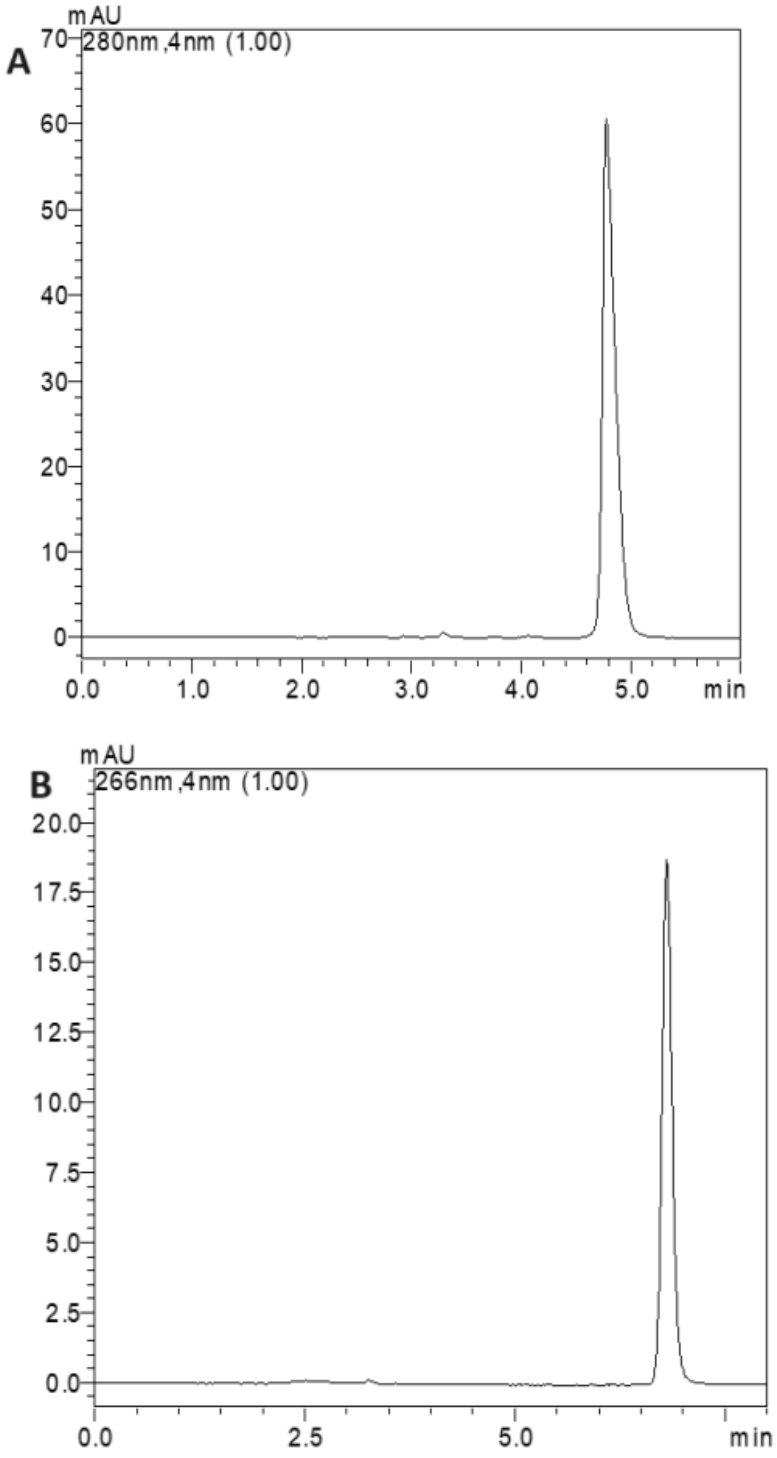

Figure 4.2. Representative chromatograms obtained under the optimum chromatographic conditions for free berberine (A) and naringenin (B) standard spiked matrix at 20ppm concentration

4.1.3. *In-Vitro* Release Study

The release study was conducted in the dark to avoid them breaking down from light exposure. To make sure the stability of B and N did not affect the results, every 2 hours changed the liquid they were in. When B and N were on their free form, they were released quickly at first. But when they were in lipo-form, they were released more slowly and steadily (Fig. 4.3). Two hours later, approximately 3.15 milligrams and 0.15 milligrams of B were released from the dialysis bags with free B and B-lipo, respectively. After 6 h, about 1.35 mg and 0.27 mg of B were released from dialysis bags containing free B and B-lipo (Fig. 4.3A).

Moreover, after 2 h, about 9.55 mg and 0.40 mg of N were released from dialysis bags with free N and N-lipo, respectively. After 6 h, about 8.93 mg and 0.49 mg of N were released from dialysis bags containing free N and N-lipo.

Furthermore, after dialysis for 4 h, the accumulative released B and N mass from the free B and N dialysis bag decreased constantly (Fig. 4.3B), while for B-lipo and N-lipo, berberine and naringenin were continuously released in the 24 h period.

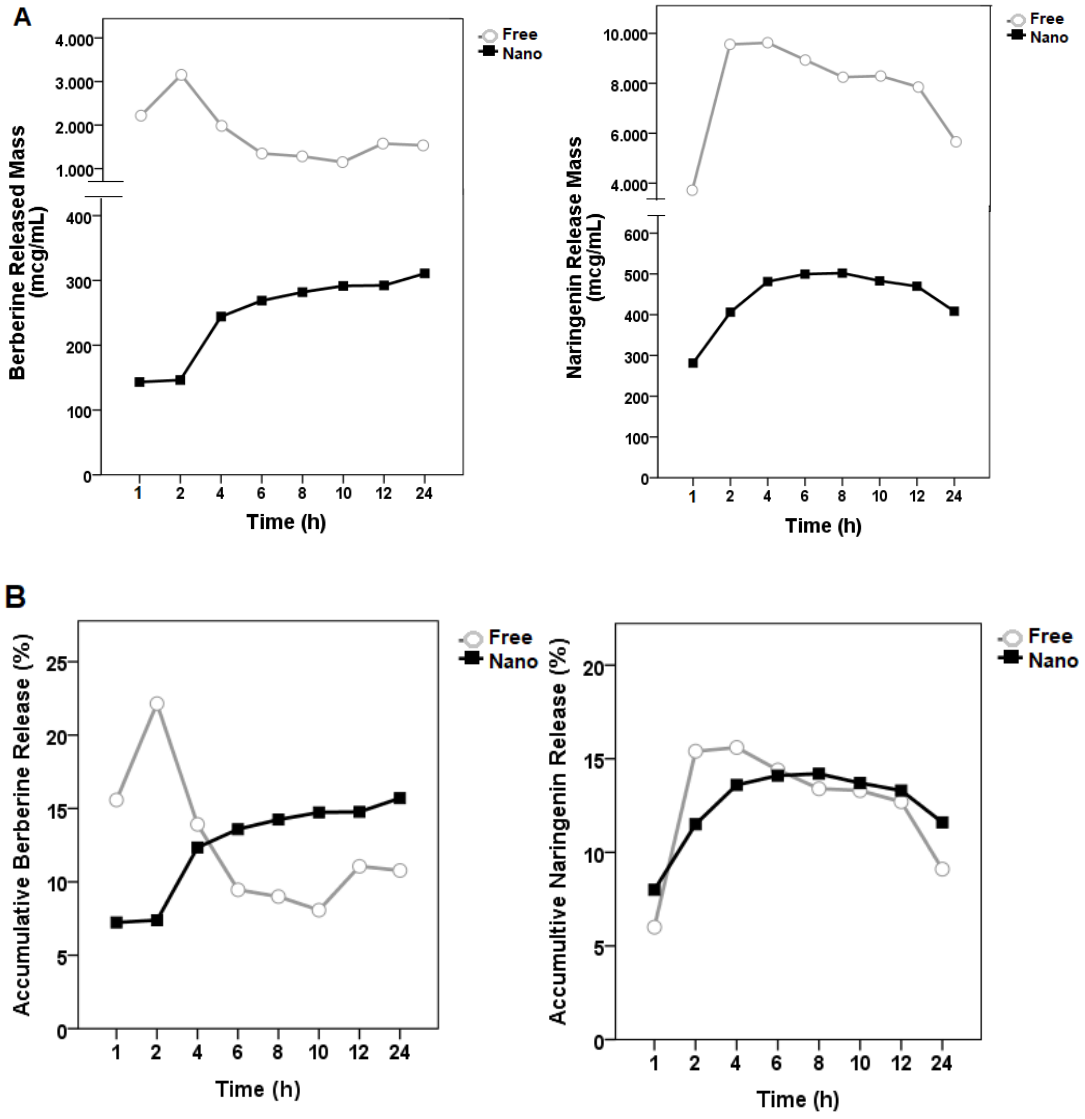

Figure 4.3. *In vitro* release profiles. Hourly (A) and accumulative (B) release for free and liposomal forms of berberine and naringenin

4.1.4. Physical and Chemical Stability

After storing both liposomal forms of B and N at 4 °C for 5 days, there were no notable alterations in their diameters and zeta potentials, while the PI values consistently stayed below 0.4, suggesting reasonably decent physical stability (Fig. 4.4 and 4.6).

Storage of both encapsulated B and N at room temperature (22 °C) for 2 days, its diameters, and PI values were increased (Fig. 4.5 and 4.7). At 37 °C, encapsulated B and N can only maintain their original size for 24 h, and its PI values were progressively increased after 2 days (Fig. 4.4 and 4.6).

The zeta potential of liposomal forms of B and N remained relatively stable at 4°C, 22°C, and 37°C over a period of 10 days, showing no significant alterations.

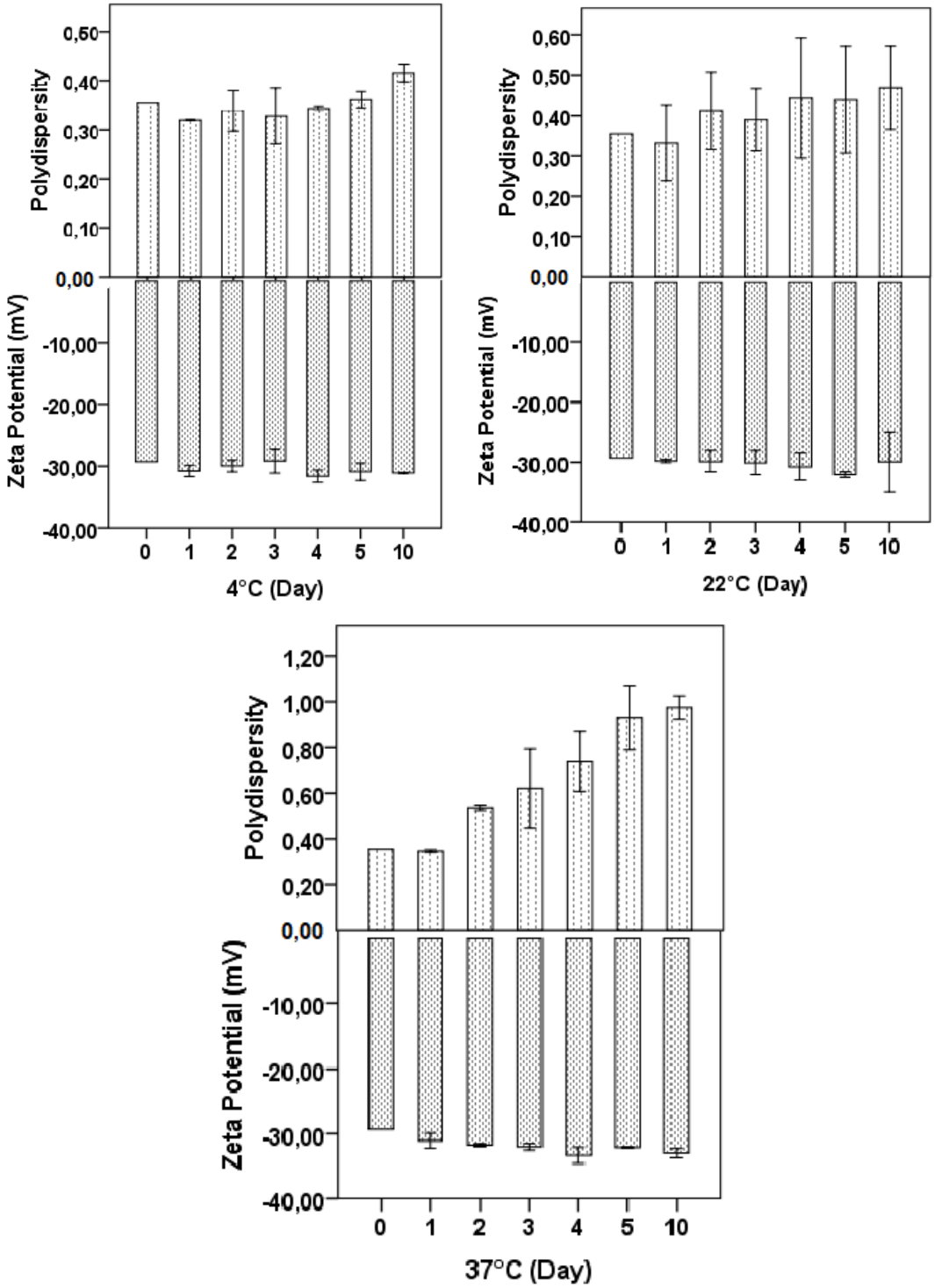

Figure 4.4. Characteristics of liposomal form of naringenin. Changes zeta potential and polydispersity index at different temperatures

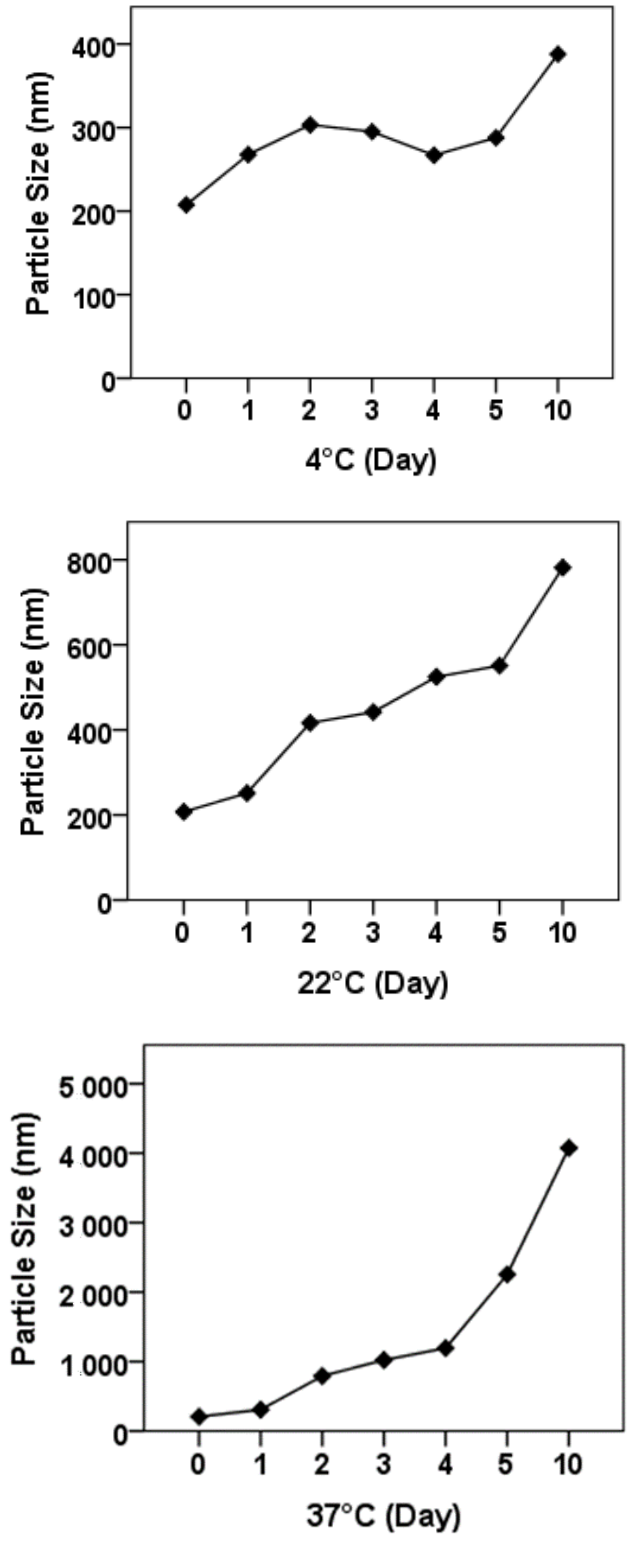

Figure 4.5. Changes in particle size of liposomal form of naringenin at different temperatures

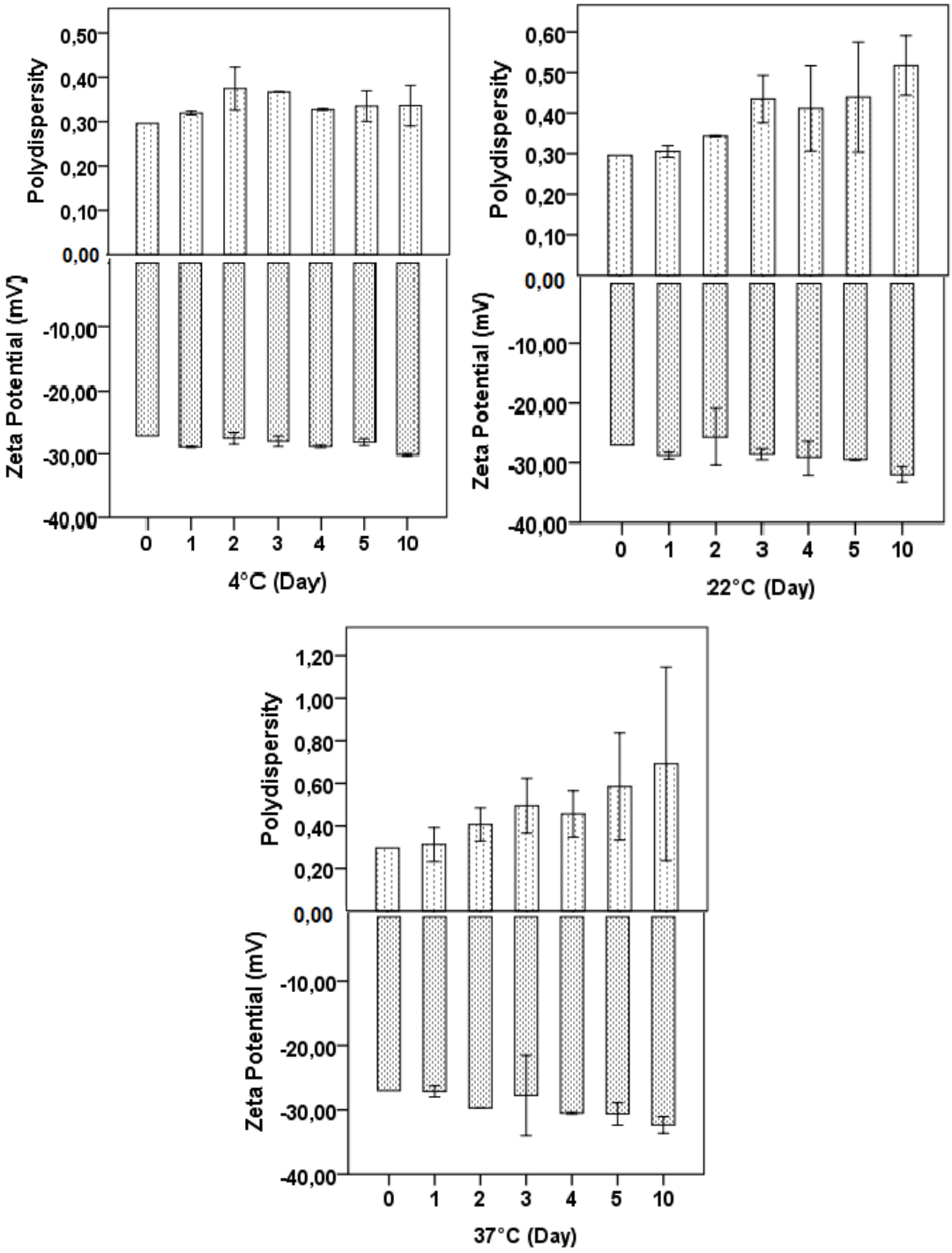

Figure 4.6. Characteristics of liposomal form of berberine. Changes zeta potential and polydispersity index at different temperatures

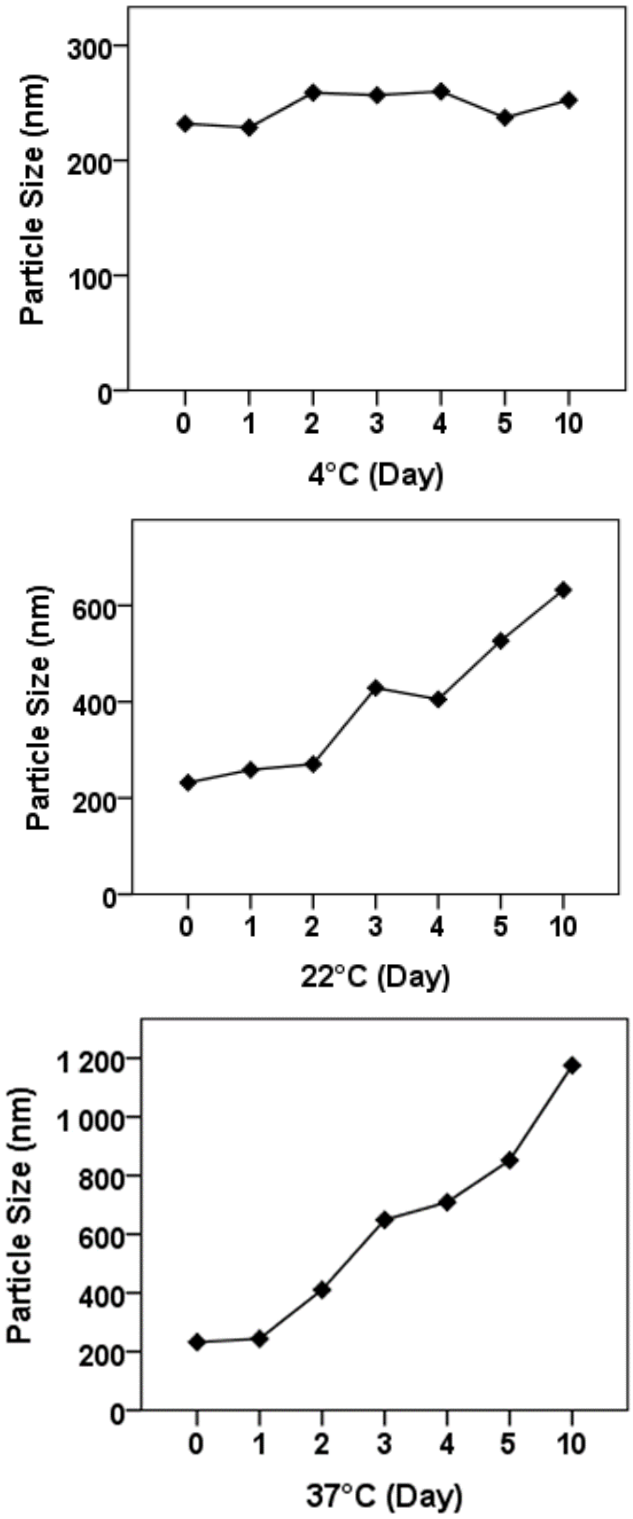

Figure 4.7. Changes in particle size of liposomal form of berberine at different temperatures

Liposomal forms of N and B also enhanced the chemical stability of phytochemicals which is sensitive to light. Free N and B were less stable under the light after 10 days (Fig.4.8A and 4.9A). Storage of free N and B in the dark decreased less the N and B degradation after 10 days (Fig.4.8B and 4.9B).

The encapsulation provided protection for N and B against degradation, irrespective of whether they were subjected to darkness or light, and their safeguarding efficacy remained consistent at temperatures of both 4°C and 22°C.

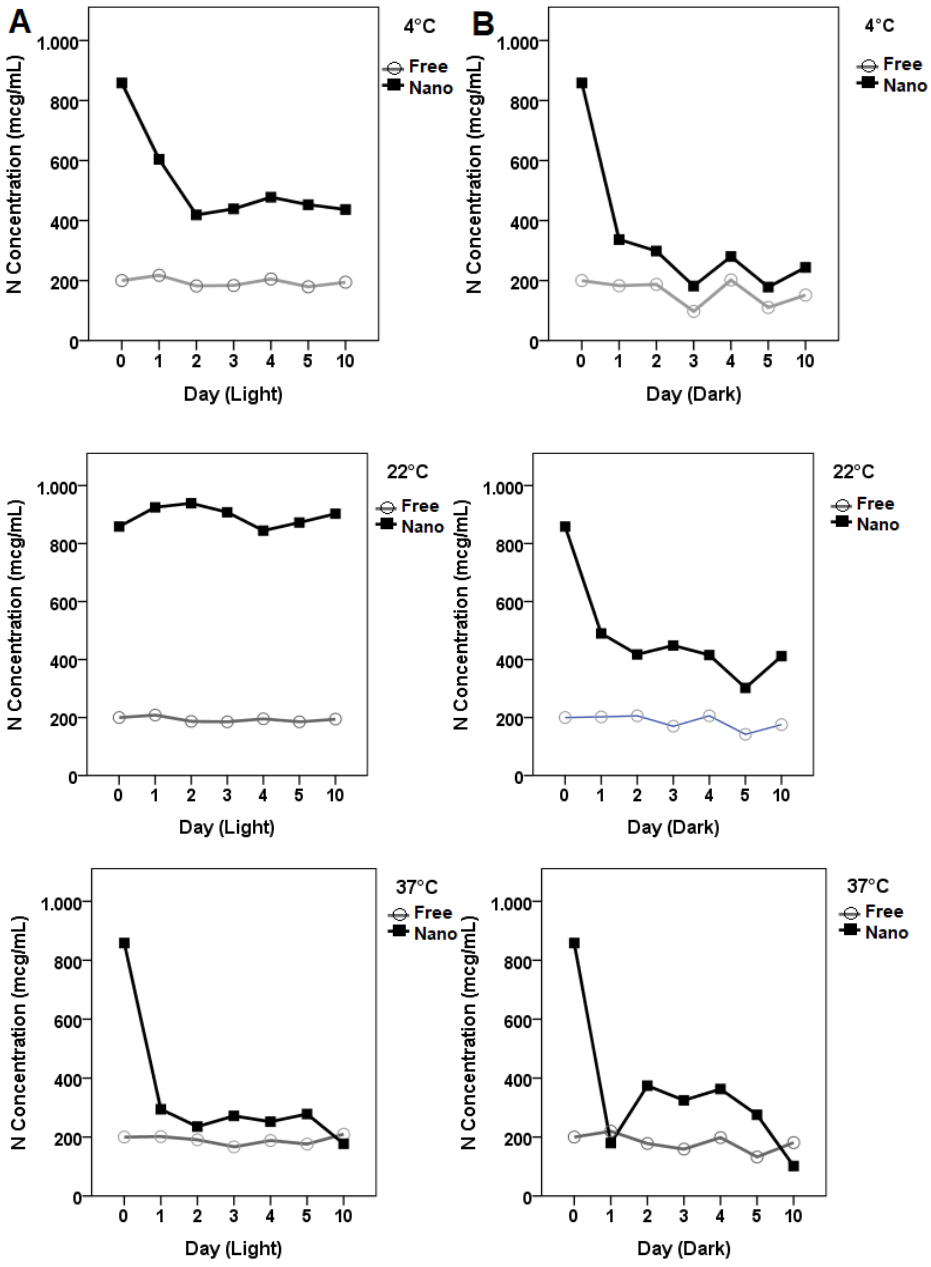

Figure 4.8. Chemical stability of free and liposomal forms of naringenin under light (A) or dark (B) at different temperatures

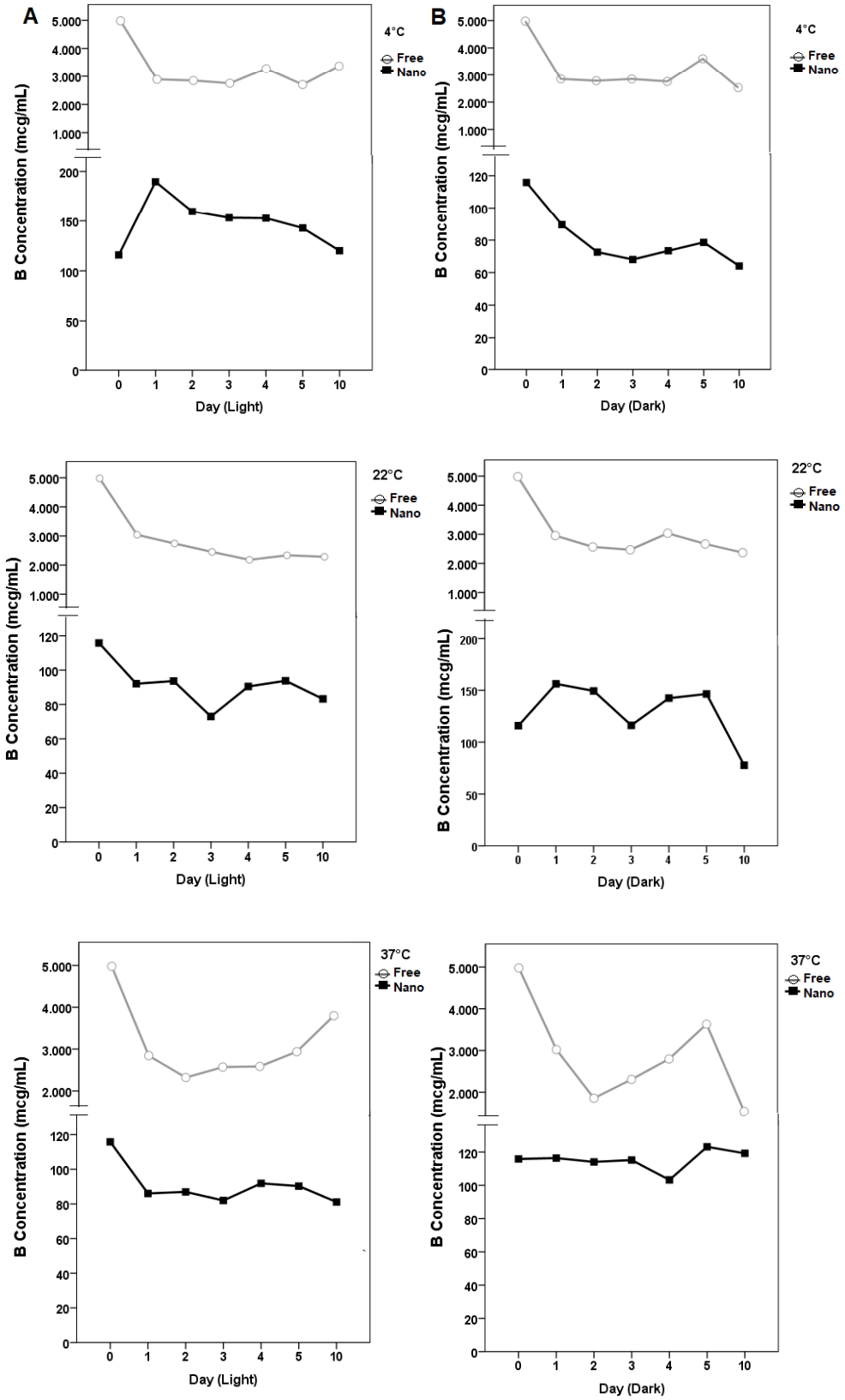

Figure 4.9. Chemical stability of free and liposomal forms of berberine under the light (A) or the dark (B) at different temperatures.

4.2. Differentiation Process

4.2.1. Gene Expression Levels

Gene expression data from RT-PCR experiments were analyzed by one-way ANOVA to compare mean gene expression levels (PPARγ, C/EBPβ, PGC1-α, CIDEA, FABP4, UCP1, PRDM16) among different types of treatment during the differentiation process. The gene were gathered in two main groups: regulators of adipogenesis (PPARγ, C/EBPβ, FABP4) and regulators of browning (PGC1α, CIDEA, UCP1, PRDM16). Furthermore, LSD or Games-Howell was used to compare the difference between the groups.

PPARγ, C/EBPβ, and FABP4, which are key regulators of adipogenesis, exhibited similar gene expression levels ($p > 0.05$) in all free D groups in the differentiation (Figure 4.10). There was no significant variance observed among the groups ($p>0.05$).

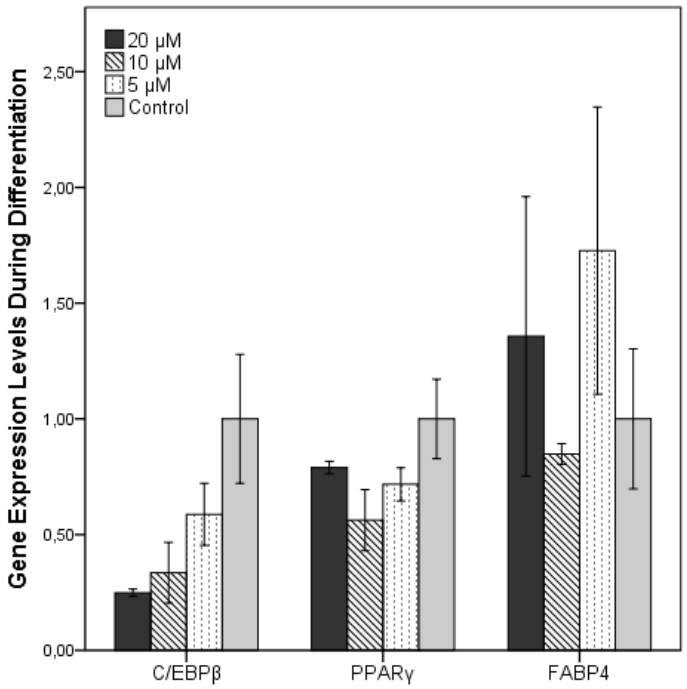

Figure 4.10. C/EBPβ, PPARγ, and FABP4 gene expression levels of delphinidin in the differentiation process.

The gene expression levels of key regulators of browning, including PGC1α, CIDEA, UCP1, and PRDM16, varied among different groups of free D (Figure 4.11). During the differentiation process, UCP-1 gene expression levels were significantly higher in the 5 μM D group compared to other groups (p = 0.038).

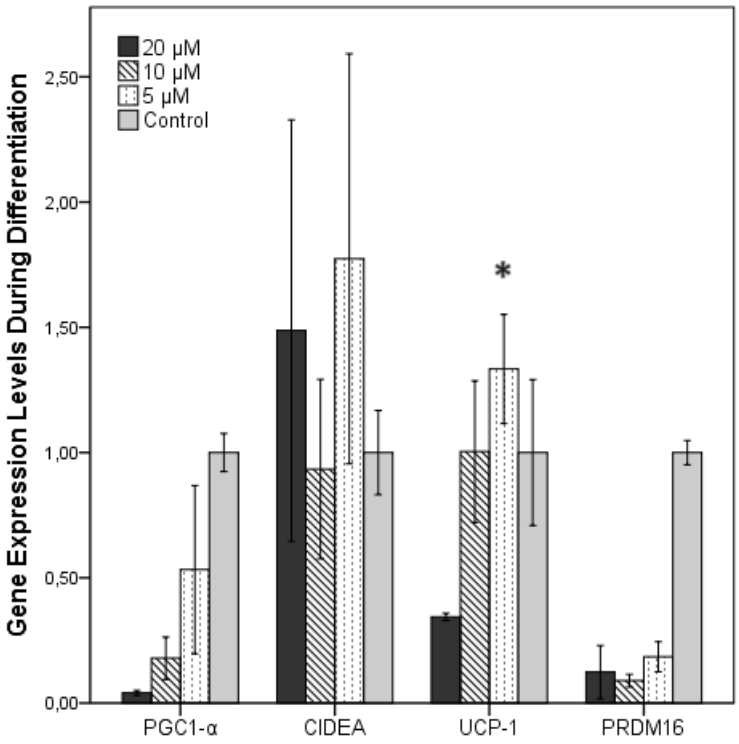

*, p < 0.05 compared to their controls.

Figure 4.11. PGC1-α, CIDEA, UCP1, and PRDM16 gene expression levels of delphinidin in the differentiation process.

In the differentiation process the key regulators of adipogenesis showed different gene expression levels for free and lipo N (Figure 4.12). There was not a significant difference for C/EBPβ and FABP4 gene expression levels (p>0.05). However, PPARγ gene expression levels in free 20 μM of D were significantly higher than lipo 20 μM (p=0.18), lipo 10 μM (p=0.08), lipo 5 μM (p=0.014), and the void (p=0.009).

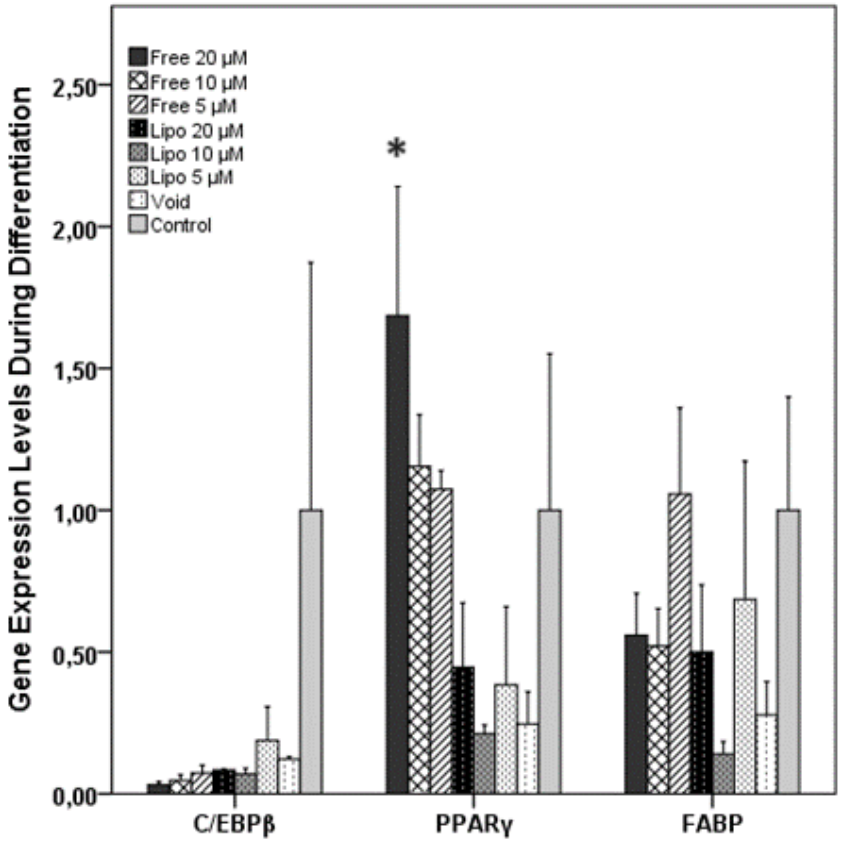

*, $p < 0.05$ compared to their controls.

Figure 4.12. C/EBPβ, PPARγ, and FABP4 gene expression levels of naringenin in the differentiation process.

The key regulators of browning in the differentiation process varied among various groups of N (Figure 4.13). PGC1-α gene expression levels in N were significantly higher in the control groups than in free 20 µM ($p=0.029$), free 10 µM ($p=0.033$), free 5 µM ($p=0.032$), and lipo 20 µM ($p=0.035$). Likewise, CIDEA gene expression levels were higher in free 20 µM groups than in lipo 20 µM ($p=0.040$), lipo 10 µM ($p=0.026$), lipo 5 µM ($p=0.025$), and the void ($p=0.025$). Another important regulator of browning is UCP1. Its gene expression levels were significantly lower in free 5 µM than in free 20 µM ($p=0.036$), lipo 20 µM ($p=0.002$), lipo 10 µM ($p=0.015$), and the void ($p=0.05$). However, PRDM16 exhibited similar gene expression levels ($p > 0.05$) for all groups of N.

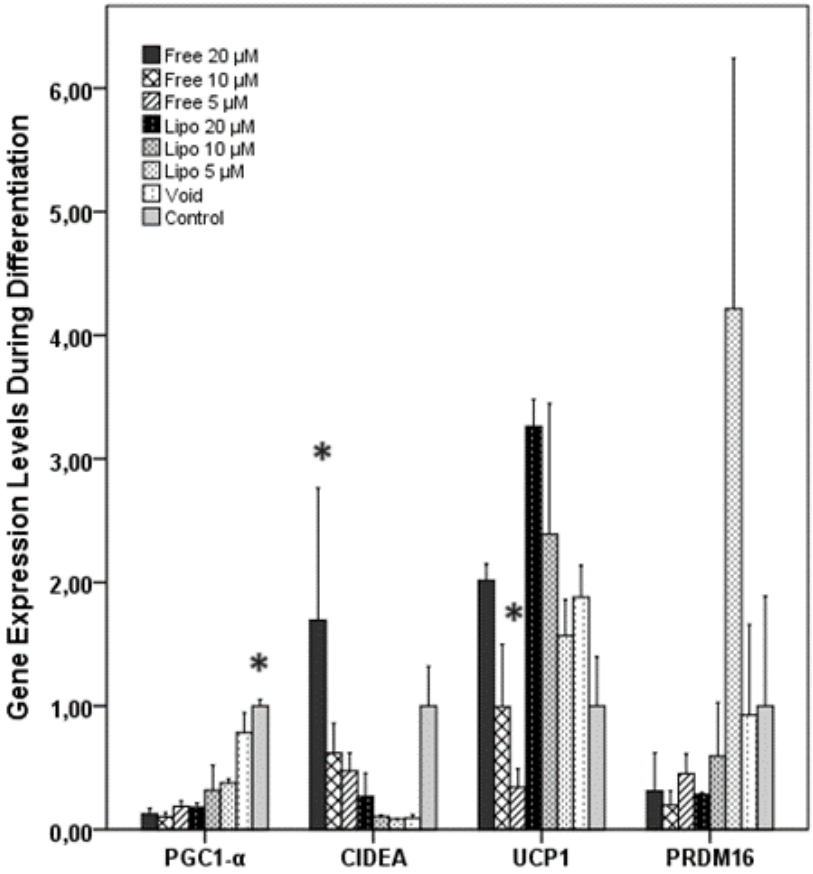

*, $p < 0.05$ compared to their controls.

Figure 4.13. PGC1-α, CIDEA, UCP1, and PRDM16 gene expression levels of naringenin in the differentiation process.

PPARγ, C/EBPβ, and FABP4 showed similar gene expression levels ($p > 0.05$) in all free B groups in the differentiation (Figure 4.14). There were no significant difference detected among the groups ($p>0.05$).

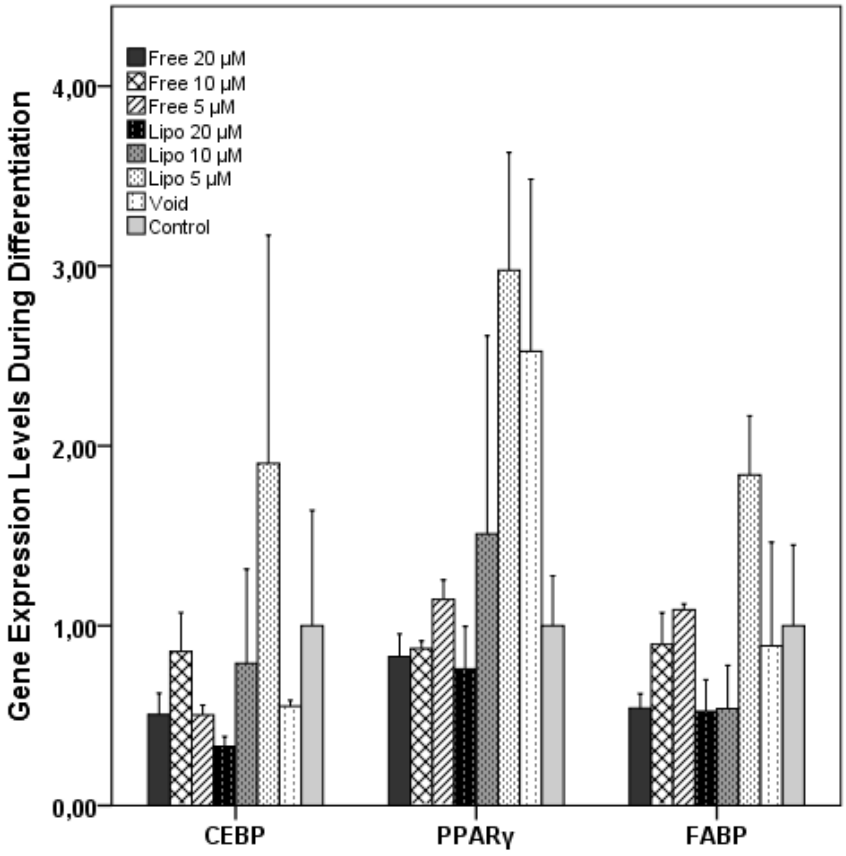

Figure 4.14. C/EBPβ, PPARγ, and FABP4 gene expression levels of berberine in the differentiation process.

During the differentiation process, the expression levels of two key regulators of browning, CIDEA and PRDM16, were similar across all forms of B ($p > 0.05$) (Figure 4.15). However, PGC1-α expression levels were higher in free 5 µM compared to lipo 20 µM ($p = 0.014$) and lipo 10 µM of B ($p = 0.032$). Furthermore, UCP1 expression was higher in free 20 µM than in lipo 20 µM ($p = 0.017$), lipo 10 µM ($p = 0.035$), and the control group ($p = 0.004$). Additionally, in free 10 µM of B, it was significantly higher than in lipo 10 µM ($p = 0.025$), the control group ($p = 0.003$), and lipo 20 µM ($p = 0.012$).

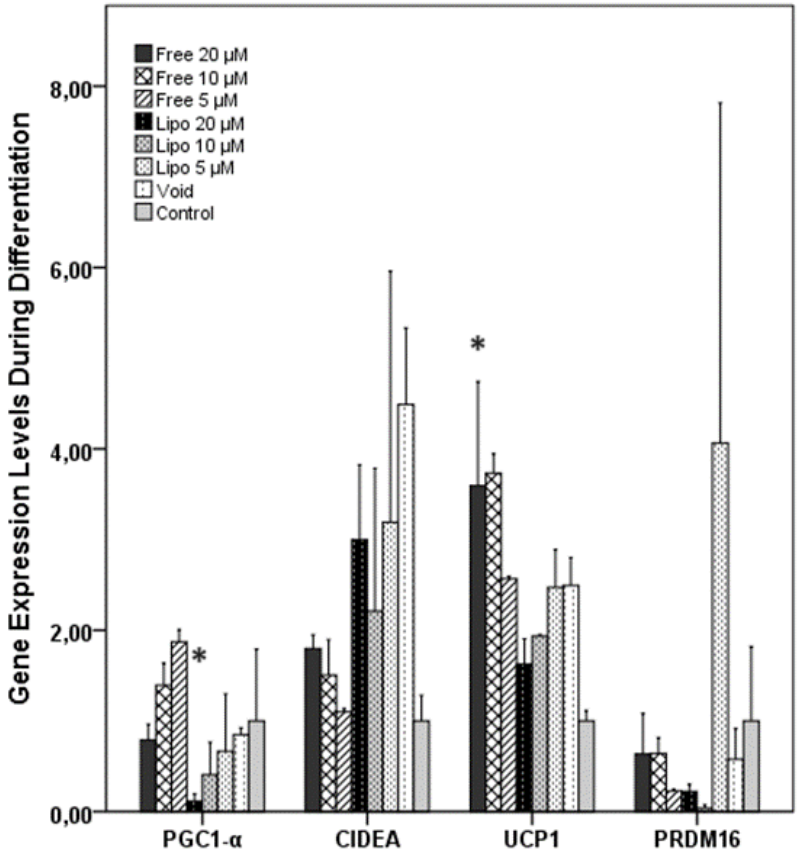

*, $p < 0.05$ compared to their controls.

Figure 4.15. PGC1-α, CIDEA, UCP1, and PRDM16 gene expression levels of berberine in the differentiation process.

4.2.2. Protein Concentration

UCP1 protein concentration for every phytochemical were compared (Table 4.4). There was not a significant difference between free D groups for UCP1 protein concentration ($p>0.05$). Moreover, there was not a significant difference for free N, free B, lipo N, and lipo B groups for UCP1 protein concentration ($p>0.05$).

PGC1-α protein concentration for every phytochemical were analyzed (Table 4.4). Free 20 µM of D was significantly higher than 5 µM and control group ($p<0.05$). PGC1-α protein concentration was significantly higher in free N 20, 10, and 5 µM than the control group. Moreover, lipo N 20 µM was significantly higher than 10, 5 µM, void, and control group. PGC1-α protein concentration was significantly lower in the control group than in free B 20, 10, and 5 µM ($p<0.05$). Finally, the control group had significantly lower PGC1-α protein concentration than lipo B 20, 10, 5 µM, and void group ($p<0.05$).

PPARγ protein concentration levels in both free and lipo D, N, and B were analyzed by one-way Anova (Table 4.1). First of all, PPARγ protein concentration for free D were compared. The control group was significantly higher than free D 20, 10, and 5 μM ($p<0.05$). Secondly, PPARγ protein concentration for free and lipo N were analyzed. The control group of free N was significantly higher than free N 5 μM ($p=0.028$). Furthermore, there was not a significant difference in PPARγ protein concentration levels in all lipo N groups and free B ($p<0.05$). Finally, the control group of lipo B was significantly higher than the void group ($p<0.05$). Lipo B 20, 10, and 5 μM were significantly higher than the void group ($p<0.05$).

Table 4.1. Effect of free and liposomal forms of delphinidin, naringenin and berberine on UCP1, PGC1-α and PPARγ concentration in the differentiation process [1, 2, 3]

	Protein Concentration (mg/dL)		
	UCP1	**PGC1-α**	**PPARγ**
Delphinidin			
Free 20	46.1 ± 4.67	40.1 ± 4.20 [a]	75.7 ± 1.73 [a]
Free 10	37.5 ± 3.42	36.8 ± 0.54 [a, b]	80.3 ± 2.52 [a]
Free 5	37.5 ± 8.81	30.9 ± 0.65 [b]	80.0 ± 2.91 [a]
Control	40.6 ± 4.14	28.6 ± 0.86 [b]	88.6 ± 2.72 [b]
	p>0.05	**p<0.05**	**p<0.05**
Naringenin			
Free 20	41.6 ± 3.78	34.6 ± 3.99 [a]	80.1 ± 5.01 [a, b]
Free 10	41.7 ± 7.92	35.5 ± 1.73 [a]	78.0 ± 0.00 [a, b]
Free 5	47.3 ± 1.80	35.3 ± 0.86 [a]	73.5 ± 2.49 [b]
Control	43.1 ± 0.54	28.1 ± 0.96 [b]	83.7 ± 2.29 [a]
	p>0.05	**p<0.05**	**p<0.05**
Lipo 20	58.4 ± 34.73	44.5 ± 3.01 [a]	80.8 ± 0.96
Lipo 10	35.8 ± 1.63	32.4 ± 5.18 [b]	81.0 ± 10.01
Lipo 5	39.8 ± 9.90	33.6 ± 0.31 [b]	77.6 ± 1.36
Void	32.7 ± 0.54	29.8 ± 0.11 [b]	79.2 ± 5.20
Control	28.9 ± 1.26	32.0 ± 0.33 [b]	85.3 ± 0.76
	p>0.05	**p<0.05**	p>0.05
Berberine			
Free 20	37.4 ± 4.31	32.5 ±1.61 [a]	80.4 ± 2.69
Free 10	66.2 ± 23.76	35.8 ± 0.44 [a]	85.3 ± 6.93
Free 5	34.0 ± 4.85	36.2 ± 2.47 [a]	78.4 ± 3.25
Control	34.0 ± 1.26	26.0 ± 0.55 [b]	89.7 ± 8.12
	p>0.05	**p<0.05**	p>0.05
Lipo 20	43.1 ± 5.22	47.6 ± 1.07 [a]	82.5 ± 2.88 [a, c]
Lipo 10	34.5 ± 0.54	43.2 ± 1.82 [a]	82.3 ± 0.00 [a, c]
Lipo 5	41.7 ± 9.35	41.0 ± 4.41 [a]	86.3 ± 2.88 [a, c]
Void	34.0 ± 3.41	40.9 ± 3.55 [a]	75.0 ± 0.76 [b]
Control	41.6 ± 13.14	26.0 ± 0.21 [b]	88.9 ± 1.92 [b, c]
	p>0.05	**p<0.05**	**p<0.05**

[1]Data were analyzed by one-way ANOVA
[2]Data are presented as mean ± SD
[3]Means within a column without a common letter differ, p<0.05

4.2.3. Triglyceride Levels

TG concentration of free and lipo D, N, and B in the differentiation process were analyzed (Table 4.2). Free 20 μM D was significantly higher than free 10, 5 μM, and the control group. There was a substantial variation evident among all groups. ($p<0.001$). TG concentration of free N was significantly higher in 5 μM than 20,10

μM, and the control group ($p<0.05$). However, there was not a significant difference between lipo groups of N ($p>0.05$).

TG concentration of free B was significantly difference between free 20, 10, 5 μM, and the control group ($p<0.05$). Moreover, lipo 10 μM had significantly higher TG concentration than lipo 20, 5 μM, void, and the control group ($p<0.001$).

Table 4.2. Effect of free and liposomal forms of delphinidin, naringenin and berberine on triglyceride concentration in the differentiation process [1, 2, 3]

	Triglyceride Concentration (mg/dL)		
	Delphinidin	**Naringenin**	**Berberine**
Free 20	67.7 ± 1.10 **a**	54.9 ± 1.99 **a**	42.3 ± 1.77 **a**
Free 10	28.8 ± 1.33 **b**	58.0 ± 6.41 **a**	57.4 ± 0.22 **b**
Free 5	43.2 ± 3.54 **c**	88.3 ± 6.85 **b**	64.4 ± 4.42 **c**
Control	52.9 ± 0.88 **d**	41.2 ± 2.43 **c**	34.4 ±0.88 **d**
	p<0.001	**p<0.05**	**p<0.05**
Lipo 20	-	19.9 ± 1.10	15.8 ± 0.22 **a**
Lipo 10	-	25.4 ± 7.51	137.6 ± 5.75 **b**
Lipo 5	-	31.6 ± 1.33	23.3 ± 1.99 **a**
Void	-	23.8 ± 10.61	22.4 ± 3.31 **a**
Control	-	20.4 ± 0.88	23.5 ± 0.00 **a**
		p>0.05	**p<0.001**

[1]Data were analyzed by one-way ANOVA
[2]Data are presented as mean ± SD
[3]Means within a column without a common letter differ, $p<0.05$

Summary of the Results in the Differentiation Process

- ✓ PPARγ, C/EBPβ, and FABP4 gene expression levels in free D were similar in all groups ($p>0.05$).
- ✓ PGC1-α gene expression levels were significantly higher in control group than 10 μM D ($p=0.047$).
- ✓ CIDEA gene expression levels in free D were similar in all groups ($p>0.05$).
- ✓ UCP-1 gene expression levels were significantly lower in 20 μM D than other groups ($p<0.05$). Moreover, 5 μM D had the highest UCP-1 gene expression levels.

- ✓ The control group had significantly higher PRDM16 gene expression levels than 20, 10, and 5 μM of D ($p<0.001$).
- ✓ C/EBPβ, and FABP4 gene expression levels in all N groups were similar in all groups ($p>0.05$).
- ✓ PPARγ gene expression levels in free 20 μM of N were significantly higher than lipo 20 μM than other groups ($p<0.05$)
- ✓ PGC1-α gene expression levels in N were significantly higher in the control groups than other groups ($p<0.05$).
- ✓ CIDEA gene expression levels were higher in free 20 μM N groups than other groups ($p<0.05$).
- ✓ UCP1 gene expression levels were significantly lower in free 5 μM than in free 20 μM ($p=0.036$), lipo 20 μM ($p=0.002$), lipo 10 μM ($p=0.015$), and the void ($p=0.05$).
- ✓ PRDM16 exhibited similar gene expression levels ($p > 0.05$) for all groups of N.
- ✓ PPARγ, C/EBPβ, and FABP4 gene expression levels in free B were similar in all groups ($p>0.05$).
- ✓ CIDEA and PRDM16, were similar across all forms of B ($p > 0.05$)
- ✓ PGC1-α expression levels were higher in free 5 μM compared to lipo 20 μM ($p =0.014$) and lipo 10 μM of B ($p =0.032$).
- ✓ UCP1 expression was higher in free 20 μM than in lipo 20 μM ($p =0.017$), lipo 10 μM ($p=0.035$), and the control group ($p =0.004$).
- ✓ There was not a significant difference between free D groups for UCP1 protein concentration ($p>0.05$).
- ✓ There was not a significant difference for free N, free B, lipo N, and lipo B groups for UCP1 protein concentration ($p>0.05$).
- ✓ PGC1-α protein concentration free 20 μM of D was significantly higher than 5 μM and control group ($p<0.05$).
- ✓ PGC1-α protein concentration was significantly higher in free N 20, 10, and 5 μM than the control group. Moreover, lipo N 20 μM was significantly higher than 10, 5 μM, void, and control group.

- ✓ PGC1-α protein concentration was significantly lower in the control group than in free B 20, 10, and 5 μM ($p<0.05$). The control group had significantly lower PGC1-α protein concentration than lipo B 20, 10, 5 μM, and void group ($p<0.05$).
- ✓ PPARγ protein concentration for free D were compared. The control group was significantly higher than free D 20, 10, and 5 μM ($p<0.05$).
- ✓ PPARγ protein concentration of control group of free N was significantly higher than free N 5 μM ($p=0.028$). Furthermore, there was not a significant difference in PPARγ protein concentration levels in all lipo N groups and free B ($p<0.05$).
- ✓ PPARγ protein concentration of lipo B 20, 10, and 5 μM were significantly higher than the void group ($p<0.05$).

4.3. Maturation Process

4.3.1. Gene Expression Levels

Gene expression data from RT-PCR experiments were analyzed by one-way ANOVA to compare mean gene expression levels (PPARγ, C/EBPβ, PGC1-α, CIDEA, FABP4, UCP1, PRDM16) among different types of treatment during the maturation process. Furthermore, LSD or Games-Howell was used to compare the difference between the groups.

PPARγ, C/EBPβ, and FABP4 showed similar gene expression levels ($p > 0.05$) in all free D concentration in the maturation process (Figure 4.16).

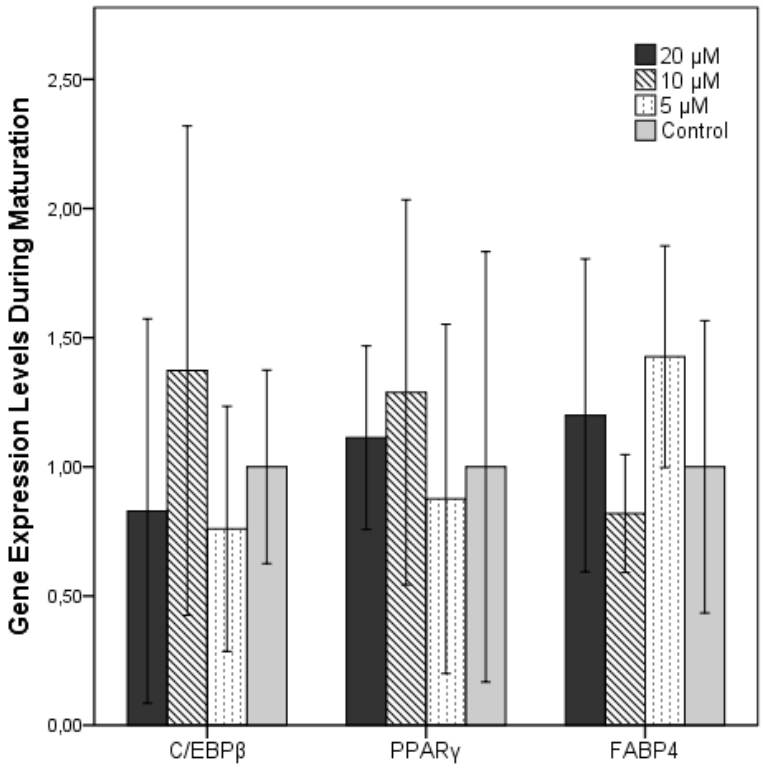

Figure 4.16. C/EBPβ, PPARγ, and FABP4 gene expression levels of delphinidin in the maturation process.

The key regulators of browning in the maturation process did not changed for PGC1-α, CIDEA, UCP1 among free D groups (Figure 4.17). Only PRDM16 gene expression levels for D were significantly higher in the 20 µM group (p= 0.037).

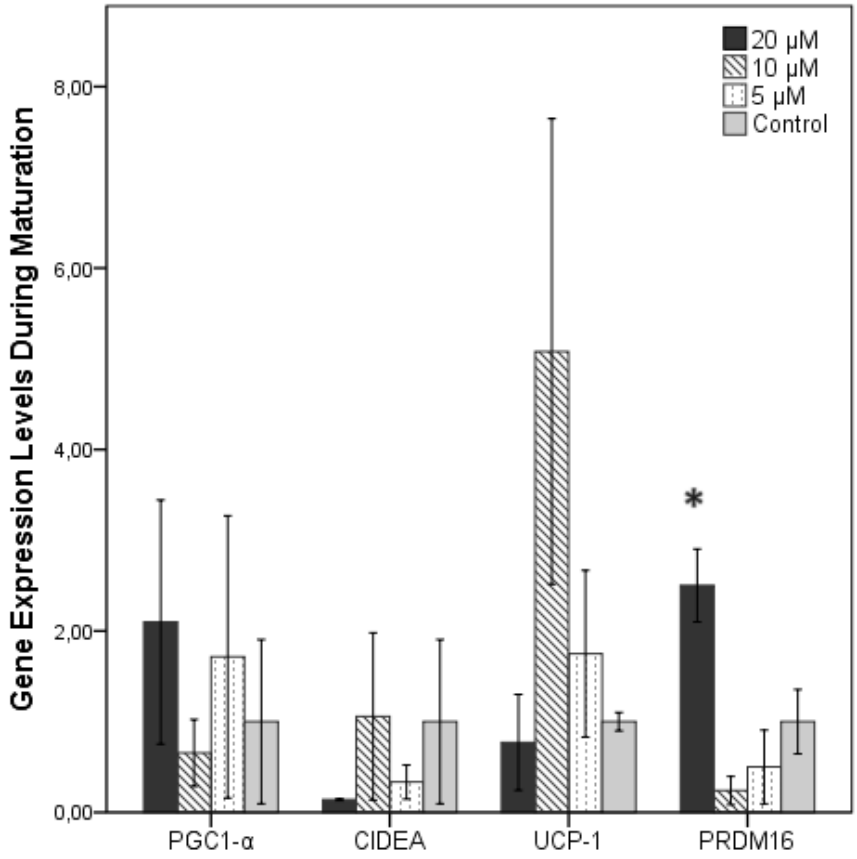

*, $p < 0.05$ compared to their controls.

Figure 4.17. PGC1-α, CIDEA, UCP1, and PRDM16 gene expression levels of delphinidin in the maturation process.

In the maturation process C/EBPβ and PPARγ exhibited similar gene expression levels ($p > 0.05$) for all groups of N (Figure 4.18). FABP4 expression levels of free 10 µM N was significantly higher than free 20 µM ($p=0.011$), free 5 µM ($p=0.026$), lipo 20 µM ($p=0.011$), lipo 10 µM ($p=0.013$), lipo 5 µM ($p=0.002$), the void ($p=0.032$), and the control groups ($p=0.017$).

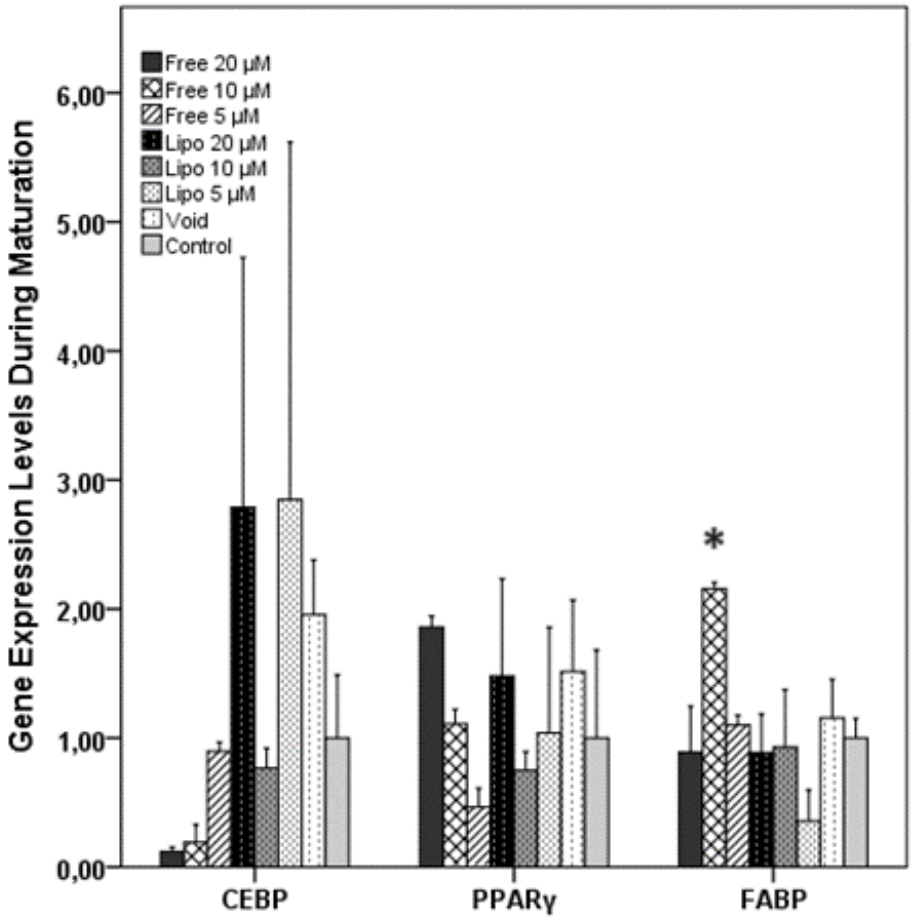

*, $p < 0.05$ compared to their controls.

Figure 4.18. C/EBPβ, PPARγ, and FABP4 gene expression levels of naringenin in the maturation process.

During the maturation process, the expression levels of CIDEA and UCP1 genes were similar across all forms of N ($p > 0.05$) (Figure 4.19). However, PRDM16 gene expression levels were significantly higher at 20 µM compared to free 20 µM ($p = 0.000$), free 10 µM ($p = 0.000$), free 5 µM ($p = 0.000$), lipo 10 µM ($p = 0.000$), lipo 5 µM ($p = 0.001$), void lipo ($p = 0.005$), and control groups ($p = 0.000$). Additionally, PGC1-α gene expression levels were significantly higher in free 5 µM than in lipo 10 µM ($p = 0.038$), lipo 5 µM ($p = 0.040$), and void ($p = 0.050$).

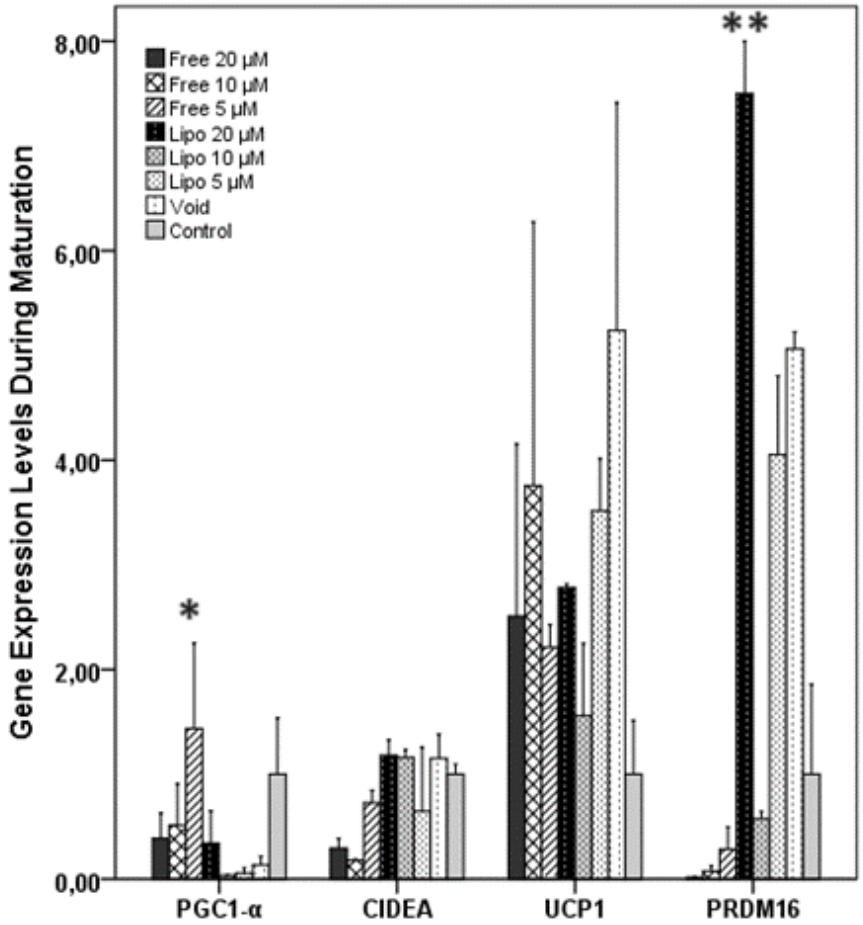

*, $p < 0.05$; **, $p < 0.01$ compared to their controls.

Figure 4.19. PGC1-α, CIDEA, UCP1, and PRDM16 gene expression levels of naringenin in the maturation process.

In the maturation process, all forms of B did not alter C/EBPβ gene expression levels (Figure 4.20). However, PPARγ gene expression levels were significantly higher in lipo 5 µM compared to free 20 µM (p=0.023), free 5 µM (p=0.013), lipo 20 µM (p=0.004), lipo 10 µM (p=0.036), and control (p=0.014). Additionally, PPARγ gene expression levels were significantly higher in free 10 µM than in lipo 20 µM (p=0.012) and control (p=0.042). Finally, FABP4 gene expression levels were significantly higher in lipo 20 µM compared to free 10 µM (p=0.021) and lipo 5 µM (p=0.029).

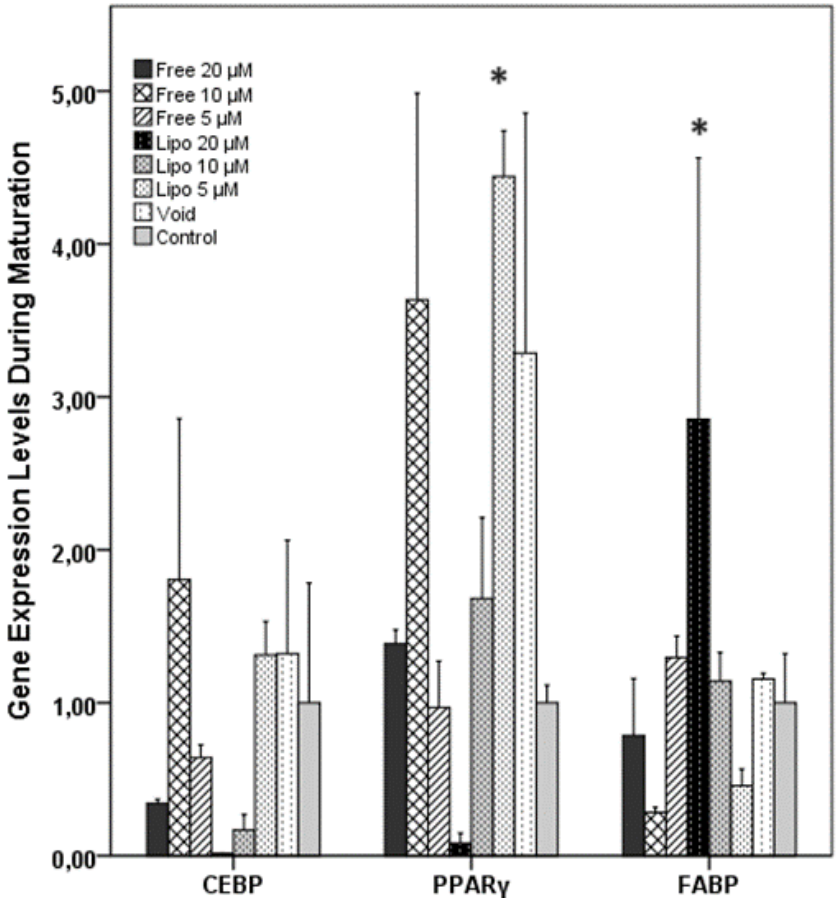

*, $p < 0.05$ compared to their controls.

Figure 4.20. C/EBPβ, PPARγ, and FABP4 gene expression levels of berberine in the maturation process.

During the maturation process, various forms of B induced significant changes in all the key regulators of browning (Figure 4.21). Firstly, PGC1-α expression was significantly higher in void groups compared to free 20 µM ($p = 0.004$), free 5 µM ($p = 0.026$), lipo 20 µM ($p = 0.002$), lipo 10 µM ($p = 0.019$), and control ($p = 0.005$). Secondly, CIDEA expression in B was significantly higher in free 10 µM compared to free 5 µM ($p = 0.009$), lipo 20 µM ($p = 0.001$), lipo 10 µM ($p = 0.001$), lipo 5 µM ($p = 0.011$), and the control group ($p = 0.004$). Thirdly, UCP1 gene expression levels were significantly lower in lipo 20 µM than in free 10 µM ($p = 0.008$) and free 5 µM ($p = 0.027$). Fourthly, PRDM16 expression levels in the void group were higher than all different groups of B; especially compared to free 20 µM ($p = 0.007$), free 10 µM

(p = 0.041), free 5 μM (p = 0.009), lipo 20 μM (p = 0.012), lipo 10 μM (p = 0.035), lipo 5 μM (p = 0.047), and control (p = 0.015).

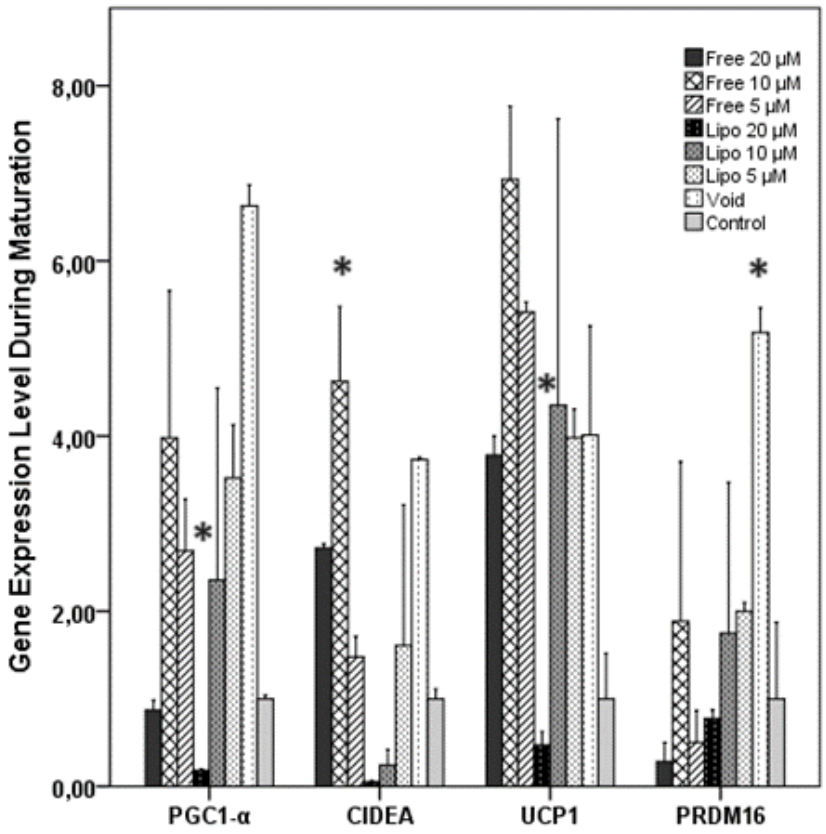

*, p < 0.05 compared to their controls.

Figure 4.21. PGC1-α, CIDEA, UCP1, and PRDM16 gene expression levels of berberine in the maturation process.

4.3.2. Protein Concentration

UCP1 protein concentration for each phytochemical were analyzed (Table 4.3). There was not a significant difference between free D groups for UCP1 protein concentration (p>0.05). Moreover, there was not a significant difference for free N, free B, and lipo N groups for UCP1 protein concentration (p>0.05). Only the control group of lipo B had significantly higher UCP1 protein concentration than lipo 20, 10, 5 μM, and void group (p<0.05).

PGC1-α protein concentration of free and lipo D, N, and B were compared (Table 4.3). Free 10 μM of D was significantly higher than 5 μM (p=0.011). PGC1-α protein concentration was significantly higher in free N 5 μM and control group than

in free 20 and 10 μM. Moreover, lipo N 20 and 10 μM was significantly lower than the 5 μM, void, and control groups ($p<0.05$). PGC1-α protein concentration in lipo and free B were not significantly different in all groups ($p>0.05$).

PPARγ protein concentration levels in both free and lipo were compared in the maturation process. First of all, PPARγ protein concentration for free D were compared. The control group was significantly lower than free D 20, 10, and 5 μM ($p<0.05$). Secondly, free and lipo N were compared. Control group of free N and 20 μM was significantly lower than free N 10 and 5 μM ($p<0.05$). Furthermore, there was not a significant difference of PPARγ protein concentration levels in all lipo N groups and lipo B ($p<0.05$). Finally, the control group of free B was significantly lower than free 5 μM ($p=0.029$).

Table 4.3. Effect of free and liposomal forms of delphinidin, naringenin and berberine on UCP1, PGC1-α and PPARγ concentration in the maturation process [1, 2, 3]

	Protein Concentration (mg/dL)		
	UCP1	**PGC1-α**	**PPARγ**
Delphinidin			
Free 20	33.5 ± 0.91	31.4 ± 1.82 [a, b]	86.3 ± 1.36 [a]
Free 10	46.8 ± 17.64	34.0 ± 0.33 [a]	87.0 ± 1.53 [a]
Free 5	41.0 ± 4.31	29.5 ± 0.33 [b]	85.2 ± 1.75 [a]
Control	35.1 ± 3.24	31.4 ± 0.75 [a, b]	72.9 ± 3.28 [b]
	p>0.05	**p<0.05**	**p<0.05**
Naringenin			
Free 20	31.0 ± 1.44	28.0 ± 0.86 [a]	79.9 ± 1.92 [a]
Free 10	34.6 ± 9.35	26.6 ± 0.21 [a]	86.4 ± 0.37 [b]
Free 5	40.5 ± 2.52	31.4 ± 1.73 [b]	84.9 ± 0.20 [b]
Control	37.7 ± 0.37	31.4 ± 0.54 [b]	77.6 ±1.36 [a]
	p>0.05	**p<0.05**	**p<0.05**
Lipo 20	44.4 ± 13.14	27.0 ± 1.82 [a]	81.9 ± 0.96
Lipo 10	34.9 ± 0.72	25.8 ± 0.33 [a]	77.1 ± 0.76
Lipo 5	34.1 ± 5.03	34.4 ± 2.57 [b, c]	87.7 ± 0.20
Void	43.3 ± 10.44	31.6 ± 1.40 [b, c]	81.8 ± 2.69
Control	31.6 ± 1.44	30.7 ± 0.42 [a, c]	88.6 ± 9.64
	p>0.05	**p<0.05**	p<0.05
Berberine			
Free 20	34.6 ± 6.83	29.0 ± 0.98	85.9 ± 2.32 [a, b]
Free 10	41.7 ± 1.80	28.0 ± 0.86	84.1 ± 3.28 [a, b]
Free 5	39.3 ± 2.35	29.3 ± 1.84	87.2 ± 2.32 [a]
Control	36.0 ± 0.89	30.6 ± 0.64	79.5 ± 0.57 [b]
	p>0.05	p>0.05	**p=0.029**
Lipo 20	37.5 ± 4.50 [a]	28.8 ± 0.76	82.1 ± 6.93
Lipo 10	37.0 ± 3.05 [a]	30.2 ± 0.33	79.5 ± 5.20
Lipo 5	35.5 ± 4.13 [a]	28.2 ± 1.40	82.6 ± 1.53
Void	37.7 ± 3.59 [a]	28.0 ± 2.36	85.1 ± 0.37
Control	52.0 ± 1.61 [b]	27.5 ± 0.10	75.1 ± 1.73
	p<0.05	p>0.05	p>0.05

[1]Data were analyzed by one-way ANOVA
[2]Data are presented as mean ± SD
[3]Means within a column without a common letter differ, p<0.05

4.3.3. Triglyceride Levels

TG concentration of free and lipo D, N, and B were compared in the maturation process (Table 4.4). Free 20 μM D was significantly higher than free 10, 5 μM ($p<0.05$). Free 10 μM D had significantly the lowest TG concentration ($p<0.05$).

The triglyceride concentration of free N was notably higher in the 20, 10, and 5 μM groups compared to the control group ($p<0.05$). Moreover, the void group's TG was significantly higher than of control and lipo 20 μM groups ($p<0.05$). A notable distinction was observed among liposomal formulations containing 20, 10, and 5 μM of N ($p<0.05$).

TG concentration of free B, there was a significant difference between free 20, 10, 5 μM, and control groups ($p<0.05$). Furthermore, the control group had significantly lower TG concentration than the void group ($p<0.05$). Lipo B 20, 10, 5 μM TG concentrations were very similar ($p>0.05$).

Table 4.4. Effect of free and liposomal forms of delphinidin, naringenin and berberine on triglyceride concentration in the maturation process [1, 2, 3]

	Triglyceride Concentration (mg/dL)		
	Delphinidin	**Naringenin**	**Berberine**
Free 20	29.4 ± 2.21 **a**	37.9 ± 2.21 **a, b**	36.0 ± 6.19 **a**
Free 10	17.7 ± 1.55 **c**	42.9 ± 9.72 **b**	33.3 ± 1.55 **a**
Free 5	21.5 ± 1.99 **c**	45.4 ± 0.88 **b**	37.4 ± 10.39 **a**
Control	52.9 ± 0.88 **b**	25.2 ± 3.33 **a**	15.1± 4.45 **b**
	p<0.05	**p<0.05**	**p<0.05**
Lipo 20	-	37.1 ± 2.87 **a, c**	23.9 ± 0.13 **a, b**
Lipo 10	-	33.2 ± 6.19 **a, b, c**	18.2 ± 3.98 **a, b**
Lipo 5	-	33.5 ± 3.98 **a, b, c**	23.2 ± 3.54 **a, b**
Void	-	42.5 ± 2.96 **a, c**	25.1 ± 4.86 **a**
Control	-	25.2 ± 3.33 **b**	15.1 ± 4.45 **b**
		p<0.05	**p<0.05**

[1]Data were analyzed by one-way ANOVA
[2]Data are presented as mean ± SD
[3]Means within a column without a common letter differ, $p<0.05$

Summary of the Results in the Maturation Process

- ✓ PPARγ, C/EBPβ, and FABP4 showed similar gene expression levels ($p > 0.05$) in all free D groups in the maturation process.
- ✓ PGC1-α, CIDEA, UCP1 exhibited similar gene expression levels ($p > 0.05$) among free D groups. PRDM16 gene expression levels for D were significantly higher in the 20 μM group.
- ✓ C/EBPβ and PPARγ exhibited similar gene expression levels ($p > 0.05$) for all groups of N.
- ✓ FABP4 expression levels of free 10 μM of N was significantly higher than all groups ($p<0.05$)
- ✓ CIDEA and UCP1 genes expression levels were similar across all forms of N ($p > 0.05$)
- ✓ PRDM16 gene expression levels were significantly higher at 20 μM compared to all groups of N ($p<0.001$).
- ✓ PGC1-α gene expression levels were significantly higher in free 5 μM of N than in lipo 10 μM ($p = 0.038$), lipo 5 μM ($p = 0.040$), and void ($p = 0.050$).
- ✓ B did not alter C/EBPβ gene expression levels. However, PPARγ gene expression levels were significantly higher in lipo 5 μM compared to other groups ($p<0.05$)
- ✓ FABP4 gene expression levels were significantly higher in lipo 20 μM compared to free 10 μM ($p=0.021$) and lipo 5 μM ($p=0.029$).
- ✓ PGC1-α expression was significantly higher in void groups compared to different group of B($p<0.05$).
- ✓ CIDEA expression in B was significantly higher in free 10 μM compared to all B groups.
- ✓ UCP1 gene expression levels were significantly lower in lipo 20 μM of B than in free 10 μM ($p = 0.008$) and free 5 μM ($p = 0.027$).
- ✓ PRDM16 expression levels in the void group were higher than all different groups of B ($p<0.05$)
- ✓ There was not a significant difference between free D groups for UCP1 protein concentration ($p>0.05$).

- ✓ There was not a significant difference for free N, free B, and lipo N groups for UCP1 protein concentration ($p>0.05$).
- ✓ PGC1-α protein concentration of free 10 μM of D was significantly higher than 5 μM ($p=0.011$).
- ✓ PGC1-α protein concentration was significantly higher in free N 5 μM than in free 20 and 10 μM. Moreover, lipo N 20 and 10 μM was significantly lower than other groups ($p<0.05$).
- ✓ PGC1-α protein concentration in lipo and free B were not significantly different in all groups ($p>0.05$).
- ✓ PPARγ protein concentration for free D were compared. Free D 20, 10, and 5 μM was significantly higher than the control group ($p<0.05$).
- ✓ Free and lipo N were compared. Free N 20 μM was significantly lower than other groups ($p<0.05$). There was not a significant difference of PPARγ protein concentration levels in all lipo N groups and lipo B ($p<0.05$).
- ✓ PPARγ protein concentration levels of free 5 μM were significantly higher than the control group of free B ($p=0.029$).

4.4. Cell Viability Assays (MTT)

Liposomal and free forms of D, N, and B at the tested doses to verify cell viability in 3T3-L1 cells were compared after 24 or 48 h (Table 4.5). Free D at different doses did not affect the cell viability negatively after 24 h ($p>0.05$). The findings indicate that both liposomal and free forms of N and B exhibited markedly reduced cell viability after 48 hours ($p<0.05$). Especially, lipo B at different doses had significantly lower cell viability.

Table 4.5. Cell viability assays of free and liposomal forms delphinidin, naringenin, and berberine [1, 2, 3]

	Cell Survival Rate %					
	24 h			48 h		
	Delphinidin	**Naringenin**	**Berberine**	**Delphinidin**	**Naringenin**	**Berberine**
Free 20	77.1 ± 6.34 [a]	77.2 ± 10.28 [a]	61.3 ± 0.47 [a]	60.2 ± 3.03 [a]	47.5 ± 1.04 [a]	43.3 ± 7.47 [a]
Free 10	82.8 ± 3.15 [a]	82.7 ± 11.64 [a]	71.6 ± 2.67 [a]	58.1 ± 4.47 [a]	63.1 ± 8.29 [b]	56.6 ± 16.72 [b]
Free 5	79.3 ± 2.64 [a]	79.4 ± 2.64 [a]	70.6 ± 2.69 [a]	69.7 ± 0.08 [a]	46.7 ± 0.24 [a]	55.7 ± 1.95 [b]
Control	95.8 ± 1.01 [a]	95.8 ± 1.01 [b]	95.8 ± 1.01 [b]	81.9 ± 3.73 [b]	81.9 ± 3.73 [b]	81.9 ± 3.73 [c]
Lipo 20	-	90.1 ± 13.30 [a]	50.4 ± 4.40 [a]	-	54.9 ± 0.72 [a]	24.6 ± 13.50 [a]
Lipo 10	-	85.7 ± 2.94 [a]	74.8 ± 1.72 [b, c]	-	62.1 ± 5.74 [b]	61.4 ± 21.37 [b]
Lipo 5	-	81.5 ± 16.33 [a, b]	80.7 ± 0.92 [b, c]	-	60.7 ± 1.91 [b]	49.7 ± 13.27 [b]
Void	-	72.8 ± 1.78 [a]	50.5 ± 0.61 [a]	-	34.5 ± 19.21 [a]	48.9 ± 5.61 [a]

[1]Data were analyzed by one-way ANOVA
[2]Data are presented as mean ± SD
[3]Means within a column without a common letter differ, $p<0.05$

5. DISCUSSION

5.1. Characteristics of Encapsulated Phytochemical

5.1.1. Morphology of Particles

New research findings suggest that the distribution of nanocarriers within tissues varied based on their size, with nanocarriers around 200 nm being predominantly found in the liver, spleen, lung, and kidney of mice. Additionally, smaller quantities of nanocarriers were detected in tissues such as the pancreas, brain, stomach, and bloodstream (202). In the present study, the particle size was around 210 nm. Therefore, it may potentially be efficiently transported into the adipose tissue of obese mice.

In drug delivery applications using liposome and nanoliposome formulations, a PI≤0.3 was considered to be acceptable and indicates homogenous phospholipid vesicles (203). Therefore, the lower PI values signify a considerable degree of uniformity in liposome size, whereas higher PI values (>0.3) suggest greater heterogeneity (196). In the present research, consistent with the preceding studies, PI of both liposomal forms of B and N were around 0.32, therefore they are homogeneous.

Nanocarriers' surface charges are crucial for cellular absorption, biodistribution, and bioavailability (196). The main surface ingredient in encapsulated liposome N and B, soy PC, generated anionic charges on the surface of the particles (196). The electric attraction of negative charges among the particles allows for their stable dispersion and they have a strong attraction towards plasma lipoprotein particles (204). In the present research, the zeta potentials of freshly made liposome of B and N were negative.

5.1.2. Encapsulation Efficiency and Loading Capacity

In the current research, the encapsulation method for B and N was developed based on the method published by Zu et al. (194). Nanoencapsulated resveratrol (R) had soy-PC bilayers and a hydrophilic core as our nanocarriers. The impressive encapsulation efficiency and loading capacity of resveratrol stemmed from the dual-

phase properties of soy-PC. The resveratrol could be integrated into the regions of the hydrophobic fatty acid tails within the soy-PC bilayer (205). A significant amount of resveratrol is also accommodated by multiple PC bilayers on liposomes. Similarly, quercetin was nanoencapsulated and it had the same encapsulation efficiency and loading capacity (206). In according to the aforementioned studies, liposome B and N, with soy-PC bilayers and a hydrophilic core had high loading capacity and encapsulation efficiency.

5.1.3. In-Vitro Release Study

Zu et al. nanoencapsulated resveratrol was continuously released compared to free resveratrol (194). Hydrophobic substances, such as resveratrol, may release more quickly in their free state than from membrane soy-PC bilayers of nanocarriers (196). This was due to resveratrol distribution in the soy-PC bilayers. Moreover, nanoencapsulated quercetin likewise had more slow and steady diffusion than free form (206). Similarly, both N and B are hydrophobic compounds with poor stability and bioavailability. Their liposomal structures, unlike the free form, had a sustained release behavior in the 24 h period due to soy-PC bilayers.

5.1.4. Physical and Chemical Stability

Previous study showed that the inclusion of cholesterol into nanoencapsulated resveratrol enhances its physical stability (194). There were no substantial alterations observed in the diameter and zeta potential of resveratrol at both 22°C and 37°C over a period of 7 days, while the PI values consistently stayed below 0.2 (194). Similarly, liposomal forms of B and N maintained their physical stability at 4°C and 22°C for 10 days. However, both lipo at 37°C increased their diameter and PI values. A possible reason of reducing their stability is due to N and B phytochemicals are sensitive to heat. Moreover, encapsulation protected resveratrol from degradation regardless of dark or light (194). The hydrophobic resveratrol, encapsulated into the solid core, increased its chemical stability. Due to this, resveratrol enhanced its stability and prolong its release (196). In line with the mentioned study, the liposome protected N and B against degradation, whether exposed to darkness or light, and their protective efficacy was comparable at both 4°C and 22°C temperatures.

5.2. Differentiation and Maturation Process

5.2.1. Gene Expression Levels and Protein Concentration

- **PPARγ**

The transformation of preadipocytes into adipocytes depends on a highly regulated multistep cascade of transcription factors, among which PPARγ and C/EBP are two crucial regulators (207). Both of them are involved in the growth arrest that is required for adipocyte differentiation (208). There are two studies that evaluated the effect of D on PPARγ protein concentration and expression level. Firstly, 3T3-L1 cells treated with D (25, 50, and 100 μM) decreased the mRNA and protein expression of PPARγ in a dose-dependent (26). The main mechanism of D to attenuate adipogenesis and to promote lipid metabolism was increased phosphorylation of adenosine monophosphate-activated protein kinase (AMPK) (26). Secondly, D suppressed the expression of intermediate markers of PPARγ in 3T3-L1 cells (96). Moreover, group of anthocyanins, composed by D-3-O-glucoside and cyanidin-3-O-glucoside, reduced 3T3-L1 differentiation by reducing the expression of PPARγ (209). Nevertheless, in the present study, PPARγ protein concentration did not significantly change after D treatment, both in differentiation and in the maturation process. Furthermore, the mRNA expression of PPARγ did not change. Therefore, present results suggest no effect on the downregulation of this gene expression and anti-adipogenic effects. These results could be partially due to a treatment with a lower dose than others studies, where the D dose was five times greater than our concentration.

There are limited research on the effect of N on PPARγ levels, especially in 3T3-L1 adipocyte cells. N was reported to activate PPARγ, therefore, N might trigger the browning process and the formation of brown fat cells to provide anti-obesity advantages (123). *In vivo* studies showed that N (20 μM) treated 3T3-L1 cells decreased PPARγ levels (210). N treatment increased the phosphorylation levels of AMPK and this suppresses lipid synthesis (211) through downregulation of PPARγ and C/EBPα (212). In diabetic rats induced by STZ, N restored blood glucose levels, liver glycogen content, and serum lipid profile by activating both the PPARγ/GLUT4 signaling pathways simultaneously (213). In contrast to these studies, N did not

change PPARγ protein and gene expression levels in maturation process, however, it changed significantly in highest free dose during differentiation.

Numerous studies have demonstrated that B suppressed the mRNA and protein expression of adipogenesis-associated transcription factors, particularly PPARγ(214-216). Moreover, in 3T3-L1 cells B, the transcriptional activity of PPARγ in a dose-dependent manner (216). In human omental preadipocytes, B inhibited cell differentiation by down-regulating PPARγ2 and C/EBPα (217). Moreover, in diabetic mice, B reduced glycemia and lipid metabolic parameters by reducing the expressions of PPARγ, C/EBP, and PGC1α. However, in the present study, after B treatment there was a downregulation of PPARγ protein concentration only in the maturation process and not in differentiation. It may be a possible a major effect of higher encapsulated phytochemicals in the later stage of adipogenesis.

- **C/EBPβ**

CCAAT/enhancer-binding proteins (C/EBP)-β and -δ represent additional transcription factors critical to the intricate transcriptional cascade, particularly in the initial stages of adipocyte differentiation. (208). After this early gene is expressed, it subsequently regulates the expression of the two master regulators of adipogenesis, PPARγ and C/EBPα (218). Only one study showed the effect on C/EBPβ expression, and it showed D treatment significantly downregulated C/EBPβ and C/EBPδ expression in 3T3-L1 cells (96). Other studies, nonetheless, analyzed the effect on the intermediate adipogenic transcription factors, such as C/EBPα expression. Recently, the blue honeysuckle berry extract effect on lipogenesis started on day 2, and the results exhibited that it significantly reduced the protein expressions of C/EBPα (219). Moreover, treatment with anthocyanin oligomers decreased adipogenesis due to the downregulation C/EBPα by 84.08% (220). Lastly, D (25, 50, and 100 μM)-treated cells showed a decrease that varies based on the dosage in the mRNA and protein expression of C/EBPα (26). Findings of the current research was different with the prior research. The mRNA expression of C/EBPβ did not significantly decrease in dose-dependent manner. These outcomes may be partly attributable to administering a smaller dosage compared to other research.

There are only one study that evaluated the effect of N on C/EBPβ levels. N treated (25-10-1 μM) 3T3-L1 pre-adipocytes did not change their level of C/EBPβ (221). Another study evaluated the effect of Pruni Cortex, rich in sakuranetin and naringenin, in hepatocyte cells (222). Sakuranetin decreased the phosphorylation of the activator isoforms of C/EBPβ. A possible reason is due to the network of transcription factors that regulates adipogenesis. In general terms, two phases can be identified: the initial phase of differentiation, overseen by C/EBPβ and SREBP1C, and the subsequent phase, governed by PPARγ and C/EBPα (218). In the present study, as the first investigation, all forms of N with similar dosages did not alter the C/EBPβ level. Therefore, N did not seem to have an anti-adipogenic effect on C/EBPβ, a crucial transcription factor in early adipocyte differentiation.

In a cell study, B treatment (0.5, 1, 5, and 10 mcg) of 3T3-L1 cells during differentiation suppressed the expressions of C/EBPα and PPARγ. These two genes are the master coordinator of adipocyte differentiation. Moreover, B prevented the expression of C/EBPβ in the early stages of differentiation (53). In porcine adipocytes, B treated cells inhibitory C/EBPβ mRNA expression levels (223). B decreased lipid accumulation that varied according to the dosage administered and increased phosphorylation of AMPKα (223). However, in the present research, all form of B did not change C/EBPβ levels both in the differentiation process and maturation. It is necessary more studies with higher dose to evaluate the effect of B on C/EBPβ.

- **FABP4**

The expression of PPARγ and C/EBPα precedes the production of adiponectin and fatty acid-binding protein 4 (FABP4), which play crucial roles in the final differentiation and development of the fat cell phenotype. (218). There are only two studies that demonstrated the effect of the D. The initial research demonstrated a significant reduction in FABP4 expression throughout the adipogenesis process, indicating that D could be an effective anti-obesity compound due to its potent inhibition of fat cell development (96). The second study indicates that D inhibited mesenchymal stem cell adipogenesis and promoted chondrogenesis, as evidenced by the decrease of adiponectin expression and FABP4 (224). However, in our study, in the maturation and differentiation process, there were no observed effects. Therefore,

additional studies are necessary to further confirm the possible impact of FABP4 expression.

There is no study on N's effect on FABP4 gene expression levels. However, an *in vitro* study on N-treated 3T3-L1 adipocytes evaluated the level of FABP5. It showed that N downregulated FABP5 levels (210). In the present research, it was expected a down-regulation, but in the differentiation did not decrease the FABP4 levels, but in the maturation lipo N significantly decrease level of this gene. There is insufficient data to comprehend the absence of FABP4 expression reduction. This possibly indicates that N may not have an effect on adipogenesis.

There are also limited studies that evaluated the effect of B on FABP4 concentration. *In vivo* study, B decreased the protein concentration of both FABP4 and FABP5 in tumor tissues of MGC803 cells (225). In a recent animal study, HFD supplemented with B downregulated the mRNA expression levels of FABP (226). In contrast to the previous studies, B did not reduce the level of FABP4 in differentiation. There was a downregulation of FABP4 with free 10 μM of B. Additional research is necessary to determine the mechanism and the effect of B on FABP4

- **UCP1**

Stimulating BAT and initiating browning within WAT trigger the upregulation of UCP1 expression (227). There are no research on the effect of D on UCP1 levels, however, there are limited studies evaluating the anthocyanidin effect on this protein. They enhanced energy consumption by diminishing mitochondrial respiration and the breakdown of the mitochondrial proton gradient (228), alongside increasing the levels of UCP1 and UCP2 in both WAT and BAT (229). In a recent study, after treatment of beige-like adipocytes with anthocyanin-rich black soybean, the concentration of UCP1 within mitochondria was quintuple the amount observed in WAT. Moreover, the extracts dose-dependently increased the expression of UCP1 (230). In another research, the blue honeysuckle berry extract led to a marked elevation in the expression levels of the UCP1 protein in 3T3-L1 cells (219). Furthermore, grape seed flour containing complex anthocyanins induced browning of WAT in cultured adipocytes or high-fat diet (HFD)-fed mice (231). Likewise, in 3T3-L1 cells subjected to treatment with anthocyanin oligomers derived from the microbial fermentation of

grape skin, there was a notable enhancement in the levels of brown-fat characteristic protein and beige-specific genes, including UCP1. (220). On the contrary, current research showed that there was not a significant difference after D treatment for UCP1 protein concentration. Our study showed that there was not a significant difference after treatment for UCP1 protein concentration. However, it was observed the highest UCP1 expression levels were in 5μM delphinidin-exposed cells during the differentiation stage. This outcome indicates that D triggered the browning process in 3T3-L1 adipocytes, particularly during the initial stages of adipogenesis, although not proportionally to the dosage. Moreover, the current study is the first that uses only D and it is limited to demonstrating the preventive role of delphinidin as a thermogenic compound in adipocytes.

In vitro and *in vivo* studies demonstrated that N had a great inhibitory effect on UCP1 levels. In differentiated human subcutaneous adipose-derived stem cells showed that N increases gene expression of UCP1 (121). In animal research, N led to a decrease in body weight alongside a rise in energy consumption in both lean mice fed a standard diet and obese mice fed a high-fat diet (HFD) with Ldlr-/- mutation (232-234). N enhanced UCP1 expression and mitochondrial uncoupling in response to β-adrenergic agonist isoproterenol in 3T3-L1 adipocytes. It supposed that N had an effect on browning through enhancement of PKA/p38/PPARγ pathway. However, a recent study showed that N at 10 μM did not increase protein expression of brown marker UCP1 at the basal condition in 3T3-L1 adipocytes (235). Our study was controversial; according to the last study, there was not a significant difference after N treatment for UCP1 protein concentration and gene expression levels in the maturation. However, as previously mentioned studies, during the differentiation process, encapsulated high doses of N increased gene expression of UCP1. In the early stage of adipogenesis, N could induce browning in 3T3-L1 adipocytes.

There are numerous studies on the positive effect of B on the browning of adipose tissue, especially on UCP1 concentrations. In a recent investigation, treatment with B elevated the expression of UCP1 and mitochondrial function in both brown and white adipocytes by reducing ATP production. (236). B treated 3T3-L1 adipocytes increased UCP2 expression by activated AMPK (237). Animal studies indicated that administering B at a dosage of 5 mg/kg of body weight enhanced total energy

consumption by 20%. This rise in energy usage, coupled with the elevated levels of UCP1 and mitochondrial content in BAT, verified B's role in stimulating BAT (199). Moreover, gene expression analysis showed that OLZ-induced suppression of UCP1 expression was restored with berberine treatment (10). B regulated the transcription of UCP1 in adipocytes through AMPK activation and PGC-1α recruitment (238). Similar to the previous study, both free and lipo B-treated cells showed increased UCP1 protein and gene expression levels during both the differentiation and maturation processes. Thereby indicating its potential as a therapeutic target for modulating browning of adipose tissue.

- **PGC1-α**

PGC1-α and PRDM16 are recognized as essential controllers of the browning process and the expression of UCP1 mRNA (175, 239). PGC1-α increased oxygen consumption via mitochondrial activation and its expression increased in BAT (240). As the UCP1, there are no studies on the effect of D on PGC1-α, however, there are limited studies evaluating the anthocyanidin effect on this protein. In a recent research, the administration of anthocyanins (500 mg/kg/day) in rat BAT cell cultures led to a dose-dependent increase in the expression of PGC1-α compared to BAT from rats that were not fed anthocyanins. (230). Similarly, in 3T3-L1 cells increased PGC-1α protein concentration after treating with anthocyanin oligomers (220). In the present research, the protein concentration of PGC1-α was dose-dependently increased during maturation. However, D did not show significant alteration in PGC1α gene expression at any stage. Lack of increase of PGC1α expression suggests that D could have no effect on the browning of adipose cells.

There are limited studies that analyzed the effect of N on PGC1α expression levels. *In vivo* study showed that N induced thermogenic PGC1α expression in human white adipocytes (121). Moreover, N stimulation increases the mRNA expression of PGC1α in tumorigenic cells (123). Similarly, an *in vivo* study showed that N increased AMPK phosphorylation and effectively up-regulated PGC1α (241). In fact, N improved mitochondrial function due to its role in the AMPK-SIRT3 signaling pathway (242). Based on these studies, the current research demonstrated an elevation in PGC1α protein concentration, specifically observed during the maturation process.

Furthermore, there was an increase in PGC1α gene expression levels following treatment with free 10 μM N during maturation. However, the findings regarding PGC1α gene expression were inconclusive, with no clear dose-dependency observed for PGC1α increase.

As the other two phytochemicals, there are also limited studies for B. A recent study demonstrated that B promoted the expression of PGC1α and other factors that regulate mitochondrial genes in skeletal muscle (243). *In vivo* study showed that daily B injections (5mg/kg-1 per day) in db/db mice for 4 weeks enhanced the PGC1 expression in both white and brown adipose tissues through AMPK-related mechanisms (12). Therefore, B enhanced BAT activity via increasing PGC1α browning marker and facilitated the development of inguinal brown-like adipocytes through a pathway implicating AMPK and PGC1α (238). Surprisingly, in the present study, B treated cells did not alter significantly the protein concentration of PGC1α. Nevertheless, there was a notable yet uncertain increase in gene expression observed in the free 5 μM group during differentiation and in the void group during the maturation process. Additional investigation is required to fully comprehend the influence of PGC1α levels in adipocyte cells.

- **CIDEA**

CIDEA, a protein linked to lipid droplets, regulates beige adipocytes by inhibiting the repression of LXRα on the UCP1 enhancer. CIDEA is connected with genes like PGC-1α and UCP1, which play roles in thermogenesis, particularly during the conversion of WAT to BAT (244). There is no study on D effect on CIDEA expression. However, after treatment with anthocyanin oligomers beige-specific genes responsible for thermogenesis, CIDEA was noticeably up-regulated (220). Moreover, anthocyanin-rich black soybean extracts significantly up-regulated the expression of thermogenesis CIDEA (230). On the contrary, in the present study, treated cells did not increase the expression levels of this gene. CIDEA expression is strictly connected with UCP1, because in adipocytes induces the expression of UCP1. Therefore, this result is consistent with the previously examined result with a change in UCP1.

There is no research on N effect on CIDEA expression however, it was expected an upregulation of this gene. As anticipated, N upregulated CIDEA

expression levels proportionately to the dosage during differentiation, similar to the UCP1 gene. However, in the present study, N did not increase the levels of CIDEA during maturation. There is insufficient research to elucidate the correlation between CIDEA expression and N treatment.

There is only one study that evaluated the effect of B on the mRNA expression levels of CIDEA. B increased the expression of CIDEA in both brown and white adipose cells through AMPK-related mechanisms (12). According to this study, free B increased the expression levels of CIDEA, but only during the maturation process. Interestingly, lipo 20 μM B downregulated CIDEA, instead of the low free dose or encapsulated version. More studies, both *in vivo* and *in vitro*, could elucidate the effect of B on CIDEA.

- **PRDM16**

PRDM16 plays a crucial role as a transcription factor in controlling the thermogenic gene expression program within brown and beige adipocytes (224). PPARγ deacetylation is strictly connected with upregulation of PRDM16, which promotes browning (245). As far as our knowledge extends, this study presents the first examination of the effects of D on PRDM16. Only one previous study has investigated the treatment of anthocyanin oligomers in 3T3-L1 cells. This study revealed a notable increase in both the expression of the PRDM16 gene and proteins. (246). Consistent with this study, the present investigation revealed an upregulation of PRDM16 expression in proportion to the dosage, specifically during the maturation process. Surprisingly, PRDM16 showed a down-regulation during the differentiation process. Further research is essential to elucidate the preventive function of D as a thermogenic agent in adipocytes.

To our knowledge, there is only one study exhibited the effect of N on PRDM16. In human white adipocyte cultures and subcutaneous abdominal adipose cells were treated with N for 7–14 days. The study found no variations in the mRNA expression levels of PRDM16 (121). According to the previous study, N did not alter the PRDM16 levels during differentiation. However, in the maturation process, lipo 20 μM significantly upregulated the expression of PRDM16. Based on our findings, it appears that the highest encapsulated dose of N has a browning effect on 3T3-L1 cells.

Finally, there are numerous research that analyzed the effect of B on PRDM16. PRDM16 seems to be indispensable for B-induced brown adipogenesis and BAT thermogenesis (247). Administration of B to adipose cells led to heightened transcription of PRDM16 by stimulating the active demethylation of the PRDM16 promoter region in DNA. This process could potentially be instigated by the activation of AMPK. Moreover, in 3T3-L1 adipocyte B treatment increased significantly different beige adipocyte-specific factors, as PRDM16 (248). In the contrast to the mentioned studies, B did not increase the mRNA expression levels of PRDM16. The void encapsulated form upregulated PRDM16 expression level compared to other groups. Further investigation is needed to ascertain the impact of PRDM16, as it remains unclear why its levels did not rise

5.2.2. Triglyceride Levels

In vitro and *in vivo* studies exhibited that treatment with free D had a great inhibitory effect on TG levels in a dose-dependent manner. D effectively reduced intracellular TG accumulation *in vitro* study. The TG accumulation in HepG2 cells was reduced by 50% with 100 μM and 59% with 180 μM of D (21). Another study showed that 25, 50, and 100 μM of D reduced intracellular TG accumulation in 3T3-L1 cells by 30%, 38%, and 58%, respectively (96). Moreover, in the same study, cells were treated with 50 μM within various periods. The amount of intracellular TG accumulation was reduced more significantly in 3T3-L1 cells treated in the early stages of differentiation than in the intermediate or late stage (96).

Not only is the dose important but also the duration of the treatment and the stage at which the preadipocyte cells are that indicate when treatment is crucial. Initial administration of D resulted in more efficient suppression of lipid accumulation compared to treatment during later stages. (96). *In vivo* study, black soybean seed coat extract, which is composed of cyanidin-3-O-glucoside, D-3-O-glucoside, and peonidin-3-O-glucoside, reduced TG levels significantly within a high-fat diet and streptozotocin (STZ)-induced diabetic mice (249). In the present study, intracellular TG accumulation was significantly reduced by D. Nevertheless, TG did not decrease proportionally with dosage. Interestingly, in both process 10 μM of D reduced intracellular TG accumulation more than 20 μM. Moreover, 10 μM reduced TG levels

in the maturation process (67%) instead of the early differentiation process (46%). One potential explanation for these findings might be the postponed impact of D treatment on the progression of the cell cycle. The reduce of lipid D is largely attributed to the early stage of adipogenesis, but along with this study, the positive effect of D appears in the intermediate and late adipogenesis phases.

In vitro and *in vivo* studies exhibited that N had a great inhibitory effect on TG levels. Previous studies showed that 20 μM and 50 μM of N reduce significantly the intracellular TG content in 3T3-L1 adipocytes (250, 251). Moreover, N improved glucose-lipid metabolism and reduced diet-induced weight gain and in animal models (123). In obese rats, N reduced body weight, TG, and TC level (252). HFD-induced NAFLD rats were administered (orally) with N at different doses (10, 30, and 90 mg/kg) for 2 weeks and their TG and TC was significantly decreased in dose dependent manner (253). Furthermore, in a clinical study, encapsulated N 200 mg/day for 4 weeks decreased serum levels of TG, TC, and LDL (254). In contrast to previous studies, in the present research, free N did not decrease TG levels in both differentiation and maturation. Surprisingly, not even lipo N had an effect on TG concentration in both process. It could be due to the mechanisms of N in the triglyceride-lowering effect. In various studies receptor PPARα with PPARα agonists, decrease plasma TAG and reduces fatty liver by inducing peroxisomal fatty acid oxidation and hepatic mitochondrial (255-257). In the present study, PPAR protein expression did not show any difference, therefore, there are not differences in TG levels.

Finally, of all three phytochemicals, B is the one most studied. There are numerous studies, both *in vitro* and *in vivo*, on the positive effects of B on TG levels. B was found to be involved in the metabolism of TG in 3T3-L1 adipocytes (258). Another study showed that B in a dose-dependent manner (10-100 μM) in mature adipocytes through the associated mechanisms related to the AMPK pathway (259). Moreover, B treatment (5-10-20 μM) significantly suppressed the TG content in adipocytes in maturation in a dose-dependent manner (26, 37 and 43%, respectively) (260). B treatment in HFD-fed C57BL/6J mice reduced hepatic TG accumulation and decreased the other TG synthesis related genes (261). A recent study showed that C57BL/6J mice treated with 50 mg/kg/d and 100 mg/kg/d B decreased TC, TG, LDL, and increased HDL-C level (262). Additionally, lipo B had a significantly lowered TG

content and inhibited hepatic steatosis in db/db mice, especially in 100 mg/kg dose (263). Furthermore, a meta-analyses suggested that B improved obesity and hyperlipidemia in T2DM patients by reducing TC, TG, and LDL in the setting of several metabolic disorders (264). In contrast to all mentioned studies, in the present research free B did not reduce TG levels in differentiation and maturation process. However, 20 μM lipo B showed a positive effect on TG concentration during the differentiation process. Therefore, encapsulation of B can increase the bioavailability of this phytochemical and resulted more beneficial than free form.

5.3. Cell Viability Assays (MTT)

Studies evaluating the effects of D, N, and B on the cell viability assay in 3T3-L1 cells are limited. In a recent study, no cytotoxicity was observed at a D concentration of 100 μM for 72 h (26). Similarly, another study showed no adverse effects on cell viability for 300 μM of D for 24 and 48 h (96). Moreover, in a study, HepG2 cells treated with 100 μM and 180 μM of D did not show any cytotoxic effects for 24 h (21).

Even for free N, significant cellular toxicity was not observed for up to 25 μM concentrations in 3T3-L1 cells for 24 h (210). Furthermore, N cytotoxicity was negligible in 3T3-L1 adipocytes for 6 h for up to 50 μM (7).

There were conflicting reports about B cell viability, on the one hand, B showed no significant effect on cell viability, that was maintained at >90% of untreated adipocytes for up 20 μM (265). On the other hand, B had a minor effect on the viability of 3T3-L1 cells for up 64 μM (266) and cells B-treated were reduced by 45% with 20 μM (267).

As previous studies, our data suggest that free D treatments did not have a negative effect on cell viability after 24 h and 48 h. However, free and lipo B and N, had adverse effects after 48 h. The results indicate that free D is safe to use in free form, but free and lipo forms of B and N after 48 h could have a cytotoxic effect on 3T3-L1 cells.

6. CONCLUSION AND RECOMMENDATIONS

6.1. Conclusion

The anti-obesity effects of plant-based bioactive compounds, including flavanones, alkaloids, and anthocyanins, have been demonstrated for some phytochemicals. However, studies focusing on delphinidin, berberine, and naringenin remain insufficient. This dissertation investigated the effects of delphinidin, naringenin, and berberine, both in their free and encapsulated liposomal forms (except for delphinidin), on the browning of adipose cells in 3T3-L1 preadipocyte cell cultures. Our findings present controversial results. The findings suggested that:

1. The encapsulated liposomal form of naringenin and berberine were successfully produced.

2. The most physically stable encapsulated naringenin and berberine were stored at +4°C in black colored tubes by Zetasizer Nanoseries-ZS.

3. Encapsulated naringenin and berberine formulation was found to be more stable than the free form of phytochemicals by HPLC measurement.

4. Delphinidin likely did not alter the expression levels of key regulators of adipogenesis (PPARγ, C/EBPβ, FABP4).

5. Delphinidin might contribute to adipose cells browning, particularly through the increased expression of PRDM16. However, delphinidin did not alter the expressions of other key regulators (PGC1-α, CIDEA, UCP1)

6. Delphinidin only reduced triglyceride levels during the maturation process.

7. Delphinidin may not have a positive effect on the brown-fat signature proteins, especially on UCP-1 levels. However, PGC1-α protein concentration increased in dose dependent manner.

8. C/EBPβ, after free and liposomal naringenin treatment, did not modify their gene expression levels. However, PPARγ gene expression levels were significantly lower after liposomal 20 μM, 10 μM, and 5 μM of naringenin. Moreover, naringenin downregulated FABP4 levels in maturation process. Based on this results, the effect of naringenin on adipogenesis is unclear.

9. PGC1-α gene expression levels after treatment with free naringenin were significantly higher in the maturation, but not in the differentiation.

10. CIDEA gene expression levels were higher in free 20 μM naringenin groups than other groups. However, naringenin treatment did not change CIDEA levels in the maturation.

11. UCP1 gene expression levels were significantly higher in liposomal encapsulated 20 μM, 10 μ, and free 10 μM naringenin forms in the differentiation process. Naringenin probably could have an effect on early stage of browning of adipose cells.

12. PRDM16 exhibited similar gene expression levels for all groups of naringenin in the differentiation, but in the maturation this gene expression levels were upregulated after naringenin treatment.

13. Both free and liposomal naringenin did not alter the protein concentration of UCP1 and PPARγ. However, naringenin increased significantly the protein concentration of PGC1-α.

14. Neither free nor liposomal naringenin decreased triglycerides levels in both differentiation and maturation phases.

15. PPARγ, C/EBPβ, and FABP4 gene expression levels after berberine treatment were similar in all groups in the differentiation, however, PPARγ gene expression levels were significantly lower in liposomal 20 μM of berberine; FABP4 gene expression levels were significantly lower in free 10 μM than other groups in the maturation. It is probable that berberine treatment may affect the adipogenesis of adipocytes.

16. CIDEA levels were similar across all forms of berberine in the differentiation, however, CIDEA expression in berberine was significantly higher in free 10 μM compared to all berberine groups.

17. PGC1-α expression levels were higher in free 5 μM compared to liposomal 20 μM and liposomal 10 μM of berberine in the differentiation process. Surprisingly, void berberine upregulated this gene in the maturation process.

18. Berberine did not significantly change PRDM16 levels in both process. Surprisingly, void B upregulated this gene in the maturation process.

19. The highest level of UCP1 expression was in free 20 μM and 10 μM of berberine in the differentiation and free 20 μM and 10 μM of berberine in the

maturation process. These results suggesting that berberine may induces browning in 3T3-L1 adipocytes.

20. There was not a significant difference for free naringenin, free berberine, liposomal naringenin, and liposomal berberine groups for UCP1 protein concentration in the differentiation.

21. PPARγ and PGC1-α protein concentration was positively affected after berberine treatment.

22. Liposomal form of berberine may reduce triglyceride level reduction only in the differentiation process.

23. The results indicate that all phytochemical may be safe to use in free form after 24 h. However, free and liposomal forms of berberine and naringenin could have adverse effects after 48 h.

The limitation of this study includes not analyzing the pathways of beige adipogenesis, which involves complex transcriptional and post-transcriptional regulation. Therefore, further study is required to fully understand the molecular mechanisms explain adipocyte browning and its metabolic effects. In conclusion, these findings may provide an important background for the development of therapeutics to combat obesity. Nonetheless, further *in vitro* and *in vivo* studies are essential to confirm the browning effect of delphinidin, naringenin, and berberine and to potentially apply these phytochemicals as practical anti-obesity therapy.

6.2. Recommendations

1. According to our study, delphinidin showed potential in promoting browning through increased PRDM16 expression. It is recommended to include delphinidin both in dietary intake and encapsulated form to increase the bioavailability of the phytochemical. Delphinidin is found mostly in dark-colored fruits and berries, such as blueberries, blackcurrants, and blackberries.

2. Given the increased UCP1 gene expression after treatment with encapsulated naringenin, it is advised to increase the consumption of naringenin both from fruits, especially those primarily present in citrus fruits like grapefruits, oranges, and from supplementation to increase the effective dose.

3. In light of the fact that berberine treatment significantly enhanced UCP1 expression and reduced triglyceride levels in differentiation, it is recommended to increase the consumption of berberine. This phytochemical is found in several plants, such as barberry, Oregon grape, and tree turmeric. However, in natural form it has a low absorption, therefore it may be use the supplementation under doctor supervision.

4. Further *in vitro* studies could analyze in detail the delivery methods of encapsulated phytochemicals. More studies should also evaluate the long-term safety and effects of these compounds in higher doses.

5. By using the encapsulation methodology outlined here, similar study could be developed for animal study to better understand the effect of these phytochemical on browning of adipose tissue.

6. In the future, it will be important to conduct well-designed clinical trials to validate the efficacy of these compounds also in humans.

7. This study underlined the increased bioavailability of encapsulated liposomal forms of the pure extract form of naringenin and berberine. Thanks to features such as increased solubility and stability, controlled release, and targeted delivery, the amount of dose administered with the encapsulation technique increases the bioavailability of naringenin and berberine. It is important to note that it is not possible to achieve the same quantity and effectiveness from consuming fruits directly, as the encapsulated forms provide a more concentrated and readily available dosage of these compounds.

8. In the context of combating obesity and its associated conditions, the treatment should include a healthy diet and physical exercise. In more complex cases, medical intervention through pharmacological therapy or even bariatric surgery might be necessary to achieve significant weight loss. However, these interventions come with their own set of challenges and risks. In this light, this technique may be a less invasive alternative that directly increase the thermogenesis of beige adipocyte by take encapsulated phytochemicals. This method, under the supervision of healthcare professionals, might serve as a complementary strategy, providing a bridge between conventional dietary measures and more invasive medical interventions.

7. REFERENCES

1. Chooi YC, Ding C, Magkos F. The epidemiology of obesity. Metabolism: clinical and experimental. 2019;92:6-10.
2. Lin X, Li H. Obesity: Epidemiology, Pathophysiology, and Therapeutics. Frontiers in endocrinology. 2021;12:706978.
3. Cheng L, Wang J, Dai H, Duan Y, An Y, Shi L, et al. Brown and beige adipose tissue: a novel therapeutic strategy for obesity and type 2 diabetes mellitus. Adipocyte. 2021;10(1):48-65.
4. Ke J-Y, Kliewer KL, Hamad EM, Cole RM, Powell KA, Andridge RR, et al. The flavonoid, naringenin, decreases adipose tissue mass and attenuates ovariectomy-associated metabolic disturbances in mice. Nutr Metab (Lond). 2015;12:1-.
5. Burke AC, Telford DE, Edwards JY, Sutherland BG, Sawyez CG, Huff MW. Naringenin Supplementation to a Chow Diet Enhances Energy Expenditure and Fatty Acid Oxidation, and Reduces Adiposity in Lean, Pair-Fed Ldlr(-/-) Mice. Molecular nutrition & food research. 2019;63(6):e1800833.
6. Karim N, Jia Z, Zheng X, Cui S, Chen W. A recent review of citrus flavanone naringenin on metabolic diseases and its potential sources for high yield-production. Trends in Food Science & Technology. 2018;79:35-54.
7. Tsuhako R, Yoshida H, Sugita C, Kurokawa M. Naringenin suppresses neutrophil infiltration into adipose tissue in high-fat diet-induced obese mice. Journal of natural medicines. 2020;74(1):229-37.
8. Naeini F, Namkhah Z, Ostadrahimi A, Tutunchi H, Hosseinzadeh-Attar MJ. A Comprehensive Systematic Review of the Effects of Naringenin, a Citrus-Derived Flavonoid, on Risk Factors for Nonalcoholic Fatty Liver Disease. Advances in nutrition (Bethesda, Md). 2021;12(2):413-28.
9. Pandey R, Gurung R, Sohng JK. Dietary Sources, Bioavailability and Biological Activities of Naringenin and its Derivatives. 2015. p. 6x9-(NBC.
10. Hu Y, Young AJ, Ehli EA, Nowotny D, Davies PS, Droke EA, et al. Metformin and berberine prevent olanzapine-induced weight gain in rats. PloS one. 2014;9(3):e93310.
11. Okla M, Kim J, Koehler K, Chung S. Dietary Factors Promoting Brown and Beige Fat Development and Thermogenesis. Advances in nutrition (Bethesda, Md). 2017;8(3):473-83.
12. Zhang Z, Zhang H, Li B, Meng X, Wang J, Zhang Y, et al. Berberine activates thermogenesis in white and brown adipose tissue. Nature communications. 2014;5:5493.
13. Silvester AJ, Aseer KR, Yun JW. Dietary polyphenols and their roles in fat browning. The Journal of nutritional biochemistry. 2019;64:1-12.
14. Kim SM, Chung MJ, Ha TJ, Choi HN, Jang SJ, Kim SO, et al. Neuroprotective effects of black soybean anthocyanins via inactivation of ASK1-JNK/p38

pathways and mobilization of cellular sialic acids. Life sciences. 2012;90(21-22):874-82.

15. Santos J, La VD, Bergeron C, Grenier D. Inhibition of host- and bacteria-derived proteinases by natural anthocyanins. J Periodontal Res. 2011;46(5):550-7.

16. Chen B, Ma Y, Li H. The antioxidant activity and active sites of delphinidin and petunidin measured by DFT, in vitro chemical-based and cell-based assays. 2019;43(9):e12968.

17. Durazzo A, Lucarini M. Polyphenols: A concise overview on the chemistry, occurrence, and human health. 2019;33(9):2221-43.

18. Moratalla-Lopez N, Bagur MJ, Lorenzo C, Salinas M, Alonso GL. Bioactivity and Bioavailability of the Major Metabolites of Crocus sativus L. Flower. Molecules (Basel, Switzerland). 2019;24(15).

19. Moriwaki S, Suzuki K, Muramatsu M, Nomura A, Inoue F, Into T, et al. Delphinidin, one of the major anthocyanidins, prevents bone loss through the inhibition of excessive osteoclastogenesis in osteoporosis model mice. PloS one. 2014;9(5):e97177.

20. Overall J, Bonney SA, Wilson M, Beermann A, Grace MH, Esposito D, et al. Metabolic Effects of Berries with Structurally Diverse Anthocyanins. Int J Mol Sci. 2017;18(2).

21. Parra-Vargas M, Sandoval-Rodriguez A, Rodriguez-Echevarria R, Dominguez-Rosales JA, Santos-Garcia A, Armendariz-Borunda J. Delphinidin Ameliorates Hepatic Triglyceride Accumulation in Human HepG2 Cells, but Not in Diet-Induced Obese Mice. Nutrients. 2018;10(8).

22. Patel K, Jain A, Patel D. Medicinal significance, pharmacological activities, and analytical aspects of anthocyanidins ‘delphinidin’: A concise report. Journal of Acute Disease. 2013;2:169–78.

23. Wang F, Li H. Effects of heat, ultrasound, and microwave processing on the stability and antioxidant activity of delphinidin and petunidin. 2019;43(5):e12818.

24. Konstantinidi M, Koutelidakis AE. Functional Foods and Bioactive Compounds: A Review of Its Possible Role on Weight Management and Obesity's Metabolic Consequences. 2019;6(3).

25. Kim HK, Kim JN, Han SN, Nam JH, Na HN, Ha TJ. Black soybean anthocyanins inhibit adipocyte differentiation in 3T3-L1 cells. Nutrition research (New York, NY). 2012;32(10):770-7.

26. Park M, Sharma A, Lee HJ. Anti-Adipogenic Effects of Delphinidin-3-O-beta-Glucoside in 3T3-L1 Preadipocytes and Primary White Adipocytes. 2019;24(10).

27. Sharif N, Khoshnoudi-Nia S, Jafari SM. Nano/microencapsulation of anthocyanins; a systematic review and meta-analysis. Food research international (Ottawa, Ont). 2020;132:109077.

28. Wang Y, Wang S, Firempong CK, Zhang H, Wang M, Zhang Y, et al. Enhanced Solubility and Bioavailability of Naringenin via Liposomal Nanoformulation: Preparation and In Vitro and In Vivo Evaluations. AAPS PharmSciTech. 2017;18(3):586-94.

29. Mirhadi E, Rezaee M, Malaekeh-Nikouei B. Nano strategies for berberine delivery, a natural alkaloid of Berberis. Biomedicine & pharmacotherapy = Biomedecine & pharmacotherapie. 2018;104:465-73.

30. Zheng T, Yin Z, Huang Q. Assessment of Digestion, Absorption, and Metabolism of Nanoencapsulated Phytochemicals Using In Vitro and In Vivo Models: A Perspective Paper. Journal of agricultural and food chemistry. 2022;70(15):4548-55.

31. Goktas Z, Zu Y, Abbasi M, Galyean S, Wu D, Fan Z, et al. Recent Advances in Nanoencapsulation of Phytochemicals to Combat Obesity and Its Comorbidities. Journal of agricultural and food chemistry. 2020;68(31):8119-31.

32. Magne TM, Alencar LMR, Carneiro SV, Fechine L, Fechine PBA, Souza PFN, et al. Nano-Nutraceuticals for Health: Principles and Applications. Revista brasileira de farmacognosia : orgao oficial da Sociedade Brasileira de Farmacognosia. 2022:1-16.

33. Derosa G, Maffioli P, Cicero A. Berberine on metabolic and cardiovascular risk factors: An analysis from preclinical evidences to clinical trials. Expert opinion on biological therapy. 2012;12:1113-24.

34. National Center for Biotechnology Information. PubChem Compound Summary for CID 2353, Berberine https://pubchem.ncbi.nlm.nih.gov/compound/Berberine.2023 [

35. Cicero AF, Colletti A. Role of phytochemicals in the management of metabolic syndrome. Phytomedicine. 2016;23(11):1134-44.

36. Singh IP, Mahajan S. Berberine and its derivatives: a patent review (2009 - 2012). Expert Opin Ther Pat. 2013;23(2):215-31.

37. Wang K, Feng X, Chai L, Cao S, Qiu F. The metabolism of berberine and its contribution to the pharmacological effects. Drug Metab Rev. 2017;49(2):139-57.

38. Sirtori CR, Pavanello C, Calabresi L, Ruscica M. Nutraceutical approaches to metabolic syndrome. Ann Med. 2017;49(8):678-97.

39. Zhao W, Xue R, Zhou ZX, Kong WJ, Jiang JD. Reduction of blood lipid by berberine in hyperlipidemic patients with chronic hepatitis or liver cirrhosis. Biomedicine & pharmacotherapy = Biomedecine & pharmacotherapie. 2008;62(10):730-1.

40. Choi BH, Ahn IS, Kim YH, Park JW, Lee SY, Hyun CK, et al. Berberine reduces the expression of adipogenic enzymes and inflammatory molecules of 3T3-L1 adipocyte. Experimental & molecular medicine. 2006;38(6):599-605.

41. Derosa G, Maffioli P, Cicero AF. Berberine on metabolic and cardiovascular risk factors: an analysis from preclinical evidences to clinical trials. Expert Opin Biol Ther. 2012;12(8):1113-24.

42. Chen W, Miao YQ, Fan DJ, Yang SS, Lin X, Meng LK, et al. Bioavailability study of berberine and the enhancing effects of TPGS on intestinal absorption in rats. AAPS PharmSciTech. 2011;12(2):705-11.

43. Liu YT, Hao HP, Xie HG, Lai L, Wang Q, Liu CX, et al. Extensive intestinal first-pass elimination and predominant hepatic distribution of berberine explain its low plasma levels in rats. Drug metabolism and disposition: the biological fate of chemicals. 2010;38(10):1779-84.

44. Spinozzi S, Colliva C, Camborata C, Roberti M, Ianni C, Neri F, et al. Berberine and its metabolites: relationship between physicochemical properties and plasma levels after administration to human subjects. Journal of natural products. 2014;77(4):766-72.

45. Yang L, Yu S, Yang Y, Wu H, Zhang X, Lei Y, et al. Berberine improves liver injury induced glucose and lipid metabolic disorders via alleviating ER stress of hepatocytes and modulating gut microbiota in mice. Bioorganic & medicinal chemistry. 2021;55:116598.

46. Fratter A, Servi B. New oral delivery system to improve absorption of berberine: Likely interaction of cationized chitosan with PG-P Pump. International Journal of Drug Delivery (Jaipur). 2015;5:33-42.

47. Och A, Podgórski R, Nowak R. Biological Activity of Berberine-A Summary Update. Toxins. 2020;12(11).

48. Godugu C, Patel AR, Doddapaneni R, Somagoni J, Singh M. Approaches to improve the oral bioavailability and effects of novel anticancer drugs berberine and betulinic acid. PloS one. 2014;9(3):e89919.

49. Tan XS, Ma JY, Feng R, Ma C, Chen WJ, Sun YP, et al. Tissue distribution of berberine and its metabolites after oral administration in rats. PloS one. 2013;8(10):e77969.

50. Kumar A, Ekavali, Chopra K, Mukherjee M, Pottabathini R, Dhull DK. Current knowledge and pharmacological profile of berberine: An update. European journal of pharmacology. 2015;761:288-97.

51. Guo Y, Pope C, Cheng X, Zhou H, Klaassen CD. Dose-response of berberine on hepatic cytochromes P450 mRNA expression and activities in mice. J Ethnopharmacol. 2011;138(1):111-8.

52. Ma JY, Feng R, Tan XS, Ma C, Shou JW, Fu J, et al. Excretion of berberine and its metabolites in oral administration in rats. Journal of pharmaceutical sciences. 2013;102(11):4181-92.

53. Zhang J, Tang H, Deng R, Wang N, Zhang Y, Wang Y, et al. Berberine Suppresses Adipocyte Differentiation via Decreasing CREB Transcriptional Activity. PloS one. 2015;10(4):e0125667.

54. Zhang Y, Li X, Zou D, Liu W, Yang J, Zhu N, et al. Treatment of type 2 diabetes and dyslipidemia with the natural plant alkaloid berberine. The Journal of clinical endocrinology and metabolism. 2008;93(7):2559-65.

55. Li Y, Zhao X, Feng X, Liu X, Deng C, Hu CH. Berberine Alleviates Olanzapine-Induced Adipogenesis via the AMPKalpha-SREBP Pathway in 3T3-L1 Cells. International journal of molecular sciences. 2016;17(11).

56. Xu X, Yi H, Wu J, Kuang T, Zhang J, Li Q, et al. Therapeutic effect of berberine on metabolic diseases: Both pharmacological data and clinical evidence. Biomedicine & Pharmacotherapy. 2021;133:110984.

57. Chen G, Lu F, Xu L, Dong H, Yi P, Wang F, et al. The anti-diabetic effects and pharmacokinetic profiles of berberine in mice treated with Jiao-Tai-Wan and its compatibility. Phytomedicine. 2013;20(10):780-6.

58. Lan J, Zhao Y, Dong F, Yan Z, Zheng W, Fan J, et al. Meta-analysis of the effect and safety of berberine in the treatment of type 2 diabetes mellitus, hyperlipemia and hypertension. J Ethnopharmacol. 2015;161:69-81.

59. Ni WJ, Ding HH, Tang LQ. Berberine as a promising anti-diabetic nephropathy drug: An analysis of its effects and mechanisms. Eur J Pharmacol. 2015;760:103-12.

60. Pang B, Zhao LH, Zhou Q, Zhao TY, Wang H, Gu CJ, et al. Application of berberine on treating type 2 diabetes mellitus. International journal of endocrinology. 2015;2015:905749.

61. Lee YS, Kim WS, Kim KH, Yoon MJ, Cho HJ, Shen Y, et al. Berberine, a natural plant product, activates AMP-activated protein kinase with beneficial metabolic effects in diabetic and insulin-resistant states. Diabetes. 2006;55(8):2256-64.

62. Yin J, Gao Z, Liu D, Liu Z, Ye J. Berberine improves glucose metabolism through induction of glycolysis. Am J Physiol Endocrinol Metab. 2008;294(1):E148-56.

63. Wang ZQ, Lu FE, Leng SH, Fang XS, Chen G, Wang ZS, et al. Facilitating effects of berberine on rat pancreatic islets through modulating hepatic nuclear factor 4 alpha expression and glucokinase activity. World J Gastroenterol. 2008;14(39):6004-11.

64. Lu SS, Yu YL, Zhu HJ, Liu XD, Liu L, Liu YW, et al. Berberine promotes glucagon-like peptide-1 (7-36) amide secretion in streptozotocin-induced diabetic rats. The Journal of endocrinology. 2009;200(2):159-65.

65. Xia X, Yan J, Shen Y, Tang K, Yin J, Zhang Y, et al. Berberine improves glucose metabolism in diabetic rats by inhibition of hepatic gluconeogenesis. PloS one. 2011;6(2):e16556.

66. Yin J, Xing H, Ye J. Efficacy of berberine in patients with type 2 diabetes mellitus. Metabolism. 2008;57(5):712-7.

67. Brusq JM, Ancellin N, Grondin P, Guillard R, Martin S, Saintillan Y, et al. Inhibition of lipid synthesis through activation of AMP kinase: an additional

mechanism for the hypolipidemic effects of berberine. J Lipid Res. 2006;47(6):1281-8.

68. Cameron J, Ranheim T, Kulseth MA, Leren TP, Berge KE. Berberine decreases PCSK9 expression in HepG2 cells. Atherosclerosis. 2008;201(2):266-73.

69. Dong H, Zhao Y, Zhao L, Lu F. The effects of berberine on blood lipids: a systemic review and meta-analysis of randomized controlled trials. Planta Med. 2013;79(6):437-46.

70. Kong W, Wei J, Abidi P, Lin M, Inaba S, Li C, et al. Berberine is a novel cholesterol-lowering drug working through a unique mechanism distinct from statins. Nat Med. 2004;10(12):1344-51.

71. Briand F, Thieblemont Q, Muzotte E, Sulpice T. Upregulating reverse cholesterol transport with cholesteryl ester transfer protein inhibition requires combination with the LDL-lowering drug berberine in dyslipidemic hamsters. Arterioscler Thromb Vasc Biol. 2013;33(1):13-23.

72. Mohammadzadeh N, Mehri S, Hosseinzadeh H. Berberis vulgaris and its constituent berberine as antidotes and protective agents against natural or chemical toxicities. Iranian journal of basic medical sciences. 2017;20(5):538-51.

73. Zhang H, Wei J, Xue R, Wu JD, Zhao W, Wang ZZ, et al. Berberine lowers blood glucose in type 2 diabetes mellitus patients through increasing insulin receptor expression. Metabolism: clinical and experimental. 2010;59(2):285-92.

74. Linn YC, Lu J, Lim LC, Sun H, Sun J, Zhou Y, et al. Berberine-induced haemolysis revisited: safety of Rhizoma coptidis and Cortex phellodendri in chronic haematological diseases. Phytotherapy research : PTR. 2012;26(5):682-6.

75. Chen Z, Zhang R, Shi W, Li L, Liu H, Liu Z, et al. The Multifunctional Benefits of Naturally Occurring Delphinidin and Its Glycosides. Journal of agricultural and food chemistry. 2019;67(41):11288-306.

76. Khoo HE, Azlan A, Tang ST, Lim SM. Anthocyanidins and anthocyanins: colored pigments as food, pharmaceutical ingredients, and the potential health benefits. Food Nutr Res. 2017;61(1):1361779.

77. Tanaka Y, Sasaki N, Ohmiya A. Biosynthesis of plant pigments: anthocyanins, betalains and carotenoids. Plant J. 2008;54(4):733-49.

78. National Center for Biotechnology Information (2023). PubChem Compound Summary for CID 68245, Delphinidin https://pubchem.ncbi.nlm.nih.gov/compound/Delphinidin2023 [

79. Yun JM, Afaq F, Khan N, Mukhtar H. Delphinidin, an anthocyanidin in pigmented fruits and vegetables, induces apoptosis and cell cycle arrest in human colon cancer HCT116 cells. Molecular carcinogenesis. 2009;48(3):260-70.

80. Calderón-Oliver M, Ponce-Alquicira E. Chapter 7 - Fruits: A Source of Polyphenols and Health Benefits. In: Grumezescu AM, Holban AM, editors. Natural and Artificial Flavoring Agents and Food Dyes: Academic Press; 2018. p. 189-228.

81. Czank C, Cassidy A, Zhang Q, Morrison DJ, Preston T, Kroon PA, et al. Human metabolism and elimination of the anthocyanin, cyanidin-3-glucoside: a (13)C-tracer study. The American journal of clinical nutrition. 2013;97(5):995-1003.

82. Fang J. Bioavailability of anthocyanins. Drug metabolism reviews. 2014;46(4):508-20.

83. Passamonti S, Vrhovsek U, Mattivi F. The interaction of anthocyanins with bilitranslocase. Biochemical and biophysical research communications. 2002;296(3):631-6.

84. Hribar U, Ulrih NP. The metabolism of anthocyanins. Current drug metabolism. 2014;15(1):3-13.

85. Andres-Lacueva C, Shukitt-Hale B, Galli RL, Jauregui O, Lamuela-Raventos RM, Joseph JA. Anthocyanins in aged blueberry-fed rats are found centrally and may enhance memory. Nutritional neuroscience. 2005;8(2):111-20.

86. Kalt W, Blumberg JB, McDonald JE, Vinqvist-Tymchuk MR, Fillmore SA, Graf BA, et al. Identification of anthocyanins in the liver, eye, and brain of blueberry-fed pigs. Journal of agricultural and food chemistry. 2008;56(3):705-12.

87. Passamonti S, Vrhovsek U, Vanzo A, Mattivi F. Fast access of some grape pigments to the brain. Journal of agricultural and food chemistry. 2005;53(18):7029-34.

88. Sharma A, Choi HK, Kim YK, Lee HJ. Delphinidin and Its Glycosides' War on Cancer: Preclinical Perspectives. International journal of molecular sciences. 2021;22(21).

89. Frank T, Netzel G, Kammerer D, Carle R, Kler A, Kriesl E, et al. Consumption of Hibiscus sabdariffa L. aqueous extract and its impact on systemic antioxidant potential in healthy subjects. Journal of the science of food and agriculture. 2012;92:2207-18.

90. Akhtar M, Murray BS, Afeisume EI, Khew SH. Encapsulation of flavonoid in multiple emulsion using spinning disc reactor technology. Food Hydrocolloids. 2014;34:62-7.

91. Thirumurugan G, Haile T, Nigusse T, Dhanaraju MD, Fereja T. Nanotechnology: An effective tool for enhancing bioavailability and bioactivity of phytomedicine. Asian Pacific journal of tropical biomedicine. 2014;4.

92. Cremonini E, Daveri E, Mastaloudis A, Adamo AM, Mills D, Kalanetra K, et al. Anthocyanins protect the gastrointestinal tract from high fat diet-induced alterations in redox signaling, barrier integrity and dysbiosis. Redox biology. 2019;26:101269.

93. Daveri E, Cremonini E, Mastaloudis A, Hester SN, Wood SM, Waterhouse AL, et al. Cyanidin and delphinidin modulate inflammation and altered redox signaling improving insulin resistance in high fat-fed mice. Redox biology. 2018;18:16-24.

94. Sandoval V, Femenias A, Martinez-Garza U, Sanz-Lamora H, Castagnini JM. Lyophilized Maqui (Aristotelia chilensis) Berry Induces Browning in the Subcutaneous White Adipose Tissue and Ameliorates the Insulin Resistance in High Fat Diet-Induced Obese Mice. 2019;8(9).

95. Hidalgo J, Flores C, Hidalgo MA, Perez M, Yañez A, Quiñones L, et al. Delphinol® standardized maqui berry extract reduces postprandial blood glucose increase in individuals with impaired glucose regulation by novel mechanism of sodium glucose cotransporter inhibition. Panminerva medica. 2014;56(2 Suppl 3):1-7.

96. Rahman N, Jeon M, Kim YS. Delphinidin, a major anthocyanin, inhibits 3T3-L1 pre-adipocyte differentiation through activation of Wnt/β-catenin signaling. BioFactors (Oxford, England). 2016;42(1):49-59.

97. Wu T, Tang Q, Gao Z, Yu Z, Song H, Zheng X, et al. Blueberry and mulberry juice prevent obesity development in C57BL/6 mice. PLoS One. 2013;8(10):e77585.

98. Les F, Cásedas G, Gómez C, Moliner C, Valero MS, López V. The role of anthocyanins as antidiabetic agents: from molecular mechanisms to in vivo and human studies. Journal of physiology and biochemistry. 2021;77(1):109-31.

99. Kato M, Tani T, Terahara N, Tsuda T. The anthocyanin delphinidin 3-rutinoside stimulates glucagon-like peptide-1 secretion in murine GLUTag cell line via the Ca2+/calmodulin-dependent kinase II pathway. PloS one. 2015;10(5):e0126157.

100. Gharib A, Faezizadeh Z, Godarzee M. Treatment of diabetes in the mouse model by delphinidin and cyanidin hydrochloride in free and liposomal forms. Planta medica. 2013;79(17):1599-604.

101. Iizuka Y, Ozeki A, Tani T, Tsuda T. Blackcurrant extract ameliorates hyperglycemia in type 2 diabetic mice in association with increased basal secretion of glucagon-like peptide-1 and activation of AMP-activated protein kinase. Journal of nutritional science and vitaminology. 2018;64(4):258-64.

102. Les F, Cásedas G, Gómez C, Moliner C, Valero MS, López V. The role of anthocyanins as antidiabetic agents: From molecular mechanisms to in vivo and human studies. Journal of physiology and biochemistry. 2021;77(1):109-31.

103. Lai D, Huang M, Zhao L, Tian Y, Li Y, Liu D, et al. Delphinidin-induced autophagy protects pancreatic β cells against apoptosis resulting from high-glucose stress via AMPK signaling pathway. Acta biochimica et biophysica Sinica. 2019;51(12):1242-9.

104. Harada G, Onoue S, Inoue C, Hanada S, Katakura Y. Delphinidin-3-glucoside suppresses lipid accumulation in HepG2 cells. Cytotechnology. 2018;70(6):1707-12.

105. Chen C-y, Yi L, Jin X, Mi M-t, Zhang T, Ling W-h, et al. Delphinidin attenuates stress injury induced by oxidized low-density lipoprotein in human umbilical vein endothelial cells. Chemico-biological interactions. 2010;183(1):105-12.

106. National Center for Biotechnology Information (2023). PubChem Compound Summary for CID 439246, Naringenin: https://pubchem.ncbi.nlm.nih.gov/compound/Naringenin; 2023 [

107. Yao LH, Jiang YM, Shi J, TomÁS-BarberÁN FA, Datta N, Singanusong R, et al. Flavonoids in Food and Their Health Benefits. Plant Foods for Human Nutrition. 2004;59(3):113-22.

108. Yang Y, Trevethan M, Wang S, Zhao L. Beneficial effects of citrus flavanones naringin and naringenin and their food sources on lipid metabolism: An update on bioavailability, pharmacokinetics, and mechanisms. The Journal of nutritional biochemistry. 2022;104:108967.

109. Barreca D, Gattuso G, Bellocco E, Calderaro A, Trombetta D, Smeriglio A, et al. Flavanones: Citrus phytochemical with health-promoting properties. BioFactors (Oxford, England). 2017;43(4):495-506.

110. Md S, Alhakamy NA, Aldawsari HM, Asfour HZ. Neuroprotective and Antioxidant Effect of Naringenin-Loaded Nanoparticles for Nose-to-Brain Delivery. Brain sciences. 2019;9(10).

111. Patel K, Singh GK, Patel DK. A Review on Pharmacological and Analytical Aspects of Naringenin. Chinese Journal of Integrative Medicine. 2018;24(7):551-60.

112. Memariani Z, Abbas SQ, ul Hassan SS, Ahmadi A, Chabra A. Naringin and naringenin as anticancer agents and adjuvants in cancer combination therapy: Efficacy and molecular mechanisms of action, a comprehensive narrative review. Pharmacological Research. 2021;171:105264.

113. Joshi R, Kulkarni YA, Wairkar S. Pharmacokinetic, pharmacodynamic and formulations aspects of Naringenin: An update. Life sciences. 2018;215:43-56.

114. Zeng X, Su W, Zheng Y, He Y, He Y, Rao H, et al. Pharmacokinetics, Tissue Distribution, Metabolism, and Excretion of Naringin in Aged Rats. Frontiers in Pharmacology. 2019;10.

115. Ahmad N, Ahmad R, Ahmad FJ, Ahmad W, Alam MA, Amir M, et al. Poloxamer-chitosan-based Naringenin nanoformulation used in brain targeting for the treatment of cerebral ischemia. Saudi Journal of Biological Sciences. 2020;27(1):500-17.

116. Harmon AW, Harp JB. Differential effects of flavonoids on 3T3-L1 adipogenesis and lipolysis. American Journal of Physiology-Cell Physiology. 2001;280(4):C807-C13.

117. Yoshida H, Takamura N, Shuto T, Ogata K, Tokunaga J, Kawai K, et al. The citrus flavonoids hesperetin and naringenin block the lipolytic actions of TNF-α in mouse adipocytes. Biochemical and biophysical research communications. 2010;394(3):728-32.

118. Claussnitzer M, Skurk T, Hauner H, Daniel H, Rist MJ. Effect of flavonoids on basal and insulin-stimulated 2-deoxyglucose uptake in adipocytes. Molecular nutrition & food research. 2011;55(S1):S26-S34.

119. Yoshida H, Watanabe W, Oomagari H, Tsuruta E, Shida M, Kurokawa M. Citrus flavonoid naringenin inhibits TLR2 expression in adipocytes. The Journal of nutritional biochemistry. 2013;24(7):1276-84.

120. Richard AJ, Amini-Vaughan Z, Ribnicky DM, Stephens JM. Naringenin inhibits adipogenesis and reduces insulin sensitivity and adiponectin expression in adipocytes. Evidence-based complementary and alternative medicine : eCAM. 2013;2013:549750.

121. Rebello CJ, Greenway FL, Lau FH, Lin Y, Stephens JM, Johnson WD, et al. Naringenin Promotes Thermogenic Gene Expression in Human White Adipose Tissue. Obesity. 2019;27(1):103-11.

122. Alam MA, Subhan N, Rahman MM, Uddin SJ, Reza HM, Sarker SD. Effect of Citrus Flavonoids, Naringin and Naringenin, on Metabolic Syndrome and Their Mechanisms of Action. Advances in Nutrition. 2014;5(4):404-17.

123. Goldwasser J, Cohen PY, Yang E, Balaguer P, Yarmush ML, Nahmias Y. Transcriptional regulation of human and rat hepatic lipid metabolism by the grapefruit flavonoid naringenin: role of PPARalpha, PPARgamma and LXRalpha. PloS one. 2010;5(8):e12399.

124. Cho KW, Kim YO, Andrade JE, Burgess JR, Kim Y-C. Dietary naringenin increases hepatic peroxisome proliferators–activated receptor α protein expression and decreases plasma triglyceride and adiposity in rats. European journal of nutrition. 2011;50(2):81-8.

125. Ortiz-Andrade RR, Sánchez-Salgado JC, Navarrete-Vázquez G, Webster SP, Binnie M, García-Jiménez S, et al. Antidiabetic and toxicological evaluations of naringenin in normoglycaemic and NIDDM rat models and its implications on extra-pancreatic glucose regulation. Diabetes, Obesity and Metabolism. 2008;10(11):1097-104.

126. Skopec MM, Green AK, Karasov WH. Flavonoids Have Differential Effects on Glucose Absorption in Rats (Rattus norvegicus) and American Robins (Turdis migratorius). Journal of Chemical Ecology. 2010;36(2):236-43.

127. Priscilla DH, Roy D, Suresh A, Kumar V, Thirumurugan K. Naringenin inhibits α-glucosidase activity: A promising strategy for the regulation of postprandial hyperglycemia in high fat diet fed streptozotocin induced diabetic rats. Chemico-biological interactions. 2014;210:77-85.

128. Li JM, Che CT, Lau CB, Leung PS, Cheng CH. Inhibition of intestinal and renal Na+-glucose cotransporter by naringenin. The international journal of biochemistry & cell biology. 2006;38(5-6):985-95.

129. Zygmunt K, Faubert B, MacNeil J, Tsiani E. Naringenin, a citrus flavonoid, increases muscle cell glucose uptake via AMPK. Biochemical and biophysical research communications. 2010;398(2):178-83.

130. Purushotham A, Tian M, Belury MA. The citrus fruit flavonoid naringenin suppresses hepatic glucose production from Fao hepatoma cells. Molecular nutrition & food research. 2009;53(2):300-7.

131. Constantin RP, Constantin RP, Bracht A, Yamamoto NS, Ishii-Iwamoto EL, Constantin J. Molecular mechanisms of citrus flavanones on hepatic gluconeogenesis. Fitoterapia. 2014;92:148-62.

132. Lin CY, Ni CC, Yin MC, Lii CK. Flavonoids protect pancreatic beta-cells from cytokines mediated apoptosis through the activation of PI3-kinase pathway. Cytokine. 2012;59(1):65-71.

133. Ortiz-Andrade RR, Sánchez-Salgado JC, Navarrete-Vázquez G, Webster SP, Binnie M, García-Jiménez S, et al. Antidiabetic and toxicological evaluations of naringenin in normoglycaemic and NIDDM rat models and its implications on extra-pancreatic glucose regulation. Diabetes, obesity & metabolism. 2008;10(11):1097-104.

134. Annadurai T, Muralidharan AR, Joseph T, Hsu MJ, Thomas PA, Geraldine P. Antihyperglycemic and antioxidant effects of a flavanone, naringenin, in streptozotocin-nicotinamide-induced experimental diabetic rats. Journal of physiology and biochemistry. 2012;68(3):307-18.

135. Kannappan S, Anuradha CV. Naringenin enhances insulin-stimulated tyrosine phosphorylation and improves the cellular actions of insulin in a dietary model of metabolic syndrome. European journal of nutrition. 2010;49(2):101-9.

136. Al-Rejaie SS, Aleisa AM, Abuohashish HM, Parmar MY, Ola MS, Al-Hosaini AA, et al. Naringenin neutralises oxidative stress and nerve growth factor discrepancy in experimental diabetic neuropathy. Neurological research. 2015;37(10):924-33.

137. Raja Kumar S, Mohd Ramli ES, Abdul Nasir NA, Ismail NHM, Mohd Fahami NA. Preventive Effect of Naringin on Metabolic Syndrome and Its Mechanism of Action: A Systematic Review. Evidence-Based Complementary and Alternative Medicine. 2019;2019:9752826.

138. Nyane NA, Tlaila TB, Malefane TG, Ndwandwe DE, Owira PMO. Metformin-like antidiabetic, cardio-protective and non-glycemic effects of naringenin: Molecular and pharmacological insights. European journal of pharmacology. 2017;803:103-11.

139. Khosravi M, Hosseini-Fard R, Najafi M. Circulating low density lipoprotein (LDL). Hormone Molecular Biology and Clinical Investigation. 2018;35(2).

140. Chen R, Qi Q-L, Wang M-T, Li Q-Y. Therapeutic potential of naringin: an overview. Pharmaceutical Biology. 2016;54(12):3203-10.

141. Yang Y, Trevethan M, Wang S, Zhao L. Beneficial Effects of Citrus Flavanones Naringin and Naringenin and Their Food Sources on Lipid

Metabolism: An Update on Bioavailability, Pharmacokinetics, and Mechanisms. The Journal of nutritional biochemistry. 2022;104:108967.

142. Sui G-G, Xiao H-B, Lu X-Y, Sun Z-L. Naringin Activates AMPK Resulting in Altered Expression of SREBPs, PCSK9, and LDLR To Reduce Body Weight in Obese C57BL/6J Mice. Journal of agricultural and food chemistry. 2018;66(34):8983-90.

143. Vekic J, Zeljkovic A, Stefanovic A, Jelic-Ivanovic Z, Spasojevic-Kalimanovska V. Obesity and dyslipidemia. Metabolism: clinical and experimental. 2019;92:71-81.

144. Barajas-Vega JL, Raffoul-Orozco AK, Hernandez-Molina D, Ávila-González AE, García-Cobian TA, Rubio-Arellano ED, et al. Naringin reduces body weight, plasma lipids and increases adiponectin levels in patients with dyslipidemia. International Journal for Vitamin and Nutrition Research. 2022;92(3-4):292-8.

145. Kanaze FI, Bounartzi MI, Georgarakis M, Niopas I. Pharmacokinetics of the citrus flavanone aglycones hesperetin and naringenin after single oral administration in human subjects. European Journal of Clinical Nutrition. 2007;61(4):472-7.

146. Rebello CJ, Beyl RA, Lertora JJL, Greenway FL, Ravussin E, Ribnicky DM, et al. Safety and pharmacokinetics of naringenin: A randomized, controlled, single-ascending-dose clinical trial. Diabetes, Obesity and Metabolism. 2020;22(1):91-8.

147. Bai Y, Peng W, Yang C, Zou W, Liu M, Wu H, et al. Pharmacokinetics and Metabolism of Naringin and Active Metabolite Naringenin in Rats, Dogs, Humans, and the Differences Between Species. Front Pharmacol. 2020;11:364.

148. Hilton C, Karpe F, Pinnick KE. Role of developmental transcription factors in white, brown and beige adipose tissues. Biochimica et biophysica acta. 2015;1851(5):686-96.

149. Chechi K, van Marken Lichtenbelt W, Richard D. Brown and beige adipose tissues: phenotype and metabolic potential in mice and men. Journal of applied physiology (Bethesda, Md : 1985). 2018;124(2):482-96.

150. Azhar Y, Parmar A, Miller CN, Samuels JS, Rayalam S. Phytochemicals as novel agents for the induction of browning in white adipose tissue. Nutr Metab (Lond). 2016;13:89.

151. Bolsoni-Lopes A, Alonso-Vale MI. Lipolysis and lipases in white adipose tissue - An update. Archives of endocrinology and metabolism. 2015;59(4):335-42.

152. Guilherme A, Virbasius JV, Puri V, Czech MP. Adipocyte dysfunctions linking obesity to insulin resistance and type 2 diabetes. Nature reviews Molecular cell biology. 2008;9(5):367-77.

153. Bolsoni-Lopes A, Alonso-Vale MIC. Lipolysis and lipases in white adipose tissue - An update. Archives of endocrinology and metabolism. 2015;59 4:335-42.

154. Heeren J, Scheja L. Brown adipose tissue and lipid metabolism. Current opinion in lipidology. 2018;29(3):180-5.

155. Cannon B, Nedergaard J. Brown adipose tissue: function and physiological significance. Physiological reviews. 2004;84(1):277-359.

156. McMillan AC, White MD. Induction of thermogenesis in brown and beige adipose tissues: molecular markers, mild cold exposure and novel therapies. Current opinion in endocrinology, diabetes, and obesity. 2015;22(5):347-52.

157. Mulya A, Kirwan JP. Brown and Beige Adipose Tissue: Therapy for Obesity and Its Comorbidities? Endocrinology and metabolism clinics of North America. 2016;45(3):605-21.

158. Montanari T, Pošćić N, Colitti M. Factors involved in white-to-brown adipose tissue conversion and in thermogenesis: a review: Factors involved in WAT browning. Obesity Reviews. 2017;18.

159. de-Lima-Júnior JC, Souza GF, Moura-Assis A, Gaspar RS, Gaspar JM, Rocha AL, et al. Abnormal brown adipose tissue mitochondrial structure and function in IL10 deficiency. EBioMedicine. 2019;39:436-47.

160. Yoneshiro T, Matsushita M, Hibi M, Tone H, Takeshita M, Yasunaga K, et al. Tea catechin and caffeine activate brown adipose tissue and increase cold-induced thermogenic capacity in humans. The American journal of clinical nutrition. 2017;105(4):873-81.

161. Kaisanlahti A, Glumoff T. Browning of white fat: agents and implications for beige adipose tissue to type 2 diabetes. Journal of physiology and biochemistry. 2019;75(1):1-10.

162. Abdullahi A, Jeschke MG. White Adipose Tissue Browning: A Double-edged Sword. Trends in endocrinology and metabolism: TEM. 2016;27(8):542-52.

163. Herz CT, Kiefer FW. Adipose tissue browning in mice and humans. The Journal of endocrinology. 2019;241(3):R97-r109.

164. Poher AL, Altirriba J, Veyrat-Durebex C, Rohner-Jeanrenaud F. Brown adipose tissue activity as a target for the treatment of obesity/insulin resistance. Frontiers in physiology. 2015;6:4.

165. Kaisanlahti A, Glumoff T. Browning of white fat: agents and implications for beige adipose tissue to type 2 diabetes. Journal of physiology and biochemistry. 2018;75.

166. Bargut TCL, Souza-Mello V, Aguila MB, Mandarim-de-Lacerda CA. Browning of white adipose tissue: lessons from experimental models. Hormone Molecular Biology and Clinical Investigation. 2017;31(1).

167. Farmer SR. Regulation of PPARgamma activity during adipogenesis. International journal of obesity (2005). 2005;29 Suppl 1:S13-6.

168. Farmer SR. Transcriptional control of adipocyte formation. Cell Metabolism. 2006;4(4):263-73.

169. Lo KA, Sun L. Turning WAT into BAT: a review on regulators controlling the browning of white adipocytes. Bioscience reports. 2013;33(5).

170. Seale P, Kajimura S, Spiegelman BM. Transcriptional control of brown adipocyte development and physiological function--of mice and men. Genes & development. 2009;23(7):788-97.

171. Qiang L, Wang L, Kon N, Zhao W, Lee S, Zhang Y, et al. Brown remodeling of white adipose tissue by SirT1-dependent deacetylation of Pparγ. Cell. 2012;150(3):620-32.

172. Roth CL, Molica F, Kwak BR. Browning of White Adipose Tissue as a Therapeutic Tool in the Fight against Atherosclerosis. Metabolites. 2021;11(5).

173. Alcalá M, Calderon-Dominguez M, Serra D, Herrero L, Viana M. Mechanisms of Impaired Brown Adipose Tissue Recruitment in Obesity. Frontiers in physiology. 2019;10:94.

174. McNeill BT, Suchacki KJ, Stimson RH. MECHANISMS IN ENDOCRINOLOGY: Human brown adipose tissue as a therapeutic target: warming up or cooling down? European Journal of Endocrinology. 2021;184(6):R243-R59.

175. Bonet ML, Oliver P, Palou A. Pharmacological and nutritional agents promoting browning of white adipose tissue. Biochimica et biophysica acta. 2013;1831(5):969-85.

176. Peschechera A, Eckel J. "Browning" of adipose tissue--regulation and therapeutic perspectives. Archives of physiology and biochemistry. 2013;119(4):151-60.

177. Čižmárová B, Hubková B, Tomečková Vr, Birková A. Flavonoids as Promising Natural Compounds in the Prevention and Treatment of Selected Skin Diseases. International journal of molecular sciences. 2023.

178. Wu Y-Y, Xu Y-M, Lau ATY. Epigenetic effects of herbal medicine. Clinical Epigenetics. 2023;15(1):85.

179. Gunasekaran S, Ko S. Rationales of Nano- and Microencapsulation for Food Ingredients. 2014. p. 43-64.

180. Pateiro M, Gómez B, Munekata PES, Barba FJ, Putnik P, Kovačević DB, et al. Nanoencapsulation of Promising Bioactive Compounds to Improve Their Absorption, Stability, Functionality and the Appearance of the Final Food Products. Molecules (Basel, Switzerland). 2021;26(6).

181. Blanco E, Shen H, Ferrari M. Principles of nanoparticle design for overcoming biological barriers to drug delivery. Nature Biotechnology. 2015;33(9):941-51.

182. Buzby JC. Nanotechnology for Food Applications: More Questions Than Answers. Journal of Consumer Affairs. 2010;44(3):528-45.

183. Kuo P-C. The Application of Nanotechnology to Functional Foods and Nutraceuticals to Enhance Their Bioactivities. 2010. p. 447-62.

184. Sekhon BS. Food nanotechnology - an overview. Nanotechnol Sci Appl. 2010;3:1-15.

185. Huang Q, Yu H, Ru Q. Bioavailability and delivery of nutraceuticals using nanotechnology. Journal of food science. 2010;75(1):R50-7.

186. da Silva Malheiros P, Daroit DJ, Brandelli A. Food applications of liposome-encapsulated antimicrobial peptides. Trends in Food Science & Technology. 2010;21(6):284-92.

187. Fathi M, Mozafari MR, Mohebbi M. Nanoencapsulation of food ingredients using lipid based delivery systems. Trends in Food Science & Technology. 2012;23(1):13-27.

188. Mozafari MR. Nanoliposomes: preparation and analysis. Methods in molecular biology (Clifton, NJ). 2010;605:29-50.

189. Panahi Y, Farshbaf M, Mohammadhosseini M, Mirahadi M, Khalilov R, Saghfi S, et al. Recent advances on liposomal nanoparticles: synthesis, characterization and biomedical applications. Artificial cells, nanomedicine, and biotechnology. 2017;45(4):788-99.

190. Akbarzadeh A, Rezaei-Sadabady R, Davaran S, Joo SW, Zarghami N, Hanifehpour Y, et al. Liposome: classification, preparation, and applications. Nanoscale research letters. 2013;8(1):102.

191. Mozafari M, Khosravi K, Borazan G, Cui J, Pardakhty A, Yurdugül S. Encapsulation of Food Ingredients Using Nanoliposome Technology. International Journal of Food Properties. 2008;11:833-44.

192. Mozafari MR, Johnson C, Hatziantoniou S, Demetzos C. Nanoliposomes and their applications in food nanotechnology. Journal of liposome research. 2008;18(4):309-27.

193. Pattni BS, Chupin VV, Torchilin VP. New Developments in Liposomal Drug Delivery. Chemical reviews. 2015;115(19):10938-66.

194. Zu Y, Overby H, Ren G, Fan Z, Zhao L, Wang S. Resveratrol liposomes and lipid nanocarriers: Comparison of characteristics and inducing browning of white adipocytes. Colloids and surfaces B, Biointerfaces. 2018;164:414-23.

195. Gao A, Hu XL, Saeed M, Chen BF, Li YP, Yu HJ. Overview of recent advances in liposomal nanoparticle-based cancer immunotherapy. Acta pharmacologica Sinica. 2019;40(9):1129-37.

196. Wang S, Su R, Nie S, Sun M, Zhang J, Wu D, et al. Application of nanotechnology in improving bioavailability and bioactivity of diet-derived phytochemicals. The Journal of nutritional biochemistry. 2014;25(4):363-76.

197. Accardo A, Morelli G. Review peptide-targeted liposomes for selective drug delivery: Advantages and problematic issues. Biopolymers. 2015;104(5):462-79.

198. Gregoire FM, Smas CM, Sul HS. Understanding adipocyte differentiation. Physiological reviews. 1998;78(3):783-809.

199. Hu X, Zhang Y, Xue Y, Zhang Z, Wang J. Berberine is a potential therapeutic agent for metabolic syndrome via brown adipose tissue activation and metabolism regulation. American journal of translational research. 2018;10(11):3322-9.

200. Zhang J, Nie S, Zu Y, Abbasi M, Cao J, Li C, et al. Anti-atherogenic effects of CD36-targeted epigallocatechin gallate-loaded nanoparticles. Journal of controlled release : official journal of the Controlled Release Society. 2019;303:263-73.

201. Chomczynski P, Sacchi N. Single-step method of RNA isolation by acid guanidinium thiocyanate-phenol-chloroform extraction. Analytical biochemistry. 1987;162(1):156-9.

202. Sonavane G, Tomoda K, Makino K. Biodistribution of colloidal gold nanoparticles after intravenous administration: Effect of particle size. Colloids and Surfaces B: Biointerfaces. 2008;66(2):274-80.

203. Danaei M, Dehghankhold M, Ataei S, Hasanzadeh Davarani F, Javanmard R, Dokhani A, et al. Impact of Particle Size and Polydispersity Index on the Clinical Applications of Lipidic Nanocarrier Systems. Pharmaceutics. 2018;10(2):57.

204. Momtazi-Borojeni AA, Abdollahi E, Jaafari MR, Banach M, Watts GF, Sahebkar A. Negatively-charged Liposome Nanoparticles Can Prevent Dyslipidemia and Atherosclerosis Progression in the Rabbit Model. Current vascular pharmacology. 2022;20(1):69-76.

205. Torchilin VP. Recent advances with liposomes as pharmaceutical carriers. Nature Reviews Drug Discovery. 2005;4(2):145-60.

206. Sun M, Nie S, Pan X, Zhang R, Fan Z, Wang S. Quercetin-nanostructured lipid carriers: Characteristics and anti-breast cancer activities in vitro. Colloids and Surfaces B: Biointerfaces. 2014;113:15-24.

207. Khalilpourfarshbafi M, Gholami K, Murugan DD, Abdul Sattar MZ, Abdullah NA. Differential effects of dietary flavonoids on adipogenesis. European Journal of Nutrition. 2019;58(1):5-25.

208. GREGOIRE FM, SMAS CM, SUL HS. Understanding Adipocyte Differentiation. Physiological Reviews. 1998;78(3):783-809.

209. Kim H-K, Kim JN, Han SN, Nam J-H, Na H-N, Ha TJ. Black soybean anthocyanins inhibit adipocyte differentiation in 3T3-L1 cells. Nutrition Research. 2012;32(10):770-7.

210. Dayarathne LA, Ranaweera SS, Natraj P, Rajan P, Lee YJ, Han CH. Restoration of the adipogenic gene expression by naringenin and naringin in 3T3-L1 adipocytes. Journal of veterinary science. 2021;22(4):e55.

211. Pu P, Gao DM, Mohamed S, Chen J, Zhang J, Zhou XY, et al. Naringin ameliorates metabolic syndrome by activating AMP-activated protein kinase in mice fed a high-fat diet. Archives of biochemistry and biophysics. 2012;518(1):61-70.

212. Kang SW, Kang SI, Shin HS, Yoon SA, Kim JH, Ko HC, et al. Sasa quelpaertensis Nakai extract and its constituent p-coumaric acid inhibit adipogenesis in 3T3-L1 cells through activation of the AMPK pathway. Food and chemical toxicology : an international journal published for the British Industrial Biological Research Association. 2013;59:380-5.

213. Singh AK, Raj V, Keshari AK, Rai A, Kumar P, Rawat A, et al. Isolated mangiferin and naringenin exert antidiabetic effect via PPARγ/GLUT4 dual agonistic action with strong metabolic regulation. Chemico-biological interactions. 2018;280:33-44.

214. Zhou L-B, Chen M, Wang X, Song H, Yang Y, Tang J, et al. Effect of berberine on the differentiation of adipocyte. Zhonghua yi xue za zhi. 2003;83(4):338-40.

215. Huang C, Zhang Y, Gong Z, Sheng X, Li Z, Zhang W, et al. Berberine inhibits 3T3-L1 adipocyte differentiation through the PPARγ pathway. Biochemical and biophysical research communications. 2006;348(2):571-8.

216. Lee YS, Kim WS, Kim KH, Yoon MJ, Cho HJ, Shen Y, et al. Berberine, a natural plant product, activates AMP-activated protein kinase with beneficial metabolic effects in diabetic and insulin-resistant states. Diabetes. 2006;55(8):2256-64.

217. Yang J, Yin J, Gao H, Xu L, Wang Y, Xu L, et al. Berberine improves insulin sensitivity by inhibiting fat store and adjusting adipokines profile in human preadipocytes and metabolic syndrome patients. Evidence-Based Complementary and Alternative Medicine. 2012;2012.

218. Farmer SR. Transcriptional control of adipocyte formation. Cell metabolism. 2006;4(4):263-73.

219. Liu X, Lv Y, Zheng M, Yin L, Wang X, Fu Y, et al. Polyphenols from blue honeysuckle (Lonicera caerulea var. edulis) berry inhibit lipid accumulation in adipocytes by suppressing lipogenesis. Journal of Ethnopharmacology. 2021;279:114403.

220. Choi M, Mukherjee S, Yun JW. Anthocyanin oligomers stimulate browning in 3T3-L1 white adipocytes via activation of the β3-adrenergic receptor and ERK signaling pathway. Phytotherapy research : PTR. 2021;35(11):6281-94.

221. Mosqueda-Solís A, Lasa A, Gómez-Zorita S, Eseberri I, Picó C, Portillo MP. Screening of potential anti-adipogenic effects of phenolic compounds showing different chemical structure in 3T3-L1 preadipocytes. Food & function. 2017;8(10):3576-86.

222. Yamauchi Y, Okuyama T, Ishii T, Okumura T, Ikeya Y, Nishizawa M. Sakuranetin downregulates inducible nitric oxide synthase expression by affecting interleukin-1 receptor and CCAAT/enhancer-binding protein β. Journal of natural medicines. 2019;73(2):353-68.

223. Yang Y, Liu F, Lu R, Jia J. Berberine Inhibits Adipogenesis in Porcine Adipocytes via AMP-Activated Protein Kinase-Dependent and -Independent Mechanisms. Lipids. 2019;54(11-12):667-78.

224. Saulite L, Jekabsons K, Klavins M, Muceniece R, Riekstina U. Effects of malvidin, cyanidin and delphinidin on human adipose mesenchymal stem cell differentiation into adipocytes, chondrocytes and osteocytes. Phytomedicine : international journal of phytotherapy and phytopharmacology. 2019;53:86-95.

225. Li L, Peng Z, Hu Q, Xu L, Zou X, Yu Y, et al. Berberine Suppressed Tumor Growth through Regulating Fatty Acid Metabolism and Triggering Cell Apoptosis via Targeting FABPs. Evidence-based complementary and alternative medicine : eCAM. 2020;2020:6195050.

226. Ming JH, Wang T, Wang TH, Ye JY, Zhang YX, Yang X, et al. Effects of dietary berberine on growth performance, lipid metabolism, antioxidant capacity and lipometabolism-related genes expression of AMPK signaling pathway in juvenile black carp (Mylopharyngodon piceus) fed high-fat diets. Fish physiology and biochemistry. 2022.

227. Porter C. Quantification of UCP1 function in human brown adipose tissue. Adipocyte. 2017;6(2):167-74.

228. Skates E, Overall J, DeZego K, Wilson M, Esposito D, Lila MA, et al. Berries containing anthocyanins with enhanced methylation profiles are more effective at ameliorating high fat diet-induced metabolic damage. Food and chemical toxicology : an international journal published for the British Industrial Biological Research Association. 2018;111:445-53.

229. Kanamoto Y, Yamashita Y, Nanba F, Yoshida T, Tsuda T, Fukuda I, et al. A black soybean seed coat extract prevents obesity and glucose intolerance by up-regulating uncoupling proteins and down-regulating inflammatory cytokines in high-fat diet-fed mice. Journal of agricultural and food chemistry. 2011;59(16):8985-93.

230. Lee M, Lee M. The Effects of C3G and D3G Anthocyanin-Rich Black Soybean on Energy Metabolism in Beige-like Adipocytes. Journal of agricultural and food chemistry. 2020;68(43):12011-8.

231. Zhou F, Yin M, Liu Y, Han X, Guo J, Ren C, et al. Grape seed flour intake decreases adiposity gain in high-fat-diet induced obese mice by activating thermogenesis. Journal of Functional Foods. 2019;62:103509.

232. Mulvihill EE, Allister EM, Sutherland BG, Telford DE, Sawyez CG, Edwards JY, et al. Naringenin Prevents Dyslipidemia, Apolipoprotein B Overproduction, and Hyperinsulinemia in LDL Receptor–Null Mice With Diet-Induced Insulin Resistance. Diabetes. 2009;58(10):2198-210.

233. Burke AC, Telford DE, Edwards JY, Sutherland BG, Sawyez CG, Huff MW. Naringenin Supplementation to a Chow Diet Enhances Energy Expenditure and Fatty Acid Oxidation, and Reduces Adiposity in Lean, Pair-Fed Ldlr−/− Mice. Molecular nutrition & food research. 2019;63(6):1800833.

234. Mehanna ET, El-sayed NM, Ibrahim AK, Ahmed SA, Abo-Elmatty DM. Isolated compounds from Cuscuta pedicellata ameliorate oxidative stress and upregulate expression of some energy regulatory genes in high fat diet induced obesity in rats. Biomedicine & Pharmacotherapy. 2018;108:1253-8.

235. Bae J, Yang Y, Xu X, Flaherty J, Overby H, Hildreth K, et al. Naringenin, a citrus flavanone, enhances browning and brown adipogenesis: Role of peroxisome proliferator-activated receptor gamma. Frontiers in nutrition. 2022;9:1036655.

236. Ferdous MR, Abdalla M, Yang M, Xiaoling L, Song Y. Berberine chloride (dual topoisomerase I and II inhibitor) modulate mitochondrial uncoupling protein (UCP1) in molecular docking and dynamic with in-vitro cytotoxic and mitochondrial ATP production. Journal of biomolecular structure & dynamics. 2022:1-11.

237. Lee YS, Kim WS, Kim KH, Yoon MJ, Cho HJ, Shen Y, et al. Berberine, a Natural Plant Product, Activates AMP-Activated Protein Kinase With Beneficial Metabolic Effects in Diabetic and Insulin-Resistant States. Diabetes. 2006;55(8):2256-64.

238. Zhang Z, Zhang H, Li B, Meng X, Wang J, Zhang Y, et al. Berberine activates thermogenesis in white and brown adipose tissue. Nature Communications. 2014;5(1):5493.

239. Richard D, Picard F. Brown fat biology and thermogenesis. Frontiers in bioscience (Landmark edition). 2011;16(4):1233-60.

240. Gill JA, La Merrill MA. An emerging role for epigenetic regulation of Pgc-1α expression in environmentally stimulated brown adipose thermogenesis. Environmental epigenetics. 2017;3(2):dvx009.

241. Yu LM, Dong X, Xue XD, Zhang J, Li Z, Wu HJ, et al. Naringenin improves mitochondrial function and reduces cardiac damage following ischemia-reperfusion injury: the role of the AMPK-SIRT3 signaling pathway. Food & function. 2019;10(5):2752-65.

242. Wu Y-X, Yang X-Y, Han B-S, Hu Y-Y, An T, Lv B-H, et al. Naringenin regulates gut microbiota and SIRT1/ PGC-1α signaling pathway in rats with letrozole-induced polycystic ovary syndrome. Biomedicine & Pharmacotherapy. 2022;153:113286.

243. Yao S, Yuan Y, Zhang H, Meng X, Jin L, Yang J, et al. Berberine attenuates the abnormal ectopic lipid deposition in skeletal muscle. Free Radical Biology and Medicine. 2020;159:66-75.

244. Jash S, Banerjee S, Lee M-J, Farmer SR, Puri V. CIDEA Transcriptionally Regulates UCP1 for Britening and Thermogenesis in Human Fat Cells. iScience. 2019;20:73-89.

245. Bargut TCL, Souza-Mello V, Aguila MB, Mandarim-de-Lacerda CA. Browning of white adipose tissue: lessons from experimental models. Hormone molecular biology and clinical investigation. 2017;31(1).

246. Cremonini E, Rodrigue-Lanzi C, Marino M, Iglesias D, Fraga C, Oteiza P. Effects of a cyanidin- and delphinidin-rich extract on mitochondrial dynamics, biogenesis and thermogenesis in adipose tissue of mice fed a high-fat diet. Free Radical Biology and Medicine. 2023;201:17.

247. Wu L, Xia M, Duan Y, Zhang L, Jiang H, Hu X, et al. Berberine promotes the recruitment and activation of brown adipose tissue in mice and humans. Cell Death & Disease. 2019;10(6):468.

248. Lin Y-C, Lee Y-C, Lin Y-J, Lin J-C. Berberine Promotes Beige Adipogenic Signatures of 3T3-L1 Cells by Regulating Post-transcriptional Events. Cells. 2019;8(6):632.

249. Chen Z, Wang C, Pan Y, Gao X, Chen H. Hypoglycemic and hypolipidemic effects of anthocyanins extract from black soybean seed coat in high fat diet and streptozotocin-induced diabetic mice. Food & function. 2018;9(1):426-39.

250. Dayarathne LA, Ranaweera SS, Natraj P, Rajan P, Lee YJ, Han C-H. Restoration of the adipogenic gene expression by naringenin and naringin in 3T3-L1 adipocytes. Journal of veterinary science. 2021;22(4).

251. Richard AJ, Amini-Vaughan Z, Ribnicky DM, Stephens JM. Naringenin Inhibits Adipogenesis and Reduces Insulin Sensitivity and Adiponectin Expression in Adipocytes. Evidence-Based Complementary and Alternative Medicine. 2013;2013:549750.

252. Do T, Mark BL, editors. Combining cooperative relaying with spectrum sensing in cognitive radio networks. 2010 IEEE Radio and Wireless Symposium (RWS); 2010 10-14 Jan. 2010.

253. Yang Y, Wu Y, Zou J, Wang Y-H, Xu M-X, Huang W, et al. Naringenin Attenuates Non-Alcoholic Fatty Liver Disease by Enhancing Energy Expenditure and Regulating Autophagy via AMPK. Frontiers in Pharmacology. 2021;12.

254. Namkhah Z, Naeini F, Mahdi Rezayat S, Mehdi Y, Mansouri S, Javad Hosseinzadeh-Attar M. Does naringenin supplementation improve lipid profile, severity of hepatic steatosis and probability of liver fibrosis in overweight/obese patients with NAFLD? A randomised, double-blind, placebo-controlled, clinical trial. International journal of clinical practice. 2021;75(11):e14852.

255. Guerre-Millo M, Gervois P, Raspé E, Madsen L, Poulain P, Derudas B, et al. Peroxisome Proliferator-activated Receptor α Activators Improve Insulin Sensitivity and Reduce Adiposity*. Journal of Biological Chemistry. 2000;275(22):16638-42.

256. Chitturi S, Farrell GC. Etiopathogenesis of Nonalcoholic Steatohepatitis. Semin Liver Dis. 2001;21(01):027-42.

257. Neve BP, Fruchart J-C, Staels B. Role of the peroxisome proliferator-activated receptors (PPAR) in atherosclerosis. Biochemical Pharmacology. 2000;60(8):1245-50.

258. Zhou L, Wang X, Yang Y, Wu L, Li F, Zhang R, et al. Berberine attenuates cAMP-induced lipolysis via reducing the inhibition of phosphodiesterase in 3T3-L1 adipocytes. Biochimica et biophysica acta. 2011;1812(4):527-35.

259. Jiang D, Wang D, Zhuang X, Wang Z, Ni Y, Chen S, et al. Berberine increases adipose triglyceride lipase in 3T3-L1 adipocytes through the AMPK pathway. Lipids in Health and Disease. 2016;15(1):214.

260. Dong SF, Yasui N, Negishb H, Kishimoto A, Sun JN, Ikeda K. Increased Oxidative Stress in Cultured 3T3-L1 Cells was Attenuated by Berberine Treatment. Natural product communications. 2015;10(6):895-7.

261. Zhu X, Bian H, Wang L, Sun X, Xu X, Yan H, et al. Berberine attenuates nonalcoholic hepatic steatosis through the AMPK-SREBP-1c-SCD1 pathway. Free Radical Biology and Medicine. 2019;141:192-204.

262. Ma C-Y, Shi X-Y, Wu Y-R, Zhang Y, Yao Y-H, Qu H-L, et al. Berberine attenuates atherosclerotic lesions and hepatic steatosis in ApoE -/- mice by down-regulating PCSK9 via ERK1/2 pathway. Annals of Translational Medicine. 2021;9(20):1517.

263. Xue M, Zhang L, Yang MX, Zhang W, Li XM, Ou ZM, et al. Berberine-loaded solid lipid nanoparticles are concentrated in the liver and ameliorate hepatosteatosis in db/db mice. International journal of nanomedicine. 2015;10:5049-57.

264. Guo J, Chen H, Zhang X, Lou W, Zhang P, Qiu Y, et al. The Effect of Berberine on Metabolic Profiles in Type 2 Diabetic Patients: A Systematic Review and Meta-Analysis of Randomized Controlled Trials. Oxidative Medicine and Cellular Longevity. 2021;2021:2074610.

265. Jang J, Jung Y, Seo SJ, Kim SM, Shim YJ, Cho SH, et al. Berberine activates AMPK to suppress proteolytic processing, nuclear translocation and target DNA binding of SREBP-1c in 3T3-L1 adipocytes. Molecular medicine reports. 2017;15(6):4139-47.

266. Hu Y, Davies GE. Berberine increases expression of GATA-2 and GATA-3 during inhibition of adipocyte differentiation. Phytomedicine : international journal of phytotherapy and phytopharmacology. 2009;16(9):864-73.

267. Hao M, Li Y, Liu L, Yuan X, Gao Y, Guan Z, et al. The design and synthesis of a novel compound of berberine and baicalein that inhibits the efficacy of lipid accumulation in 3T3-L1 adipocytes. Bioorganic & Medicinal Chemistry. 2017;25(20):5506-12.

8. APPENDICES

Appendix 1: Copy of ethical committee approval

T.C.
HACETTEPE ÜNİVERSİTESİ
Hayvan Deneyleri Yerel Etik Kurulu

Sayı : 52338575 – ١٤١

23.10.2019

Doç. Dr. Zeynep GÖKTAŞ
Sağlık Bilimleri Fakültesi
Beslenme ve Diyetetik Bölümü
Öğretim Üyesi

Sayın Doç. Dr. GÖKTAŞ,

Kurulumuza değerlendirilmek üzere sunduğunuz 09.07.2018 tarihli dilekçeniz ile danışmanı olduğunuz Dyt. Elif Didem ÖRS'ün ***"Naringenin, Berberin ve Delfinidin Fitokimyasal Bileşenlerinin 3T3-L1 Preadipozit Hücrelerinin Kahverengileşmesi Üzerine Etkisi"*** başlıklı tez projesinde ATCC firmasından temin ederek kullanacağınız 3T3-L1 fare hücre hattının tedarikçi bir firmadan satın alınacağı ve bu amaçla canlı omurgalı bir hayvan kullanılmayacağı anlaşılmaktadır. Hücre Kültürü Deneyleri, eğer canlı omurgalı hayvan kullanımını içermiyorsa, Hayvan Deneyleri Etik Kurullarının Çalışma Usul ve Esaslarına Dair Yönetmelik kapsamı dışında kalmakta ve Hayvan Deneyleri Etik Kurul onayı gerektirmemektedir.

Bilgilerinize rica ederim.

Prof. Dr. Sema ÇALIŞ
Başkan

Hacettepe Üniversitesi Hayvan Deneyleri Yerel Etik Kurulu 06100 Sıhhiye-Ankara
Telefon: 0 (312) 305 1090-1082 • Faks: 0 (312) 310 0580
www.etikkurul.hacettepe.edu.tr/index_hdk.php
Ayrıntılı Bilgi için:

HACETTEPE ÜNİVERSİTESİ
HAYVAN DENEYLERİ ETİK KURULU İMZA SİRKÜLERİ

TOPLANTI TARİHİ : 23.10.2019 (ÇARŞAMBA)
TOPLANTI SAYISI : 2019/11
TOPLANTI SAATİ : 14.00
KARAR NUMARASI : 2019/11-09

Prof. Dr. Sema ÇALIŞ (Başkan)	Prof. Dr. Nüket Örnek BÜKEN (Üye)	Prof. Dr. M. Yıldırım SARA (Üye)
Prof. Dr. Mehmet Ali ONUR (Üye)	(İZİNLİ) Prof. Dr. Güneş ESENDAĞLI (Üye)	Prof. Dr. Abdullah C. AKMAN (Üye)
(İZİNLİ) Prof. Dr. Ersoy KONAŞ (Üye)	Prof. Dr. Aytekin AKYOL (Üye)	Doç. Dr. Meltem TUNCER (Üye)
Doç. Dr. İlyas ÜNBAŞILAR (Üye)	(İZİNLİ) Doç. Dr. M. Alper ÇETİNKAYA (Üye)	Dr. Öğr. Üyesi Banu Cahide TEL (Üye)
(İZİNLİ) Mevlüt ÖKSÜZOĞLU (Üye)	Serdar ÇAKIROĞLU (Üye)	Avukat Yasemin ÖZSELÇUK (Üye)

Appendix 2: Protocols

RNA Extraction Protocol

Chemicals

- Chloroform
- Isopropyl alcohol
- 75% Ethanol
- RNAse free water/DEPC treated water

Glassware

- 1.5 ml tube
- Glass tubes
- Glass beaker
- Pipettor

Equipment

- Centrifuge
- UV cabin
- Heat Block
- Nanodrop

Procedure

1. Homogenization: Collection of cells. One Step RNA reagent 500 µL (Biobasic-BS410A) was used instead of triazole for cell collection and RNA isolation.

2. Phase Separation

- Cells stored at -80°C were thawed at room temperature for 5 min.
- Add 100 µL of chloroform to each sample (Add 0.2 mL of chloroform per 1 mL of ONE-STEP Reagent).
- Cap the tubes and shake by hand for 15 seconds.
- Incubate the samples stand at room temperature for 2-3 minutes.
- Centrifuge for 15 minutes at 12,000 rpm and 4°C.

- Following centrifugation, the mixture separates into a lower phase (DNA and protein) and in upper aqueous phase (RNA).

3. RNA Precipitation

- Transfer carefully the aqueous phase to a fresh tube.
- Add 250 μL of isopropyl alcohol to the samples (Use 0.5mL of isopropyl alcohol per 1mL of ONE STEP-RNA Reagent used for the initial homogenization).
- Incubate samples at room temperature for 10 minutes.
- Centrifugate for 10 minutes at 12,000 rpm and 4°C.
- After centrifugation RNA precipitate on the bottom of the tube.

4. RNA wash

- Remove the supernatant (wash the RNA pellet once with 75% ethanol. Add at least 1mL of 75% ethanol per 1mL ONE STEP-RNA Reagent used for the initial homogenization)
- Vortex the sample and centrifuge for 5 minutes at 9000 rpm and 4°C.

5. Redissolving the DNA

- Aspirate ethanol from the tubes.
- Open the caps of the tubes for 5-10 minutes and dry the ethanol. It is important not to let the RNA pellet dry completely.
- Add 30 μL of RNAse-free water to the RNA pellet and pipetting up and down.
- Incubate the samples at 55°C for 10 minutes on the heat block.
- Finally measure the samples to the nanodrop.

Reverse Transcriptase Protocol

cDNA was obtained from RNA with following reverse transcriptase protocol.

Chemicals

- Total RNA
- Random Primers
- dNTP (10 mM)
- 5X RT Buffer
- Nuclease-Free Sterile, Distilled Water
- RNase inhibitors
- OneScript® Plus RTase
- Ice

Glassware

- 0.2mL Microcentrifuge Tubes
- 0.2mL Tube Holder
- Ice bucket

Equipment

- Bench-top Spinner
- 0.2 mL Tube Rotor
- Eppendorf Gradient Cycler
- Heat block

Procedure

1. Reverse Transcriptase reactions should be assembled in an RNase-free environment. Thoroughly thaw and mix the following components before use on ice:

- 4 µl of 5X RT Buffer

- 1 µl of dNTP

- 1 µl of Primers

-1 ng- 2 µg/rxn of Total RNA or poly(A) + mRNA Variable

- 1 µl of OneScript® Plus RTase

- Nuclease-free H2O up to 20 µl

2. Gently mix the reaction and briefly centrifuge.

3. Incubate tube for 15 minutes at 50-55°C in the cycler.

4. Stop the reaction by heating at 85°C for 5 minutes in the cycler.

5. The synthesized first-strand cDNA is ready for amplification in PCR.

Real-Time PCR for Primer Testing

Before starting the Real-Time PCR sample testing, all the designed primers were tested for efficiency and specifically with following protocol.

Chemicals

- BlasTaq 2X qPCR MasterMix (catolog no: G891)
- Nuclease-free water
- 10 mcM Primerler (Forward-F ve Reverse-R)
- 4 ng/µL cDNA (real sample)

Glassware

- 0.5 mL RNase-free eppendorf tubes
- 96-well plate
- Optical adhesive Cover

Equipment

- Real-time PCR Cycler (LightCycler 480)
- Spinner
- Mini-shaker

Procedure

1. Dilute cDNA into 20 ng, 4 ng, 0.8 ng, 0.16 ng, 0.032 ng, 0.0064 ng/µL (5-series dilution) with nuclease-free water.

2. Mix BlasTaq 2X qPCR MasterMix, primer, and nuclease-free water as the following

Master mix 10 µL, primer 0.5 µL, nuclease-free water 5 µL.

3. Load 16 µL of the mixture into the well (duplicate)

4. Load 5 µL of the different cDNA concentrations and nuclease free water (as blank) into the wells (duplicate).

An example template;

	1	2	3	4	5	6	7	8	9	10	11	12
A	20ng	20ng										
B	4ng	4ng										
C	0.8ng	0.8ng										
D	0.16ng	0.16ng										
E	0.032ng	0.032ng										
F	0.0064ng	0.0064ng										
G	Blank	Blank										
H												

5. Cover the plate with optical adhesive cover and shake carefully.

6. Put the plate into LightCycler 480 real-time PCR cycler.

7. Format the plate layout and fill in the PCR specification

8. Set the equipment as following

Programs

Program Name	pre-incubation						
Cycles	1	Analysis Mode	None				
Target (°C)	Acquisition Mode	Hold (hh:mm:ss)	Ramp Rate (°C/s)	Acquisitions (per °C)	Sec Target (°C)	Step size (°C)	Step Delay (cycles)
95	None	00:03:00	4.40		0	0	0

Program Name	amplification						
Cycles	45	Analysis Mode	Quantification				
Target (°C)	Acquisition Mode	Hold (hh:mm:ss)	Ramp Rate (°C/s)	Acquisitions (per °C)	Sec Target (°C)	Step size (°C)	Step Delay (cycles)
95	None	00:00:15	4.40		0	0	0
60	Single	00:01:00	2.20		0	0	0

Program Name	melting curve						
Cycles	1	Analysis Mode	Melting Curves				
Target (°C)	Acquisition Mode	Hold (hh:mm:ss)	Ramp Rate (°C/s)	Acquisitions (per °C)	Sec Target (°C)	Step size (°C)	Step Delay (cycles)
95	None	00:00:05	4.40		0	0	0
65	None	00:01:00	2.20		0	0	0
97	Continuous		0.11	5	0	0	0

Program Name	cooling						
Cycles	1	Analysis Mode	None				
Target (°C)	Acquisition Mode	Hold (hh:mm:ss)	Ramp Rate (°C/s)	Acquisitions (per °C)	Sec Target (°C)	Step size (°C)	Step Delay (cycles)
40	None	00:00:30	2.20		0	0	0

9. Save the file and click on green arrow to run the PCR. The whole run will take about 1 hours and 30 minutes.

10. After finishing the run, check the amplification curve.

11. After exporting the results as an excel file, make standard curve (x-axis is Lg cDNA amount, y-axis is Ct), and make delta Ct curve (x-axis is Lg cDNA amount, y-axis is delta Ct (target-endogenous gene)).

12. The slope of standard curve should be between 3.2-3.4 the slope of delta Ct curve should be $<\pm 0.1$.

Real-Time PCR for Sample Testing

Sample cDNA were tested with following Real-Time PCR protocol to measure gene expression levels.

Chemicals

- BlasTaq 2X qPCR MasterMix (catolog no: G891)
- Nuclease-free water
- 10 mcM Primers (designed)
- 4 ng/μL cDNA (real sample)

Glassware

- 0.5 mL RNase-free tubes
- 96-well plate
- Optical Adhesive Cover

Equipment

- Real-time PCR Cycler (LightCycler 480)
- Mini-shaker

Procedure

1. Dilute the sample cDNA into 4ng/μL with nuclease-free water.

2. Calculate how many wells will be needed and mix BlasTaq MasterMix, primer (β-actin, PPARγ, C/EBPβ, PGC1-α, CIDEA, FABP4, 36B4, UCP1, PRDM16), and nuclease-free water as the following;

10 μL BlasTaq * number of wells, 1 μL primer * number of wells, 5μL RNase free water * number of wells.

3. Load 16 μL of the mixture into the wells.

4. Load 4 μL of the cDNA to the designated wells.

5. Cover the plate with optical adhesive cover and shake carefully.

6. Put the plate into LightCycler 480 real-time PCR cycler.

7. Format the plate layout and fill in the PCR specification

8. Set the equipment as following

Programs

Program Name	pre-incubation						
Cycles	1	Analysis Mode	None				
Target (°C)	Acquisition Mode	Hold (hh:mm:ss)	Ramp Rate (°C/s)	Acquisitions (per °C)	Sec Target (°C)	Step size (°C)	Step Delay (cycles)
95	None	00:03:00	4.40		0	0	0

Program Name	amplification						
Cycles	45	Analysis Mode	Quantification				
Target (°C)	Acquisition Mode	Hold (hh:mm:ss)	Ramp Rate (°C/s)	Acquisitions (per °C)	Sec Target (°C)	Step size (°C)	Step Delay (cycles)
95	None	00:00:15	4.40		0	0	0
60	Single	00:01:00	2.20		0	0	0

Program Name	melting curve						
Cycles	1	Analysis Mode	Melting Curves				
Target (°C)	Acquisition Mode	Hold (hh:mm:ss)	Ramp Rate (°C/s)	Acquisitions (per °C)	Sec Target (°C)	Step size (°C)	Step Delay (cycles)
95	None	00:00:05	4.40		0	0	0
65	None	00:01:00	2.20		0	0	0
97	Continuous		0.11	5	0	0	0

Program Name	cooling						
Cycles	1	Analysis Mode	None				
Target (°C)	Acquisition Mode	Hold (hh:mm:ss)	Ramp Rate (°C/s)	Acquisitions (per °C)	Sec Target (°C)	Step size (°C)	Step Delay (cycles)
40	None	00:00:30	2.20		0	0	0

9. Save the file and click on green arrow to run the PCR. The whole run will take about 1 hours and 30 minutes.

10. After finishing the run, check the amplification curve. Check that there is only one amplicon peak.

7. Format the plate layout and fill in the PCR specifications.

8. After exporting results, calculation is performed as the following;

- deltaCt (ΔCt) of target gene in experimental group= Ct (target gene)- Ct (endogenous gene)
- ΔCt of target gene in control group= Ct (target gene) – Ct (endogenous gene)
- ΔΔCt =ΔCt of target gene in experimental group - ΔCt of target gene in control group
- Fold change=$2^{*\Delta\Delta Ct}$

Protein Extraction Protocol

Protein extraction was used for isolate proteins from the sample.

Chemicals

- Isopropyl alcohol
- Urea
- SDS
- Ethanol

Glassware

- Pipettor
- 2mL centrifuge tubes
- Pipette tips

Equipment

- Centrifuge
- Heat block
- Vortex
- Precision scale

Procedure

1. Precipitate the protein

- After RNA was separated in the tube remaining DNA and protein. However, RNA may have remained in the upper phase. Remove as much as possible with a pipettor the upper phase.
- Add 150 μL of 100% ethanol (for every 1 mL of ONE Step Reagent, add 0.3 mL of ethanol)
- Close the cap of the tube and mix by hand several times and incubate for 2-3 minutes.
- Centrifuge for 5 minutes at 5,000 rpm at 4°C to precipitate DNA.
- Transfer the supernatant to a new 2mL tube.
- Add 750μL of isopropanol to the supernatant and incubate for 10 minutes.
- Centrifuge for 10 minutes at 12,000 rpm at 4°C to precipitate proteins.

- Discard the supernatant with a micro pipettor.

2. Wash the proteins

- Prepare a wash solution of 0.9009 g of urea in 95% ethanol (5% water with DEPC).
- *Resuspend the pellet with 1 mL of wash solution (use 2 mL of wash solution for 1 mL of ONE Step Reagent).
- *Incubate for 20 minutes.
- *Centrifuge at 9,000 rpm for 5 minutes at 4°C.
- *Discard the supernatant with a micro pipettor.
- Repeat the starred steps twice.
- Add 2 mL of 100% ethanol, then vortex briefly.
- Incubate for 20 minutes.
- Centrifuge for 5 minutes at 9,000 rpm at 4°C.
- Discard the supernatant with a micro pipettor.
- Air dry the protein pellet for 5-10 minutes.

3. Solubilize the proteins

- Resuspend the pellet in 200 µL of 1% SDS by pipetting up and down.
- To ensure complete resuspension of the pellet, incubate the sample at 50°C in a heat block.
- Centrifuge for 10 minutes at 11,000 rpm at 4°C to remove insoluble materials.
- Transfer the supernatant to a new tube and store the supernatant at -20°C until use.

BCA Protein Assay

BCA protein assay kit was used for protein quantification of the samples.

Chemicals

- Pierce BCA Protein Assay Kit (thermo Scientific 23225)
- BCA Reagent A
- BCA Reagent B
- RIPA Buffer
- Albumin Standards

Glassware

- 2mL centrifuge tube
- 96-well flat bottom transparent plate
- Adhesive plate covers

Equipment

- Water bath
- Shaker
- Plate reader

Procedure

1. Prepare standards from Albumin

- Standard A; 600mL albumin stock and 600mL RIPA
- Standard B; 600mL Standard A and 600mL RIPA
- Standard C; 600mL Standard B and 600mL RIPA
- Standard D; 600mL Standard C and 600mL RIPA
- Standard E; 600mL Standard D and 600mL RIPA
- Standard F; 600mL Standard E and 600mL RIPA
- Standard G; 600mL Standard F and 600mL RIPA
- Blank; 600mL RIPA

2. Calculate the amount of the BCA working reagent using the following formula; (number of standards + number of samples) * 2 *200 µL working reagent= total volume of working reagent

3. Mix 50 parts of Reagent A with 1 part of Reagent B.

4. Load 25 µL of standards and sample into the wells.

5. Load 200 µL working reagent into the wells.

6. Shake the plate on a shaker for 1 minute.

7. Put the plate into water bath at 37°C for 30 minutes.

8. Cool the plate to the room temperature.

9. Measure the absorbance at 562nm with the plate reader.

10. Export the Blank 562 to the excel file.

11. Calculate a curve and the sample concentrations.

ELISA Protocol

UCP1, PPAR-γ, PGC1-α protein concentration of protein extracts were measured by using Sandwich enzyme immunoassay (ELISA) kit (ELK Biotechnology, Wuhan) with following protocol.

Chemicals

- Microplate, coated with mouse cell
- Wash Buffer 25X
- HRP Diluent
- Detection Antibody
- Detector 100X
- Antibody Diluent
- Standard (lyophilized)
- Substrate Solution
- Stop Solution
- De-ionized Water

Glassware

- Adhesive Covers
- Glass cylinders
- Multi-channel pipettor
- Wipes

Equipment

- Plate reader
- High-speed centrifuge
- Water bath

Preparation of the Solutions

1. Wash Buffer 10X has to be diluted with de-ionized water 1:25 before use to obtain Wash Buffer 1X.

2. Standard working solution has to be reconstitutes with 1.0mL of Standard Diluent. The concentration of the standard in the stock solution is 10 ng/mL. Prepare 7 tubes

containing 0.5mL Standard Diluent and use the diluted standard to produce a double dilution series. Mix each tube thoroughly before the next transfer. Use the new standard solution for each experiment.

Procedure

1. Add 100μL of standard working Buffer or 100μL of sample to each well, incubate at 37°C for 80 minutes.

2. Discard the liquid in the plate, add 200μL of Wash Buffer to each well, and wash the plate 3 times. After the last wash, complete removal of liquid is essential for good performance. You may tap the plate on a wipe.

3. Spin-drying and add 100μL Antibody working solution to each well, incubate at 37°C for 50 minutes.

4. Discard the liquid in the plate, add 200μL Wash Buffer to each well, and wash the plate 3 times. After the last wash, complete removal of liquid is essential for good performance. You may tap the plate on a wipe.

5. After drying, add 100μL of the diluted Detector to each well, incubate at 37°C for 50 minutes.

6. Discard the liquid in the plate, add 200μL Wash Buffer to each well, and wash the plate 5 times. After the last wash, complete removal of liquid is essential for good performance. You may tap the plate on a wipe.

7. After spin-drying, add 90μL Substrate Solution to each well, incubate at 37°C for 20 minutes.

8. Add 50μL stop solution to each well, read plate at 450nm.

Triglyceride Protocol

Triglyceride Colorimetric Assay kit was used for triglyceride quantification of the samples.

Chemicals

- Triglyceride Standard
- Standard Diluent Assay Reagent (5X)
- NP40 Substitute Assay Reagent (5X)
- Triglyceride Enzyme Mixture
- Sodium Phosphate Assay Buffer
- Distilled water

Glassware

- Test tubes
- 15 mL centrifuge tube
- Aluminum foil
- Multi-channel pipettor
- 96-well solid plate
- Plate Cover

Equipment

- Plate reader
- Sonicator
- Centrifuge

Preparation of the Sample

1. Collect cells. Resuspend the cell pellet in 1-2 mL of cold diluted Standard Diluent.

2. Sonicate the cell suspension 20X at one second bursts and centrifuge cell suspension at 10,000 x g for 10 minutes at 4°C.

3. Remove the supernatant and store on ice.

4. Before assaying diluted the samples 1:2-1:3 with diluted Standard Diluent.

Preparation of the Standard

- Label eight clean test tubes A-H and add 200 µl of the diluted Standard Diluent to tubes B-H.
- Add 400 µl of diluted Standard Diluent to tube A. Add 100 µl of Triglyceride Standard to tube A and mix thoroughly. The concentration of tube A is 200 mg/dL.
- Serially dilute the standard by removing 200 µl from tube A and adding it to tube B; mix thoroughly.
- Remove 200 µl from tube B and place it into tube C; mix thoroughly. Repeat this process for tubes D-G. Tube H only has diluted Standard Diluent and used as the blank.

Procedure

1. Add 10 µl of Triglyceride standard (tubes A-H) to the designated wells on the plate.

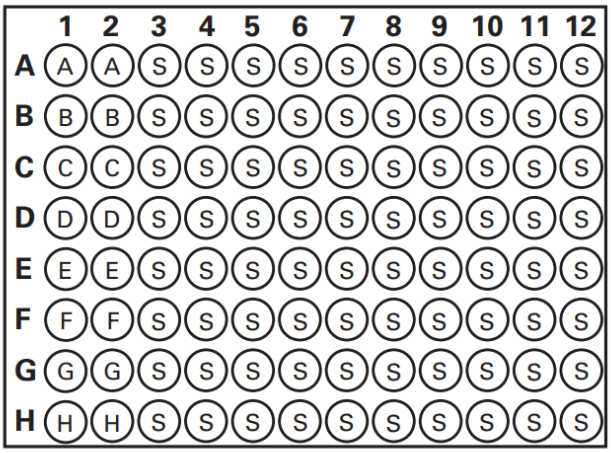

A-H = Standards
S = Samples

2. Add 10 µl of sample to two or three wells, after add 150 µl of diluted Enzyme Mixture solution to each well.

4. Cover with the plate cover. Shake the plate for a few seconds to mix.

5. Incubate the plate for 30 minutes at 37°C or 60 minutes at room temperature.

6. Measure the absorbance at 530-550 nm using a plate reader.

Cell Viability Assays (MTT) Protocol

MTT Assay Kit was used in cell proliferation and cytotoxicity detection.

Chemicals

- DMSO
- PBS
- MTT (5X)
- MTT Substrate

Glassware

- 2mL centrifuge tube
- 96-well plate
- Pipettor

Equipment

- Water bath
- Shaker
- Plate reader

Preparation of the Standard

1. MTT(5X) was diluted with MTT Substrate to 1XMTT working solution before use (e.g. 100μL MTT(5X) + 400μL MTT Substrate) to obtain 1XMTT working solution.

Procedure

1. Add 100 μL of cell suspension per well, incubate at 37°C, 5% CO2 Cell incubator for 24 h.

2. Add 10 μL of Nano encapsulated phytochemicals or free form to each well to stimulate the cells. Add two blank wells with the same volume of PBS or void for control groups.

3. Incubate at 37°C, 5% CO2 and 100% humidity Cell incubator for appropriate time.

4. Add 50 μL1XMTT working solution to each well, incubate at 37°C, 5%CO2 Cell incubator for 4 h.

5. Remove the supernatant, add 150μL DMSO to each to dissolve the formazan format on the last step, shake the well with a flat shaker.

6. Measure the absorbance at 570 nm.

Appendix 3: Turnitin Report

EFFECTS OF NARINGENIN, BERBERINE, AND DELPHINIDIN PHYTOCHEMICAL COMPOUNDS ON BROWNING OF 3T3-L1 PREADIPOCYTE CELLS

ORIGINALITY REPORT

3%	2%	4%	0%
SIMILARITY INDEX	INTERNET SOURCES	PUBLICATIONS	STUDENT PAPERS

PRIMARY SOURCES

1	theinterstellarplan.com Internet Source	1%
2	worldwidescience.org Internet Source	1%
3	Zeynep Goktas, Yujiao Zu, Mehrnaz Abbasi, Shannon Galyean, Dayong Wu, Zhaoyang Fan, Shu Wang. "Recent Advances in Nanoencapsulation of Phytochemicals to Combat Obesity and Its Comorbidities", Journal of Agricultural and Food Chemistry, 2020 Publication	1%
4	Yang Yang, Myah Trevethan, Shu Wang, Ling Zhao. "Beneficial Effects of Citrus Flavanones Naringin and Naringenin and Their Food Sources on Lipid Metabolism: An Update on Bioavailability, Pharmacokinetics, and Mechanisms", The Journal of Nutritional Biochemistry, 2022 Publication	1%

Appendix 4: Digital Receipt

turnitin

Digital Receipt

This receipt acknowledges that Turnitin received your paper. Below you will find the receipt information regarding your submission.

The first page of your submissions is displayed below.

Submission author:	Elif Örs Demet
Assignment title:	tez
Submission title:	EFFECTS OF NARINGENIN, BERBERINE, AND DELPHINIDIN P...
File name:	Elif_Didem_RS_DEMET_tez.docx
File size:	1.86M
Page count:	118
Word count:	23,361
Character count:	132,037
Submission date:	13-Mar-2024 11:44AM (UTC+0300)
Submission ID:	2298712541

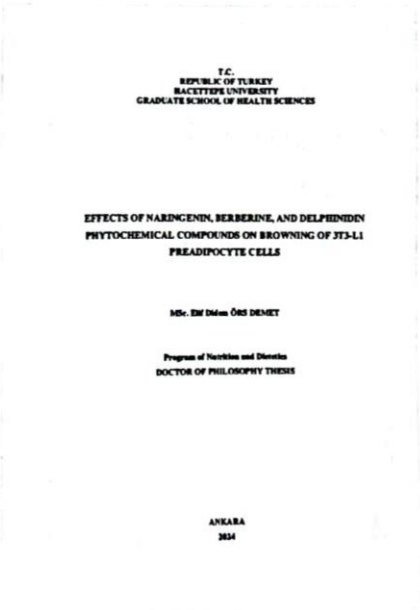

T.C.
REPUBLIC OF TURKEY
HACETTEPE UNIVERSITY
GRADUATE SCHOOL OF HEALTH SCIENCES

EFFECTS OF NARINGENIN, BERBERINE, AND DELPHINIDIN PHYTOCHEMICAL COMPOUNDS ON BROWNING OF 3T3-L1 PREADIPOCYTE CELLS

MSc. Elif Didem ÖRS DEMET

Program of Nutrition and Dietetics
DOCTOR OF PHILOSOPHY THESIS

ANKARA
2024

Copyright 2024 Turnitin. All rights reserved.

9. CURRICULUM VITAE